https://doi.org/10.35662/unine-thesis-3002

Power-scaling of ultrafast thin-disk laser oscillators for intra-oscillator high harmonic generation

A dissertation submitted to

University of Neuchâtel
Faculty of Science

Presented by

Julian Benedikt Fischer

Submitted on 12.09.2022 to the jury

Prof. Dr. Thomas Südmeyer	Director
Prof. Dr. Uwe Morgner	Examiner
Dr. Valentin Wittwer	Examiner

Neuchâtel, 2022

UNIVERSITÉ DE NEUCHÂTEL

Faculté des Sciences
Secrétariat-décanat de Faculté
Rue Emile-Argand 11
2000 Neuchâtel – Suisse
Tél : + 41 (0)32 718 21 00
E-mail : secretariat.sciences@unine.ch

IMPRIMATUR POUR THESE DE DOCTORAT

La Faculté des sciences de l'Université de Neuchâtel autorise l'impression de la présente thèse soutenue par

Monsieur Julian Benedikt FISCHER

Titre:

"Power-scaling of ultrafast thin-disk laser oscillators for intra-oscillator high harmonic generation"

sur le rapport des membres du jury composé comme suit:

- Prof. Thomas Südmeyer, directeur de thèse, Université de Neuchâtel, Suisse
- Dr Valentin Wittwer, Université de Neuchâtel, Suisse
- Prof. Uwe Morgner, Leibniz Universität Hannover, Allemagne

Neuchâtel, le 3 novembre 2022

Le Doyen, Prof. R. Bshary

Abstract

This thesis describes (i) the development of an efficient, high peak-power, sub-100-fs thin-disk laser (TDL) oscillator; and (ii) the development of a single-stage, megahertz-repetition-rate, coherent extreme-ultraviolet (XUV) light source based on high harmonic generation (HHG) inside an ultrafast TDL oscillator.

The short-pulse-duration high-peak-power TDL oscillator is an attractive single-stage source for driving nonlinear interactions at megahertz repetition rates. The developed Kerr lens mode-locked (KLM) Yb:YAG TDL oscillator operates in the regime of strong intra-cavity self-phase modulation (SPM). It delivers not only in an extreme configuration of 27 fs the shortest pulses of any ultrafast TDL oscillator, but also presents with 102 MW peak-power at 52 fs pulse duration the first more than 100-MW peak-power ultrafast laser oscillator. The achieved results show that TDL oscillators operating with strong intra-cavity SPM can generate efficiently short pulses with an optical bandwidth exceeding the available Yb:YAG gain bandwidth by a factor of more than two. Furthermore, the results show that the industry-standard Yb:YAG gain material is currently still the best choice for reaching shortest pulses and highest peak powers from TDL oscillators. This statement also holds in the sub-100-fs pulse duration regime, where Yb:YAG by far exceeds the performance achieved by TDL oscillators based on more broadband gain materials. The output of the 102-MW peak-power 52-fs TDL oscillator is well-suited for consecutive temporal pulse compression and a $\sim$7 fs pulse duration is expected to be reached within a single gas-filled multi-pass compression cell. The close to single-cycle compressed pulses should feature a superior pulse contrast in comparison to systems requiring several consecutive compression stages. This makes this source highly attractive for attosecond applications at megahertz repetition rates.

The developed single-stage intra-oscillator HHG source generates coherent XUV light at megahertz repetition rates (MHz-HHG) and features compared to other MHz-HHG approaches a considerably reduced system complexity. The presented system utilizes the intra-oscillator enhancement available inside a mode-locked laser oscillator for driving HHG directly inside a tight intra-cavity focus. The two major challenges of building an intra-oscillator MHz-HHG source are intra-cavity peak-power scaling of the driving laser and finding efficient and broadband intra-cavity XUV out-coupling mechanisms. The achieved 2 GW

of intra-cavity peak power within a 51-fs KLM Yb:YAG TDL oscillator represents the highest intra-cavity peak-power of any ultrafast laser oscillator. Additionally, two broadband and efficient intra-oscillator XUV out-coupling approaches, i.e., a coated grazing-incidence plate (GIP) and a pierced mirror will be discussed. The during this thesis developed and for the first time intra-cavity-implemented coated GIP features more than 25% of XUV reflectivity in the photon energy range from 10 to 60 eV. In combination with an improved driving intra-oscillator performance, this allowed to scale the out-coupled XUV average power from intra-oscillator HHG sources by more than four orders of magnitude while simultaneously more than doubling the out-coupled photon energy. The out-coupled XUV flux of 1.3 µW in a single harmonic at 37 eV from argon approaches for the first time the state-of-the-art XUV power levels of femtosecond enhancement cavity (fsEC) MHz-HHG sources operating at comparable photon energies. Preliminary results for the first successful out-coupling of intra-oscillator generated high harmonics from a KLM TDL by a pierced mirror will be presented. A pierced mirror enables efficient and spectrally not-limited XUV out-coupling towards high photon energies. Replacing the infrared-transmissive XUV out-couplers of previous intra-oscillator HHG systems by a pierced mirror has allowed reaching a significantly increased intra-cavity peak power. The to 1.2 GW increased peak-power, 1.1 kW average-power system has enabled HHG in neon with photon energies up to 71 eV. A combination of the demonstrated 2 GW intra-cavity peak-power TDL with the pierced mirror XUV out-coupling should soon enable a 100-eV intra-oscillator MHz-HHG source. Single-stage 100-eV coherent-XUV sources are highly attractive for coherent diffraction imaging and find broad applications especially in the semiconductor industry for optical inspection.

Keywords:

Mode-locked lasers, ultrafast lasers, Yb-doped gain materials, Kerr lens mode-locking, thin-disk laser oscillators, megahertz repetition rate, intra oscillator, high harmonic generation, coherent extreme-ultraviolet light, coated grazing-incidence plate, pierced mirror.

Résumé

Cette thèse se décompose en deux parties. Dans un premier temps, elle décrit le développement d'un laser à disque fin (TDL) à haute efficacité optique, capable de générer des impulsions de plus de 100 MW de puissance de crête et de durées inférieures à 100 fs. La deuxième partie présente le développement d'une source XUV cohérente basée sur la génération d'harmoniques d'ordre élevé (HHG) produites directement à l'intérieure de la cavité d'un laser à haute puissance de crête. Ce système compact d'un seul étage permet la génération d'impulsions XUV ultracourtes, à des taux de répétions de plusieurs mégahertz.

Capable de délivrer des impulsions optiques ultracourtes à hautes puissances de crêtes, le TDL est une source compacte et prometteuse pour générer des interactions non-linéaires à des taux de répétition de l'ordre du mégahertz. Le TDL décrit dans cette thèse se base sur un cristal Yb:YAG et utilise le procéder de blocage de mode par lentille de Kerr (KLM) pour générer des impulsions de moins de 100 fs. Il fonctionne dans le régime de forte automodulation de phase (SPM) où la largeur spectrale des impulsions excède considérablement celle de la bande d'émission du cristal Yb:YAG. Opéré dans une première configuration, ce laser est capable de générer des impulsions de 27 fs. Cela représente la durée d'impulsion la plus courte jamais atteinte par un TDL. D'autre part, dans une seconde configuration on mesure jusqu'à 102 MW de puissance de crête avec 52 fs de durée d'impulsion. Il constitue ainsi la première source laser femtoseconde capable de dépasser les 100 MW de puissance de crête. Ces résultats démontrent que les TDLs fonctionnant avec un fort taux de SPM peuvent générer efficacement des impulsions ultrabrèves dont la largeur spectrale dépasse celle du matériau Yb:YAG d'un facteur supérieur à deux. En outre, ces résultats soulignent le fait que le matériau à gain Yb:YAG, fortement présent dans l'industrie, reste actuellement le meilleur choix pour obtenir des impulsions courtes à hautes puissances de crête à partir de TDLs. Cette affirmation est également valable dans le régime de durée d'impulsion inférieure à 100 fs, où l'Yb:YAG dépasse de loin les performances obtenues par les oscillateurs TDL basés sur des matériaux de gain à plus large bande. La configuration permettant d'atteindre 102 MW de puissance de crête est prometteuse pour la compression temporelle des impulsions en sortie de laser. Il est potentiellement possible de compresser les 52 fs de durée d'impulsion jusqu'à $\sim$7 fs en focalisant la sortie

du laser dans une seule cellule de compression multi-passe remplie de gaz. Ces impulsions ainsi compressées se rapprochent d'un cycle optique et devraient permettre d'obtenir un contraste supérieur aux systèmes nécessitant plusieurs étapes de compression. Par conséquent, ce système constitue une source optique très attractive pour les applications attosecondes à des taux de répétition de l'ordre du mégahertz.

La source XUV décrite dans la deuxième partie est capable de générer des impulsions cohérentes dans l'ultraviolet extrême à des taux de répétition de l'ordre du mégahertz (MHz-HHG). Basé sur la génération d'harmoniques d'ordre élevé directement à l'intérieur de la cavité laser, ce système mono étage à l'avantage d'être plus simple et plus compact que la plupart des autres sources XUV. Le fait de produire la HHG directement à l'intérieur de la cavité où le faisceau est le plus focalisé permet de bénéficier de puissances et intensités de crête bien supérieures à celles disponibles en sortie du laser. Le développement d'une source MHz-HHG intra-oscillateur présente deux défis principaux. D'une part, l'optimisation de la cavité pour maximiser la puissance de crête intra-cavité, d'autre part, le développement du mécanisme permettant d'extraire les impulsions XUV de manière efficace sur une large bande spectrale. La puissance de crête maximale atteinte à l'intérieure de la cavité est de 2 GW avec une durée d'impulsion de 51 fs. Il s'agit de la puissance de crête intra-cavité la plus élevée de tous les oscillateurs laser femtoseconde. Deux mécanismes permettant l'extraction de la lumière XUV de manière efficaces et large bande sont présentés. Une première approche se base sur l'utilisation d'une plaque à incidence rasante (GIP) revêtue de couches minces optique. La deuxième technique se base sur l'utilisation d'un miroir percé. La GIP développée au cours de cette thèse et mise en œuvre pour la première fois à l'intérieur d'une cavité, présente une réflectivité XUV de plus de 25% dans la gamme d'énergie de photon de 10 à 60 eV. L'amélioration des performances intra-cavité combinée avec l'utilisation de cette GIP a permis l'augmentation de la puissance XUV extraite de plus de quatre ordres de grandeur et l'augmentation de l'énergie de photon d'un facteur deux, en comparaison avec d'autres systèmes de HHG intra-oscillateur. En utilisant un gaz d'argon, le flux XUV hors cavité contenu dans l'harmonique d'énergie 37 eV atteint 1.3 µW. Ce résultat s'approche pour la première fois des niveaux de puissance XUV des meilleures sources MHz-HHG, à savoir celles utilisant des résonnateurs optiques passifs femtoseconde (fsEC), opérant à des énergies de photon comparables. Dans la partie suivante, on présente les résultats relatifs à l'extraction de la lumière XUV à l'aide d'un miroir percé, utilisés pour la première fois dans un oscillateur KLM TDL. Le miroir percé permet une extraction XUV efficace avec une gamme spectrale non limité, même à plus hautes énergies de photon. L'utilisation des miroirs per-

cés dans les sources HHG intra-oscillateurs a permis d'atteindre une puissance de crête intra-cavité considérablement accrue. Avec une puissance de crête de 1.2 GW et une puissance moyenne de 1.1 kW, le système est désormais capable de générer des harmoniques dans le néon, atteignant des énergies de photon de 71 eV. En combinant la puissance de crête intra-cavité de 2 GW, précédemment démontrée, avec le miroir percé, cette source MHz-HHG intra-oscillateur devrait permettre de produire des photons jusqu'à des énergies atteignant 100 eV. De telles sources XUV cohérentes et compactes capables d'atteindre 100 eV, sont très attractives pour l'imagerie par diffraction cohérente et trouvent de nombreuses applications, notamment pour l'inspection optique dans l'industrie des semi-conducteurs.

Mots clés:

Lasers à verrouillage de mode, Lasers ultrarapides, Matériaux à gain Ytterbium, Verrouillage de mode par effet Kerr, Lasers à disque fin, Taux de répétition MHz, intra cavité, Génération d'harmoniques d'ordre élevé, rayonnement cohérent dans l'ultraviolet extrême, lame à incidence rasante avec revêtement optique, miroir percé.

Contents

List of acronyms

FCPA	Fiber chirped pulse amplifier
fsEC	Femtosecond enhancement cavity
FWHM	Full width at half maximum
GDD	Group delay dispersion
GIP	Grazing-incidence plate
HHG	High harmonic generation
KLM	Kerr lens mode-locking
NLM	Non-linear mirror
ROC	Radius of curvature
SESAM	Semiconductor saturable absorber mirror
SPM	Self-phase modulation
TDL	Thin-disk laser
XUV	Extreme ultraviolet
Yb:CALGO	Ytterbium doped calcium gadolinium aluminum oxide (Yb:$CaGdAlO_4$)
Yb:Lu_2O_3	Ytterbium doped lutetium oxide (Yb:Lu_2O_3)
Yb:YAG	Ytterbium doped yttrium aluminum garnet (Yb:$Y_3Al_5O_{12}$)

Publications

Parts of this thesis are published or submitted in the following journal papers. All papers are as originally published and reprinted with the permission from the corresponding publishers. The copyright of the original publications are held by the respective copyright holders.

Journal publications

1. Fischer, J., Drs, J., Labaye, F., Modsching, N., Müller, M., Wittwer, V. J. & Südmeyer, T. Efficient XUV-light out-coupling of intra-cavity high harmonics by a coated grazing-incidence plate. *Optics Express* **30**, 30969 (2022).
2. Drs, J., Fischer, J., Modsching, N., Labaye, F., Müller, M., Wittwer, V. J. & Südmeyer, T. A decade of sub-100-fs thin-disk laser oscillators. *Submitted to: Laser & Photonics Reviews* (2022).
3. Fischer, J., Drs, J., Modsching, N., Labaye, F., Wittwer, V. J. & Südmeyer, T. Efficient 100-MW, 100-W, 50-fs-class Yb:YAG thin-disk laser oscillator. *Optics Express* **29**, 42075 (2021).
4. Drs, J., Fischer, J., Modsching, N., Labaye, F., Wittwer, V. J. & Südmeyer, T. Sub-30-fs Yb:YAG thin-disk laser oscillator operating in the strongly self-phase modulation broadened regime. *Optics Express* **29**, 35929 (2021).
5. Modsching, N., Drs, J., Brochard, P., Fischer, J., Schilt, S., Wittwer, V. J. & Südmeyer, T. High-power dual-comb thin-disk laser oscillator for fast high-resolution spectroscopy. *Optics Express* **29**, 15104 (2021).
6. Fischer, J., Drs, J., Labaye, F., Modsching, N., Wittwer, V. & Südmeyer, T. Intra-oscillator high harmonic generation in a thin-disk laser operating in the 100-fs regime. *Optics Express* **29**, 5833 (2021).
7. Modsching, N., Drs, J., Fischer, J., Paradis, C., Labaye, F., Gaponenko, M., Kränkel, C., Wittwer, V. J. & Südmeyer, T. Sub-100-fs Kerr lens mode-locked Yb:Lu_2O_3 thin-disk laser oscillator operating at 21 W average power. *Optics Express* **27**, 16111 (2019).

Conference contributions (first author)

8. Fischer, J., Drs, J., Labaye, F., Modsching, N., Müller, M., Wittwer, V. J. & Südmeyer, T. *Broadband and Efficient Out-Coupling of Intra-Cavity High Harmonics by a Coated Grazing-Incidence Plate* in *Pacific Rim Conference on Lasers and Electro-Optics 2022 (CLEO Pacific Rim, CLEO-PR)* (Optica Publishing Group, 2022), paper CThP2I, Promoted Invited talk.
9. Fischer, J., Drs, J., Müller, M., Modsching, N., Labaye, F., Wittwer, V. J. & Südmeyer, T. *Efficient high-peak-power 50-fs-class Yb:YAG thin-disk laser oscillator* in *Conference on Lasers and Electro-Optics 2022* (Optica Publishing Group, 2022), paper SF4E.4.
10. Fischer, J., Drs, J., Labaye, F., Modsching, N., Müller, M., Wittwer, V. J. & Südmeyer, T. *Coated grazing incidence plate for XUV out-coupling of intracavity high harmonics from a thin-disk laser oscillator* in *Conference on Lasers and Electro-Optics 2022* (Optica Publishing Group, 2022), paper STh4L.1.
11. Fischer, J., Drs, J., Labaye, F., Modsching, N., Müller, M., Wittwer, V. J. & Südmeyer, T. *High Harmonic Generation Inside Thin-Disk Laser Oscillators – An Efficient and Single-Stage XUV Source* in *Optica High-brightness Sources and Light-driven Interactions Congress 2022* (Optica Publishing Group, 2022), paper HW2B.3.
12. Fischer, J., Drs, J., Labaye, F., Modsching, N., Wittwer, V. J. & Südmeyer, T. *Recent Progress and Perspectives of Intra-Oscillator High Harmonic Generation Using Thin-Disk Lasers* in *Conference on Lasers and Electro-Optics Europe and European Quantum Electronics Conference 2021* (Optica Publishing Group, 2021), paper cf_4_3.
13. Fischer, J., Drs, J., Labaye, F., Modsching, N., Wittwer, V. J. & Südmeyer, T. *Microwatt-class intra-oscillator high harmonic generation in argon, krypton, and xenon* in *European Optical Society Annual meeting 2021* (European Optical Society, 2021), paper TOM13 S04: 2.
14. Fischer, J., Drs, J., Modsching, N., Labaye, F., Wittwer, V. J. & Südmeyer, T. *Powerful Sub-40-fs Yb:YAG Thin-Disk Laser Oscillator Operating in the Regime of Strong Self-Phase Modulation* in *Laser Congress 2021 (ASSL,LAC)* (Optica Publishing Group, 2021), paper AW2A.2.
15. Fischer, J., Drs, J., Modsching, N., Labaye, F., Wittwer, V. J. & Südmeyer, T. *69 W average power sub-100-fs Yb:YAG thin-disk laser* in *Conference on Lasers and Electro-Optics 2021* (Optica Publishing Group, 2021), paper SF2M.4.

16. Fischer, J., Drs, J., Labaye, F., Modsching, N., Wittwer, V. J. & Südmeyer, T. *Intra-Oscillator High Harmonic Generation in a ~100-fs Kerr-Lens Mode-Locked Yb:YAG Thin-Disk Laser* in *Laser Congress 2020 (ASSL, LAC)* (Optica Publishing Group, 2020), paper AF3A.2.

17. Fischer, J., Drs, J., Labaye, F., Modsching, N., Kränkel, C., Wittwer, V. J. & Südmeyer, T. *Intra-Oscillator High Harmonic Generation in a ~100-fs Kerr-Lens Mode-Locked Thin-Disk Laser* in *Conference on Lasers and Electro-Optics 2020* (Optica Publishing Group, 2020), paper SF3H.3.

Awards and honors

1. Fischer, J., Drs, J., Labaye, F., Modsching, N., Müller, M., Wittwer, V. J. & Südmeyer, T. *High Harmonic Generation Inside Thin-Disk Laser Oscillators – An Efficient and Single-Stage XUV Source* in *Optica High-brightness Sources and Light-driven Interactions Congress 2022 (2022)* (Optica Publishing Group, 2022), paper HW2B.3, "Best Student Paper Award" winner.
2. Fischer, J., Drs, J., Müller, M., Modsching, N., Labaye, F., Wittwer, V. J. & Südmeyer, T. *Efficient high-peak-power 50-fs-class Yb:YAG thin-disk laser oscillator* in *Conference on Lasers and Electro-Optics (2022)* (Optica Publishing Group, 2022), paper SF4E.4, "Maiman Paper Competition" finalist.
3. Fischer, J., Drs, J., Modsching, N., Labaye, F., Wittwer, V. J. & Südmeyer, T. *Powerful Sub-40-fs Yb:YAG Thin-Disk Laser Oscillator Operating in the Regime of Strong Self-Phase Modulation* in *Laser Congress 2021 (ASSL,LAC) (2021)* (Optica Publishing Group, 2021), paper AW2A.2, "Best Student Paper Award" winner.
4. Fischer, J., Drs, J., Labaye, F., Modsching, N., Wittwer, V. J. & Südmeyer, T. *Intra-Oscillator High Harmonic Generation in a ~100-fs Kerr-Lens Mode-Locked Yb:YAG Thin-Disk Laser* in *Laser Congress 2020 (ASSL, LAC) (2020)* (Optica Publishing Group, 2020), paper AF3A.2, "Best Student Paper Award" winner.

1 Introduction

1.1 Motivation

Coherent extreme-ultraviolet (XUV) light sources enable a plethora of applications in science and technology. High harmonic generation (HHG) in a noble gas target driven by ultrafast lasers is hereby the most common approach and has enabled table-top coherent XUV light sources. The extremely high peak intensities ($>10^{13}$ W/cm^2) required for HHG have been historically delivered by Ti:sapphire laser amplifier systems. Due to thermal limitations in the bulk gain material, these systems typically operate with only a few watts of average output power, restricting HHG to kilohertz repetition rates. With the rapid development of Yb-doped laser systems in the last decades, significantly higher average powers in the kilowatt range can nowadays be reached, enabling HHG at megahertz repetition rates (MHz-HHG). MHz-HHG sources enable, inter alia, shorter measurement acquisition times in for instance space-charge-effect limited photoelectron spectroscopy experiments.

Placing the HHG gas target directly inside the tight intra-cavity focus of an ultrafast thin-disk laser (TDL) oscillator is a young and promising technology capable of driving MHz-HHG. Compared to established MHz-HHG systems based on high-power fiber chirped pulse amplifier (FCPA) systems or femtosecond enhancement cavities (fsEC), the single-stage intra-oscillator approach comes with the advantage of a considerably reduced system complexity. It neither requires temporal pulse compression nor any active stabilization. Intra-oscillator HHG was first demonstrated in this research group in 2017 [1]. This doctoral thesis aims to further investigate power-scaling of ultrafast TDL oscillator and its subsequent application for intra-oscillator HHG to increase the delivered XUV flux and provided photon energy.

This PhD thesis is based on a cumulative format of peer-reviewed journal articles. The following section 1.2 defines the main objectives and introduces the structure of the thesis.

1.2 Thesis objectives and organization

Starting from the proof-of-principle demonstration of HHG inside an ultrafast TDL oscillator in 2017 [1], generating less than 1 nW within a single harmonic order at 13 eV, the main objective of this thesis can be defined as follows: Reach state-of-the-art megahertz repetition rate XUV output power levels with the intra-oscillator HHG approach. Depending on the desired photon energy and repetition rate, reaching state-of-the-art XUV output power corresponds to delivering µW to mW XUV power levels in a single harmonic order [2, 3]. The XUV output had to be increased by at least four orders of magnitude, therefore.

The efficiency of the HHG process is highly nonlinear and depends strongly on the peak intensity inside the tight focus of the noble gas jet. A strong focus of the thesis was set on investigating current limitations and finding solutions further improving the intra-cavity and output performance of the driving TDL oscillator. The results of the studies are described in chapter 2 and include an investigation about performance benefits using higher round-trip gain by implementing a double-pass over the disk (section 2.2), the push towards the shortest pulse duration (section 2.3), as well as to the first >100 MW peak-power ultrafast TDL oscillator (section 2.4).

Chapter 3 summarizes the intra-oscillator HHG results using the developed ultrafast TDL oscillator. In a first step, the pulse formation mechanism was switched from semiconductor saturable absorber mirror (SESAM) to Kerr lens mode-locking (KLM), which is generally beneficial for the generation of shorter pulse durations. Furthermore, the gain medium was switched from Yb:Lu_2O_3 to the industrial-standard thin-disk material Yb:YAG. In this configuration, intra-oscillator HHG was driven with 365 MW peak-power in 105-fs pulses and 0.4 µW of XUV light was generated in a single harmonic at 30 eV in argon (section 3.1). A major challenge of intra-oscillator HHG is efficient out-coupling of the generated XUV light. Here, the generated XUV light needs to be separated from the co-propagating driving laser field without compromising the driving laser performance. To overcome this challenge, a coated grazing-incidence plate (GIP) has been developed and for the first time successfully implemented for efficient out-coupling of intra-cavity generated high harmonics (section 3.2). The intra-oscillator HHG source based on a coated GIP, featuring a broadband XUV reflectivity of >25% for photon energies ranging from 10 to 60 eV, generated an XUV flux of 4.3 µW in a single harmonic at 37 eV in argon and 18.0 µW at 25 eV in xenon. Another approach for efficient and towards higher photon energies spectrally not limited out-coupling of intra-cavity higher harmonics is the pierced mirror. Preliminary results of the first successful out-coupling of intra-oscillator generated high harmonics from a KLM TDL by a pierced mirror

are presented in section 3.3. Replacing the transmissive XUV out-couplers of previous intra-oscillator HHG systems by a pierced mirror has allowed reaching a significantly increased intra-cavity peak power of 1.2 GW. The increased peak power has enabled HHG in neon with photon energies up to 71 eV.

The last part, chapter 4, briefly summarizes the main results of the PhD thesis and provides an outlook about the up-coming challenges towards further improving the performance of single-stage MHz-HHG sources based on intra-oscillator HHG.

References

1. Labaye, F., Gaponenko, M., Wittwer, V. J., Diebold, A., Paradis, C., Modsching, N., Merceron, L., Emaury, F., Graumann, I. J., Phillips, C. R., Saraceno, C. J., Kränkel, C., Keller, U. & Südmeyer, T. Extreme ultraviolet light source at a megahertz repetition rate based on high-harmonic generation inside a mode-locked thin-disk laser oscillator. *Optics Letters* **42**, 5170 (2017).
2. Fischer, J., Drs, J., Labaye, F., Modsching, N., Müller, M., Wittwer, V. J. & Südmeyer, T. Efficient XUV-light out-coupling of intra-cavity high harmonics by a coated grazing-incidence plate. *Optics Express* **30**, 30969 (2022).
3. Klas, R., Kirsche, A., Gebhardt, M., Buldt, J., Stark, H., Hädrich, S., Rothhardt, J. & Limpert, J. Ultra-short-pulse high-average-power megahertz-repetition-rate coherent extreme-ultraviolet light source. *PhotoniX* **2**, 1 (2021).

2 High peak-power sub-100-fs thin-disk laser oscillators

Thin-disk laser (TDL) oscillators directly emit high peak-power, close to transform-limited soliton pulses with excellent beam profile. This makes them an attractive single-stage alternative to more complex amplifier systems for applications benefitting from megahertz repetition rates. A detailed introduction as well as an overview of the state-of-the-art of the TDL technology is provided by a submitted review article written during this thesis (section 2.1). The development of high-power TDL oscillators has always been a major focus of this research group and this thesis continues these efforts by pushing the boundaries of the technology further towards the shortest pulses (section 2.3) as well as towards highest peak powers (section 2.4).

An overview of output peak power against pulse duration for TDL oscillators is shown in Fig. 2.1. At the beginning of this thesis, the highest peak power achieved in the sub-100-fs regime was based on an Yb:Lu_2O_3 TDL oscillator and limited to 1.8 MW within 88-fs pulses [1]. Higher peak powers (62 to 88 MW) were achieved from Yb:YAG gain material, however, only at longer pulse durations (140 to 1070 fs) [2–4]. Initially, a strong focus was put on pushing the performance further using Yb:Lu_2O_3 disks as gain material. Yb:Lu_2O_3, which directly supports the generation of ∼90-fs pulses within its 13-nm FWHM gain bandwidth, features a broader gain bandwidth than industrial-standard Yb:YAG, supporting the generation of ∼140-fs pulses within its 8-nm FWHM gain bandwidth. Short pulse durations of several few tens of femtoseconds facilitate reaching highest peak-power pulses and are beneficial for suppressing detrimental plasma effects in HHG. As a first result achieved during this thesis, a 21 W average output-power, 4.1 MW output peak-power, and 95 fs pulse-duration Kerr lens mode-locked (KLM) TDL oscillator was demonstrated using Yb:Lu_2O_3 gain material with a double pass over the disk in 2019 (section 2.2). Further optimization approaches on the system led to damage of the Yb:Lu_2O_3 disks and commercially available disks based on Yb:YAG gain material were used thereafter. Against the expectation of previous literature [5], even shorter pulse durations compared to Yb:Lu_2O_3 at significantly higher peak powers could be demonstrated from Yb:YAG during this thesis. Such short pulses are enabled

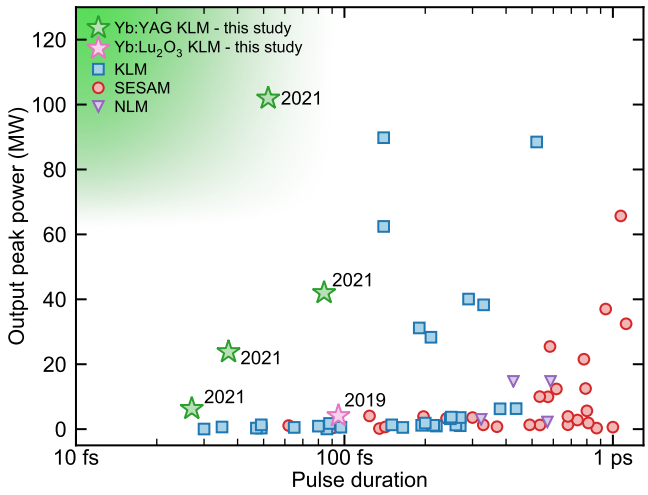

Figure 2.1: Overview of output peak power against pulse duration for different TDL oscillators. The favored direction of the development towards highest output peak power and shortest pulse duration is highlighted by the green shaded corner. Selected results are labeled by year of publication. The marker symbol emphasizes the employed mode-locking technique. KLM: Kerr lens mode-locking; SESAM: semiconductor saturable absorber mirror; NLM: non-linear mirror. The star markers show the results achieved during this thesis. The first result published in 2019 was based on a KLM Yb:Lu_2O_3 TDL oscillator (section 2.2). The following results published in 2021 were based on a KLM Yb:YAG TDL oscillator (section 2.3 and 2.4).

by operating a TDL oscillator in the regime of strong intra-cavity self-phase modulation. In a push towards shortest pulses, 27 fs were demonstrated from a KLM Yb:YAG TDL oscillator (section 2.3), presenting the shortest pulse duration so far achieved directly from the output of any TDL oscillator. The result even surpassed the shortest pulse duration of 30 fs achieved with significantly more broadband Yb:CALGO gain material, which directly supports the generation of sub-20-fs pulses within its 64-nm FWHM gain bandwidth [6]. Optimized towards highest output peak power, 102 MW within 52-fs pulses were achieved, representing the first >100 MW peak-power ultrafast laser oscillator (section 2.4). The KLM Yb:YAG TDL oscillator delivered an average power of 103 W and operated at 26% optical-to-optical efficiency, which is comparable to the optical-to-optical efficiency of TDL oscillators working within their available gain bandwidth. The short pulse duration, high peak-power pulses achieved with the KLM Yb:YAG TDL oscillator developed during this thesis show that Yb:YAG is currently still the best choice for the development of

powerful sub-100-fs TDL oscillators.

References

1. Paradis, C., Modsching, N., Wittwer, V. J., Deppe, B., Kränkel, C. & Südmeyer, T. Generation of 35-fs pulses from a Kerr lens mode-locked Yb:Lu_2O_3 thin-disk laser. *Optics Express* **25**, 14918 (2017).
2. Kanda, N., Eilanlou, A. A., Imahoko, T., Sumiyoshi, T., Nabekawa, Y., Kuwata-Gonokami, M. & Midorikawa, K. *High-Pulse-Energy Yb:YAG Thin Disk Mode-Locked Oscillator for Intra-Cavity High Harmonic Generation* in *Advanced Solid State Lasers Congress* (Optical Society of America, 2013), paper AF3A.
3. Saraceno, C. J., Emaury, F., Schriber, C., Hoffmann, M., Golling, M., Südmeyer, T. & Keller, U. Ultrafast thin-disk laser with 80 µJ pulse energy and 242 W of average power. *Optics Letters* **39**, 9 (2014).
4. Brons, J., Pervak, V., Bauer, D., Sutter, D., Pronin, O. & Krausz, F. Powerful 100-fs-scale Kerr-lens mode-locked thin-disk oscillator. *Optics Letters* **41**, 3567 (2016).
5. Südmeyer, T., Kränkel, C., Baer, C. R. E., Heckl, O. H., Saraceno, C. J., Golling, M., Peters, R., Petermann, K., Huber, G. & Keller, U. High-power ultrafast thin disk laser oscillators and their potential for sub-100-femtosecond pulse generation. *Applied Physics B* **97**, 281 (2009).
6. Modsching, N., Paradis, C., Labaye, F., Gaponenko, M., Graumann, I. J., Diebold, A., Emaury, F., Wittwer, V. J. & Südmeyer, T. Kerr lens mode-locked Yb:CALGO thin-disk laser. *Optics Letters* **43**, 879 (2018).

A decade of sub-100-fs thin-disk laser oscillators

Jakub Drs, Julian Fischer, Norbert Modsching, François Labaye, Michael Müller, Valentin J. Wittwer, Thomas Südmeyer*

Laboratoire Temps-Fréquence (LTF), Institut de Physique, Université de Neuchâtel, Avenue de Bellevaux 51, 2000 Neuchâtel, Switzerland
E-mail: jakub.drs@unine.ch

Keywords: thin-disk laser, Kerr-lens mode-locking, SESAM mode-locking, high harmonic generation

Abstract

Thin-disk lasers (TDL) are best known for their high-power continuous-wave industrial applications. Nonetheless, the thin-disk geometry is also highly attractive for ultrafast laser oscillators. The short propagation distance and large beam diameter inside the gain crystal allows for very low induced nonlinearity, low dispersion, and extreme peak powers inside the laser cavity. The path toward TDL oscillators directly delivering high average power at ultrafast pulse duration required for many scientific applications has, however, been tangled and is still ongoing. A decade ago, the first sub-100-fs laser oscillator was demonstrated, initiating the pursuit of even shorter pulses. Since then, many gain materials have been investigated in the thin-disk geometry as well as various mode-locking mechanisms for their suitability for efficient short-pulse operation. In this review, we will discuss the fast-evolving development trends of TDL oscillators, as well as their scientific applications, and prospects.

1. Introduction

The thin-disk laser (TDL) concept, first demonstrated in 1993 [1], has been designed and optimized for most efficient cooling of the laser gain material while maximizing the beam size inside the gain crystal. This endowed the TDL technology with a unique suitability for high-power applications. A single thin-disk gain crystal with a ~100-µm thickness can provide several kilowatts of average power [2] and withstand many gigawatts of peak power [3]. The small thickness of the disk directly contacted onto a very good heat sink, nowadays diamond in most systems, results in a very uniform single-dimensional heat flow inside the disk, minimizing the induced thermal lens [1]. In addition, the very short interaction length in the crystal keeps the dispersive and nonlinear response of the gain medium at a very low level, benefitting ultrafast operation.

The most common use of TDLs are high-power continuous-wave (CW) industrial lasers. Here, the thin-disk geometry allows to efficiently convert the high average power of low-brightness laser diodes into a high-brightness laser beam suitable for remote welding and cutting applications [4–6]. The vast use in industrial applications have led to the development of highly efficient multi-pass pumping solutions. Pumping TDL heads with up to 72-passes through the disk are nowadays commercially available, allowing for nearly 100% absorption of the pump power inside the gain crystal. Similarly, the production of high-quality industrial-grade Yb:YAG disks has been optimized to near perfection.

These developments later also benefitted pulsed operation of TDLs. Most notably, multi-pass and regenerative amplifiers have reached tremendous success, both industrially and scientifically. Up to 1.9 kW of average power in 1.3-ps pulses have been demonstrated from a multi-pass TDL amplifier [3] as well as 200 mJ in 1-ps pulses and 1 kW of average power out of a regenerative amplifier [7].

However, due to the narrow gain bandwidth of Yb:YAG disks, the pulse duration of these amplifier systems is typically limited to ~200 fs. Shorter pulses can be achieved by operating TDLs as high-power mode-locked laser oscillators. Thanks to the soliton mode-locking, TDL oscillators can reach significantly shorter pulse durations than Yb-based laser amplifier systems. In addition, ultrafast TDL oscillators typically emit nearly transform-limited soliton pulses with clean sech^2 spectrum in an excellent transverse-mode TEM_{00} Gaussian beam.

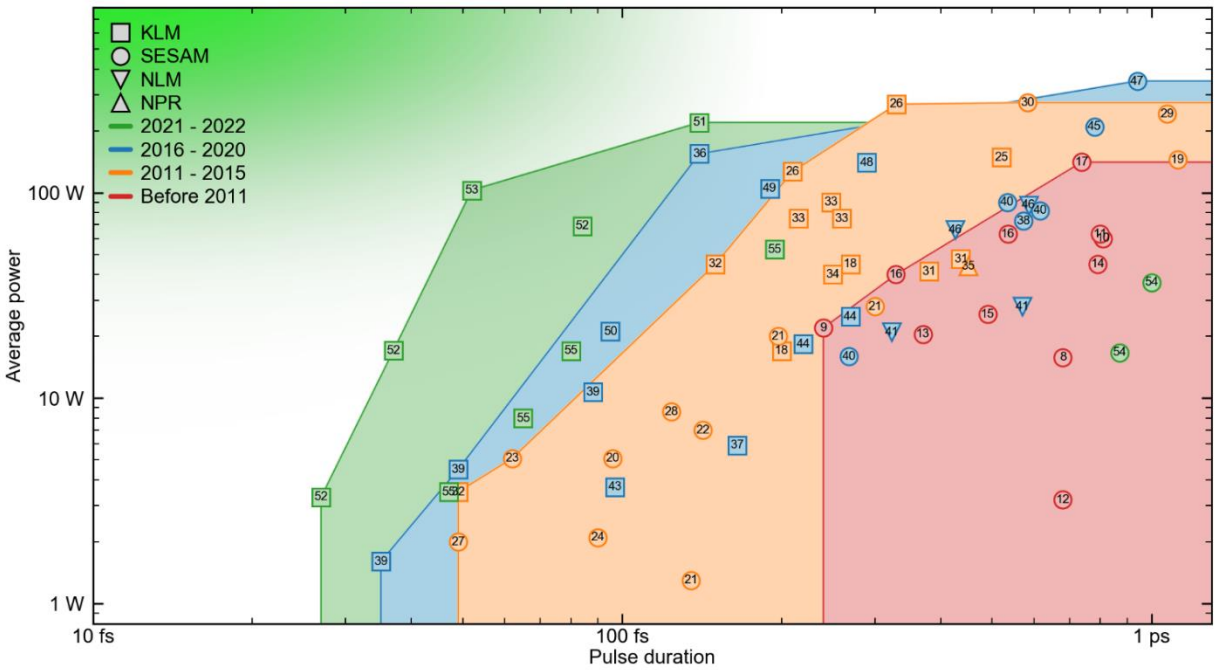

Figure 1. Overview of state-of-the-art TDL oscillators operating with > 1 W of average power and sub-picosecond pulse duration. The markers depict the mode-locking scheme: KLM – Kerr-lens mode-locking, SESAM – semiconductor saturable absorber mirror mode-locking, NLM – nonlinear mirror mode-locking, NPR – nonlinear polarization rotation mode-locking. The color scheme shows the historical evolution of the technology, categorizing the individual results into several time frames. A trade-off between average power and pulse duration can be observed within each time frame, which is moving over time toward the green-shaded corner indicating the desired parameter range. The numbers in the markers correspond to references [8–55].

Development of mode-locked TDL oscillators, thus, became an important research direction aiming for obtaining ultrafast pulses from Yb-doped gain materials at tens to hundreds of watts of average power and megahertz repetition rates. In Fig. 1, we show a historical overview of state-of-the-art TDL oscillators in terms of pulse duration and average output power. The color scheme together with the colored polygons categorize the results into several time frames revealing a trade-off between achievable pulse duration and average power within each time frame. During the first decade of development indicated in red, TDL oscillators strongly increased their average power starting from initial 16 W [8] up to 141 W [17] and reached pulse durations as short as 240 fs [9]. In 2012, the first sub-100-fs TDL oscillator was demonstrated [20] triggering the pursuit of even shorter pulses. Within the following decade the frontier of achievable performance shown by the colored polygons has been pushed strongly into the sub-100-fs domain. This transition was allowed by using broadband Yb-doped gain materials as well as by the transition from semiconductor saturable absorber mirror (SESAM) mode-locking to Kerr-lens mode-locking (KLM). Interestingly, a very large step in this direction has been made only since 2021 as could be seen from the green markers. The strive towards short pulse duration at high-power levels is still a highly active research direction and will most likely enable many research and industrial

breakthroughs. In this paper, we will discuss in detail this progress into the sub-100-fs domain and identify the current trends and prospects of the technology.

We will start with a discussion on the gain materials for ultrafast TDLs in section 2. Initially, it appeared mandatory to switch to more broadband gain materials than Yb:YAG in order to progress into the sub-100-fs regime [56]. Numerous materials were evaluated and optimized in the thin-disk geometry, which will be discussed. Over time it turned out that in high-power ultrafast TDLs the mode-locking method is more important than initially considered, which will be discussed in section 3. Surprisingly, it has been shown that efficient ultrafast operation can be also achieved with Yb:YAG in KLM TDL oscillators. In section 4, we will focus on nonlinear pulse compression, where the clean $sech^2$ optical spectrum and beam quality of TDL oscillators provides an ideal starting point for reaching few-cycle pulses. In section 5, we will review the methods of carrier-envelope-offset stabilization of these lasers, which is a necessary ingredient for frequency comb and attosecond science applications. Finally, these lasers have been successfully used for further nonlinear conversion toward longer wavelengths for field-resolved mid-infrared (MIR) [57] and terahertz [58–62] spectroscopy applications or toward shorter wavelengths through high harmonic generation (HHG) [63]. The high average power from the laser oscillator has been also harnessed by single-cavity dual-comb systems [64,65]. Another very important potential of TDL oscillators is driving nonlinear processes at extremely high intensities directly inside the laser cavity such as intra-oscillator HHG [66–68]. In section 6 we provide a quick overview on those application areas for sub-100-fs TDLs.

2. Gain materials

After the first demonstration of a mode-locked TDL oscillator in 2000 based on Yb:YAG and SESAM mode-locking [8], one development direction soon oriented toward shorter pulses. The evolution of the shortest achieved pulse duration with respect to mode-locking scheme and gain materials is depicted in Fig. 2. During the first decade of development, mode-locked TDL oscillators have been enabled by SESAM technology. The initial studies showed that decreasing the pulse duration of SESAM mode-locked Yb:YAG TDL oscillators is very difficult due to the narrow gain bandwidth of Yb:YAG. This can be also seen in the Fig. 2 from the green circle markers, which show that the pulse duration of these lasers has decreased only marginally since the first demonstration. The focus was therefore put on mode-locking studies using more broadband Yb-doped gain materials. Already in 2002, the pulse duration dropped from the initial 730 fs [8] down to 240 fs using an Yb:KYW disk [9].

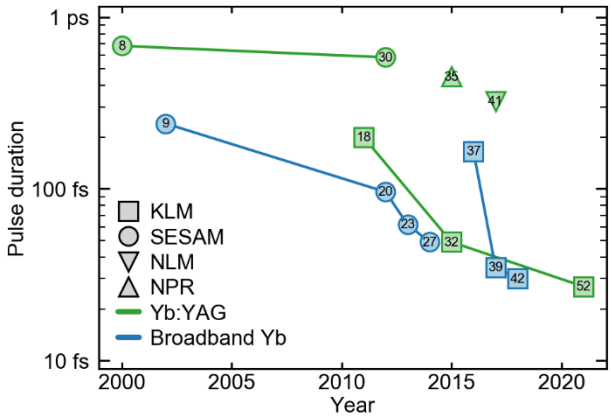

Figure 2. Historical evolution of the shortest pulse duration achieved by TDL oscillators. The markers depict the mode-locking scheme, while the color code differentiates between Yb:YAG and other more broadband Yb-doped host materials. SESAM mode-locked lasers have achieved short-pulse operation only with broadband gain materials, whereas KLM laser can reach the short pulses also with Yb:YAG.

The direction toward even shorter pulses was outlined in 2009 in a detailed review article highlighting the challenges and necessary steps for TDL oscillators operating in the sub-100-fs regime [56]. The first TDL oscillator which reached the 100-fs milestone was demonstrated three years later in 2012 using Yb:LuScO as gain medium and an optimized fast-recovery-time SESAM [20]. Many other gain materials have been utilized in the thin-disk geometry in order to allow for efficient short-pulse operation including Yb:KLuW [15], Yb:CALGO [21,23,24,27,42], Yb:LuO [13,16,17,22,39,40,50], Yb:ScO [28], and Yb:LuScO [20], as shown in Fig. 3. Another development direction of TDL oscillators leads toward operation at longer wavelength of 2 µm based on Ho:YAG [44,54]. The 2-µm TDLs have been recently reviewed in detail in [69] and will not be discussed further in the context of this review.

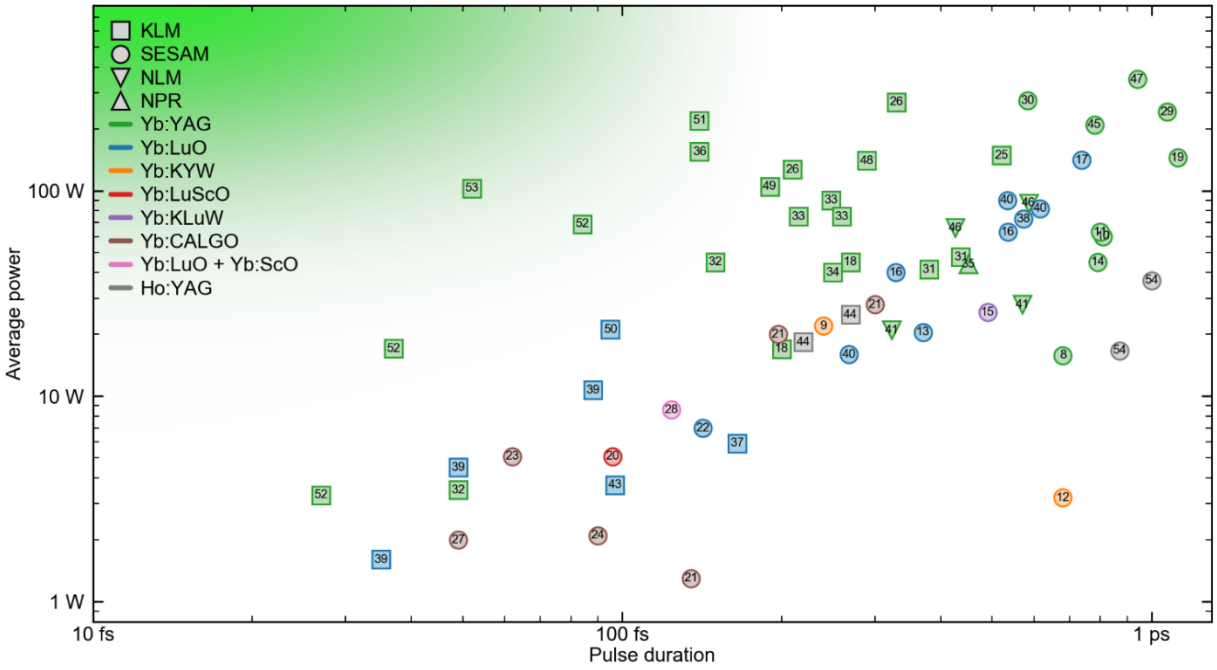

Figure 3. Overview of average power and pulse duration of TDL oscillators with respect to the gain materials used, depicted by the color scheme. The green-shaded corner shows the desired parameter range.

A great challenge for gain materials in the thin-disk geometry is not only the gain bandwidth but equally important the thermal properties, achievable doping concentration, and homogeneity. A high thermal conductivity is required for efficient heat removal and reduced thermal lensing. A high homogeneity in terms of thermo-mechanical and optical properties over the disk is a necessary ingredient for efficient operation in TEM_{00} mode.

Among all tested gain materials shown in Fig. 3, we will focus on the most abundant ones of Yb:YAG, Yb:LuO, and Yb:CALGO, which also form a good representative sample of the Yb-doped family in terms of performance trade-offs and technical challenges. The first and also by far the most used material in the thin-disk geometry has been Yb:YAG. It was selected as an industrial standard for high-power CW applications and optimized to a great degree for the thin-disk geometry in terms of crystal growth quality, doping concentration, thermal properties, and bonding procedure. It features a relatively narrow gain bandwidth of 8-nm full-width at half maximum (FWHM), shown in Fig. 4. The thermal conductivity amounts to 11 W m^{-1} K^{-1}, which however drops for high doping concentrations down to 7 W m^{-1} K^{-1} [70]. The crystal can be optically pumped at wavelengths around 940 nm or 969 nm.

Yb:LuO was introduced to the TDL family in 2001 as the most promising representative of Yb-doped sesquioxides and a potential successor of Yb:YAG for shorter pulse durations [71]. It features a broader gain bandwidth of ~13 nm (Fig. 4.) and slightly higher thermal conductivity of 12.8 W m^{-1} K^{-1} compared to Yb:YAG. Thanks to the very close weight ratio between lutetium and ytterbium, Yb:LuO allows for higher doping concentrations than Yb:YAG without compromising the thermal conductivity

of the gain crystal [70]. Initial studies characterizing Yb:LuO disks also showed unprecedented multimode slope efficiencies, exceeding 80% with > 70% of optical-to-optical efficiency in CW operation [70,72]. In mode-locked operation, also very promising initial results were demonstrated, reaching 141 W of average power in 738 fs pulses and 40% optical-to-optical efficiency [17].

These first results and the remarkable properties of Yb:LuO have motivated many further mode-locking studies with this material [13,16,17,22,39,40,50], as shown in Fig. 3. However, despite the theoretical advantage of Yb:LuO, up to nowadays, these lasers have not yet managed to outperform the ones based on Yb:YAG, as can be clearly seen in Fig. 3. This rather surprising outcome can be mostly attributed to the great difficulty of growing Yb:LuO crystals connected to its high melting point of ~2500°C [73]. This temperature exceeds the capabilities of the commonly used iridium crucibles. Rhenium is the only suitable material sustaining such temperatures and allowing for the use of the Czochralski growth method. Unfortunately, the production of rhenium crucibles is very costly and time consuming, since it involves galvanic deposition of the material. This technical difficulty has resulted in only few growth attempts of Yb:LuO crystals for thin disk laser applications, which have not yet allowed to reach a comparable level of optimization as for Yb:YAG.

A promising approach towards further development in this direction is based on compositions of Lu_2O_3 with other sesquioxides such as Sc_2O_3 and Y_2O_3, which have significantly lower melting temperatures. Recently, the first high-quality mixed sesquioxides crystal has been grown by conventional Czochralski method using an iridium crucible [74]. This approach might allow for a new generation of Yb-doped sesquioxide crystals with suitable properties for the thin-disk geometry in the near future [75].

Yb:CALGO is another notable gain material for TDLs. It offers a very broad gain bandwidth with > 60 nm FWHM (Fig. 4). In principle, such bandwidth should support ~20 fs pulse durations without requiring any further nonlinear spectral broadening effects. Its thermal conductivity of 6.3 W m^{-1} K^{-1} is lower than for Yb:YAG, but still sufficiently high for the use in TDLs. The first CW Yb:CALGO TDL oscillator was demonstrated in 2011 and showed a 40% slope efficiency with 32% optical-to-optical efficiency [76]. A SESAM mode-locked version followed already in 2012 [21]. The laser was operated in three configurations, delivering 28 W with 300 fs pulses, 20 W with 200 fs, and 1.3 W with 135 fs, respectively. Later studies showed even shorter pulse durations of 62 fs and 49 fs using SESAM mode-locking [23,27] and 30 fs using a KLM TDL oscillator [42]. All these short-pulse lasers, however, operated at rather low average powers for TDLs of < 6 W.

In contrast to the TDL results, Yb:CALGO lasers have proven to be very successful in the bulk geometry, where they even outperform their thin-disk counterparts. In CW operation, slope efficiencies of 73% with optical-to-optical efficiencies up to 65% have been demonstrated [77]. In mode-locked operation, up to 12.5 W has been obtained from a 94-fs laser oscillator with 20% optical-to-optical efficiency [78]. Shorter pulse durations of 22 and 31 fs at average powers of 0.7 W and 1.6 W have been shown using another Yb:CALGO bulk oscillator [79]. The bottleneck hindering the efficient operation of Yb:CALGO lasers in the thin-disk geometry seems to be again connected

to the crystal growth quality. So far, the distorted crystalline structure of Yb:CALGO has not provided sufficiently homogeneous gain over the disk surface [23,27,42], which prevents efficient operation in the fundamental TEM_{00} mode and limits the performance in mode-locked operation.

Up to nowadays, the production of high-quality thin disks comes at a great effort and has been difficult to achieve outside of an industrial environment. It can be also noticed, that several research groups have been recently returning back to Yb:YAG [47,49,53]. The commercial availability and the suitability for high average powers seem to outweigh the narrower gain bandwidth. Moreover, with the recent progress of Kerr-lens mode-locked TDL oscillators, it has been shown that the narrow gain bandwidth can be compensated by the self-phase modulation (SPM) inside the laser [32,39,52], as will be discussed in the next section. Recently, the shortest pulse durations achieved with Yb:LuO and Yb:CALGO TDL oscillators have been even surpassed by an Yb:YAG laser [52]. We, thus, expect that Yb:YAG will continue to dominate the realm of 1-µm TDL oscillators also in the next years.

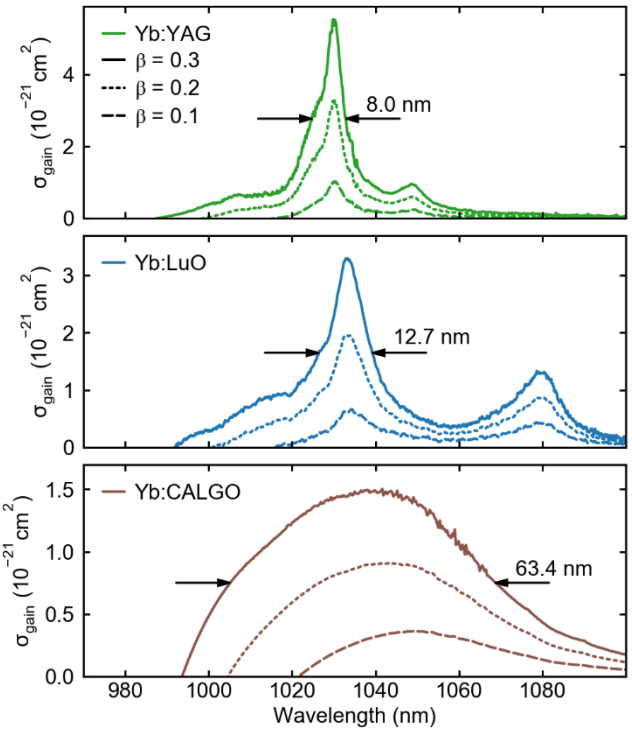

Figure 4. Gain cross-section of Yb:YAG, Yb:LuO and Yb:CALGO which are the three most commonly used gain materials in thin-disk lasers. The gain cross sections, σ_{gain}, are calculated from the emission and absorption cross sections as $\sigma_{gain} = \beta \cdot \sigma_{emission} - (1 - \beta) \cdot \sigma_{absorption}$, for the inversion levels of $\beta = 0.1$, 0.2, and 0.3. The underlying data was obtained from [56,77].

3. Mode-locking mechanisms

Nearly every ultrafast TDL oscillator operates in the soliton mode-locked regime yielding high-contrast soliton pulses without pre- or post-temporal features, typically at very good transverse beam quality with M^2 values < 1.1. TDLs are known to be power-scalable, meaning that the average power can be scaled by increasing the pumped surface of the disk and adapting the cavity to adjust the laser mode. This power-scaling principle is easily applicable in CW operation of these lasers, where the average power has been pushed toward the 10-kW levels. In mode-locked operation, the bottleneck is often the mode-locking mechanism itself, which needs to withstand the high peak and average powers, while providing sufficient self-amplitude modulation for soliton mode-locking. Various trade-offs are typically involved in the design of these lasers including the selection of the mode-locking mechanism in order to meet the desired parameters. The historical evolution of the highest average power with respect to pulse duration is shown in Fig. 5. It can be clearly identified that the technology has been constantly evolving and that both SESAM and KLM lasers have their important role in this evolution.

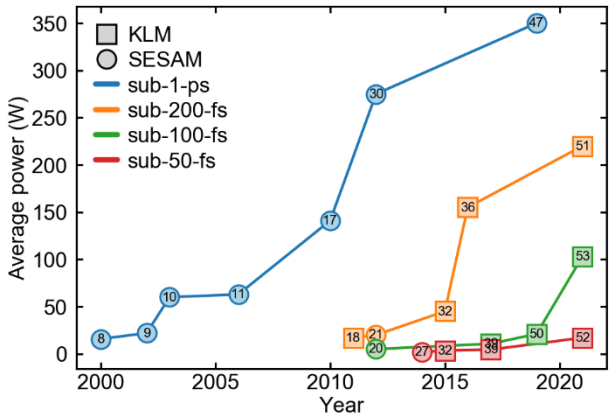

Figure 5. Historical evolution of the highest average power achieved by mode-locked TDL oscillators. SESAM mode-locked lasers depicted by circles dominate the long pulse duration category, whereas KLM lasers depicted by squares excel in shorter pulse durations.

3.1. SESAM mode-locking

SESAM mode-locked TDLs have opened up the possibility of obtaining tens to hundreds of watts directly from a laser oscillator, while also offering the favorable self-starting operation. Initial designs of SESAMs were originally inspired by saturable absorbers used for all-optical switches based on InGaAs/GaAs quantum wells grown on AlAs/GaAs dielectric Bragg reflector mirror [80,81]. But since the first demonstration, the technology has been constantly evolving and experiencing strong improvements [40,82–85].

There are various requirements for SESAMs operating inside high-power TDL oscillators. They need to provide sufficient modulation depth, typically around 1%, for stable mode-locking, while featuring fast recovery time for short-pulse operation. For reaching high average power and high pulse energies inside the oscillator, low non-saturable losses and high damage threshold as well as a reflectivity rollover shifted

towards highest fluences are essential. Since some residual losses always occur in the SESAM, efficient heat removal is also of high importance to prevent thermal lensing.

As these parameters have been improving, SESAM mode-locked TDLs have been continuously pushing the frontier of high-power laser oscillators, as can be seen in Fig. 5. The hundred-watt-level was reached in 2010 using Yb:LuO gain material [17]. In 2012, this level has been pushed to 275 W [30] and in 2019, 350 W was demonstrated using Yb:YAG [47].

On the other hand, decreasing the pulse duration of SESAM mode-locked TDLs has been much more challenging. Due to the moderate modulation depth of only few percent, SESAM mode-locked TDLs require broadband gain materials to reach short pulse durations. Further, the requirement of a short recovery time typically comes at a trade-off with other SESAM parameters required for high-power operation, such as damage threshold or rollover fluence [40,84]. Thus, in shorter pulse durations below 200 fs, SESAM mode-locked TDLs have not allowed for high average power, so far. Nevertheless, at lower powers below 10 W, shorter pulse duration has been achieved. For instance the first sub-100-fs TDL oscillator was based on SESAM mode-locking [20], and a pulse duration as short as 49 fs has been demonstrated using Yb:CALGO [27].

3.2. Nonlinear polarization rotation mode-locking

The concept of nonlinear polarization rotation (NPR), commonly utilized in fiber-based laser oscillators, has been demonstrated inside a TDL oscillator in 2015 [35].
Here, the nonlinear polarization rotation was induced by a phase-mismatched second harmonic generation in an LBO nonlinear crystal. The study used two nonlinear crystals at orthogonal orientation with 20-mm and 19-mm lengths, where the effective propagation length corresponds to the difference between both crystals. This allowed for a long interaction length inside the crystal for strong polarization rotation while maintaining broadband properties. The mode-locked laser emitted 44 W of average power with ~500 fs pulse duration. Although this more exotic mode-locking mechanism offers some theoretical advantages compared to the SESAM mode-locking, such as no absorptive losses and instantaneous response of the second order nonlinear process, the required propagation trough centimeter-long nonlinear crystals would likely prevent significant power-scaling or decrease of pulse duration.

3.3. Nonlinear mirror mode-locking

Another mode-locking scheme aiming to reduce the pulse duration of TDL oscillators is frequency-doubling nonlinear mirror mode-locking (NLM). In this scheme, the saturable losses are formed by an intracavity second harmonic nonlinear crystal followed by a spectrally tailored output coupler, having partial reflection for the fundamental wavelength but full reflection at the second harmonic wavelength. This way, the low intensity light passes through the nonlinear crystal without significant second harmonic conversion and experiences a partial transmission on the output coupler. In contrast, the high intensity light is partially transferred to the second harmonic which experiences complete reflection on the output coupler. On the way back through the nonlinear crystal, the second harmonic light is back-converted to the fundamental wavelength through optical parametric amplification.

The NLM concept has been first applied to a TDL oscillator in 2017 [41]. Compared to the bulk oscillators operating with NLM, the TDL oscillators are much more promising candidates for this technique. Thanks to the high peak intensities inside TDL cavities, it is possible to use much shorter nonlinear crystals and thus increase the mode-locking bandwidth and reach shorter pulse durations. The first NLM mode-locked TDL oscillator has reached 323 fs pulse duration at 21 W of average power using a 0.5-mm long BBO crystal. In a later study, the authors combined the NLM with SESAM mode-locking, reaching more than three times higher average power of 66 W with 426 fs pulses in a self-starting laser operation [46].

3.4. Kerr-lens mode-locking

The most commonly used approach for reaching shortest pulses is Kerr-lens mode-locking (KLM). Accidently discovered in 1990 [86] together with the novel Ti:sapphire gain material [87], KLM has revolutionized the ultrafast world. Conventionally, KLM lasers utilize the naturally occurring self-focusing inside the gain crystal, which leads to better pump overlap for high intensity light, so called soft-aperture mode-locking. The same effect can be used in combination with a physical hard aperture inside the laser, so called hard-aperture mode-locking. Here, the self-focused high-intensity light passes better through the aperture and experiences lower losses. The instantaneous effect of the Kerr lens together with high reachable modulation losses allow for the shortest pulse generation of all mode-locking mechanisms [88].

In TDLs, the large beam size inside the gain material usually does not provide sufficient self-focusing for KLM. For this purpose, an additional Kerr medium is placed close to an intra-cavity focus and a hard aperture is used for KLM. An often-emphasized drawback of KLM lasers is the coupling between the self-amplitude modulation required for the mode-locking and the cavity dynamics, leading toward changing beam size between CW and mode-locked operation. This also makes it difficult to quantitatively characterize the modulation losses inside the laser. The KLM mechanism cannot be easily taken out of the cavity and independently characterized as it is in the case for the SESAM, thus hindering theoretical studies. Another difficulty originates from the requirement of a laser perturbation to initiate the mode-locked operation, since KLM lasers are typically not self-starting. Typically, this is achieved via shaking or moving a cavity mirror. Nevertheless, the short achievable pulse duration and the simple implementation makes this approach very popular.

The first KLM TDL was demonstrated in 2011 [18] and reached a pulse duration of 200 fs at 17 W of average power using Yb:YAG gain material. This was by far the shortest pulse duration achieved by any Yb:YAG TDL oscillator, way below the 680 fs of SESAM mode-locked TDLs [8]. The next demonstration in 2016 has manifested the potential even clearer, showing a 155-W Yb:YAG TDL oscillator delivering 140-fs pulses [36]. The bandwidth of the demonstrated pulses has fully covered the available gain bandwidth of Yb:YAG, suggesting that the optimal operation point in terms of pulse duration for Yb:YAG has been reached.

Several attempts have been made to reach even shorter pulse durations using more broadband gain materials such as Yb:LuO or Yb:CALGO in the KLM TDL

configuration. These lasers have reached very short pulse durations of 35 fs [39], or 30 fs [42], however, at relatively low average powers of 1.5 W and 150 mW, respectively. KLM TDLs typically operate at higher cavity losses compared to SESAM mode-locked ones. This requires sufficient roundtrip gain to cover these losses while maintaining comparably high output coupling rate in order to operate efficiently. Unfortunately, the more broadband gain materials typically provide lower gain compared to Yb:YAG. The roundtrip cavity gain can be increased by implementing several bounces over the disk in order to allow for higher output coupling rates and reach more efficient operation. This has been shown by several studies [26,44,48,50]. However, implementing several passes over the disk also increases the sensitivity of the laser cavity to the thermal lens induced by the disk. So far, the highest power of broadband Yb-doped gain material TDLs in the sub-200-fs category has been limited to ~20 W, utilizing a double pass over an Yb:LuO disk [50].

The so far limited performance of the broadband gain material disks and the narrow gain bandwidth of Yb:YAG hindered power scaling in the sub-100-fs regime for a long time. In 2015, it was shown that by placing several additional Brewster plates inside the cavity, the pulse duration of a KLM Yb:YAG TDL oscillator can be significantly decreased down to 49 fs [32]. The corresponding 23-nm FWHM optical bandwidth by far exceeded the 8 nm gain bandwidth of Yb:YAG. A similar result was shown in 2017, reaching 35-fs pulses using an Yb:LuO disk, exceeding the gain bandwidth by a similar factor [39]. This operation beyond gain bandwidth was allowed by strong SPM inside the laser cavity, which generated the additional frequencies not covered by the gain material. Nevertheless, both these results showed only several watts of average power at a few percent optical-to-optical efficiency. Up to very recently, it was not believed that efficient operation is feasible with the pulse spectral bandwidth exceeding the gain bandwidth.

In spite of these assumptions, two recent studies have shown that the narrow gain bandwidth of Yb:YAG is not as a strongly limiting factor for reaching short pulse durations as originally expected. The first study investigated the limits of decreasing the pulse duration of a KLM Yb:YAG TDL oscillator operating in a strongly SPM-broadened regime [52]. It showed an overall better performance of Yb:YAG in the sub-100-fs regime compared to the more broadband Yb-doped hosts. The higher gain cross-section of Yb:YAG combined with the SPM-broadened regime has outperformed the broadband gain materials both in terms of average power, demonstrating 69 W at 84 fs, as well as in pulse duration, reaching the shortest pulses of any TDL oscillator with a duration of 27 fs at 3.3 W of average power. The second study utilizing the same laser system has pushed the frontier in the sub-100-fs regime even further by demonstrating 100 W of average power at 52 fs pulse duration [53]. Importantly, the latter result was achieved at an optical-to-optical efficiency of 26% which is comparable to the TDL oscillators operating within their gain bandwidth.

These experimental results seem to be enabled by using broadband dispersive mirrors and by operation at high intracavity peak power in the gigawatt range allowed by a vacuum environment. Both these technologies have been, however, long available in the domain and to fully explain this sudden gain in performance, a quantitative simulation will be needed. Nevertheless, these results suggest that further power scaling in the sub-100-fs regime is well within reach, even without development of any new

technology. For instance, a 220-W, 140-fs TDL oscillator operating at 24% efficiency has been recently demonstrated [51] and it seems reasonable to assume that the pulse duration of this laser could be also significantly reduced without compromising the efficiency.

3.5. Comparison of mode-locking schemes

Each of the individually discussed mode-locking schemes has its favored parameter range and different operating conditions. The SESAM mode-locked lasers have been pushing the highest achievable average powers, whereas KLM shines at short pulse durations. For the NPR and NLM, at the current state of development, the performance cannot yet compete with the well-established KLM and SESAM mode-locked TDLs.

One of the crucial parameters for TDL oscillators, as a high-power laser technology, is the optical-to-optical efficiency. Operation at high efficiency is crucial for decreasing the demand on high-power pump diodes while limiting the excessive parasitic heat, which typically causes further problems such as thermal lensing or misalignment. An overview of the achieved optical-to-optical efficiency with respect to pulse duration and average power is shown in Fig. 6. It can be seen that the highest efficiency of up to 40% [17] as well as highest average power has been achieved using SESAM mode-locked TDLs. This is due to the very low non-saturable losses in the range of a few per mil for SESAMs which allows for efficiencies close to the CW operation. The high efficiency together with the high average power of SESAM mode-locked lasers have allowed for significant pulse energies. Up to 80 µJ has been demonstrated at 3 MHz repetition rate and 1-ps pulse duration [29]. However, the long pulse duration puts SESAM mode-locked TDLs in competition with Yb-based laser amplifier systems, which easily outperform them both in terms of average power and pulse energy. Although much shorter pulses have been achieved using SESAM mode-locked TDLs, extending far into the sub-100-fs domain, we assume that several of these lasers could have been SESAM-assisted soft-aperture KLM due to the presence of a Brewster plate for polarization selection and additional SPM, similarly as implemented in [18].

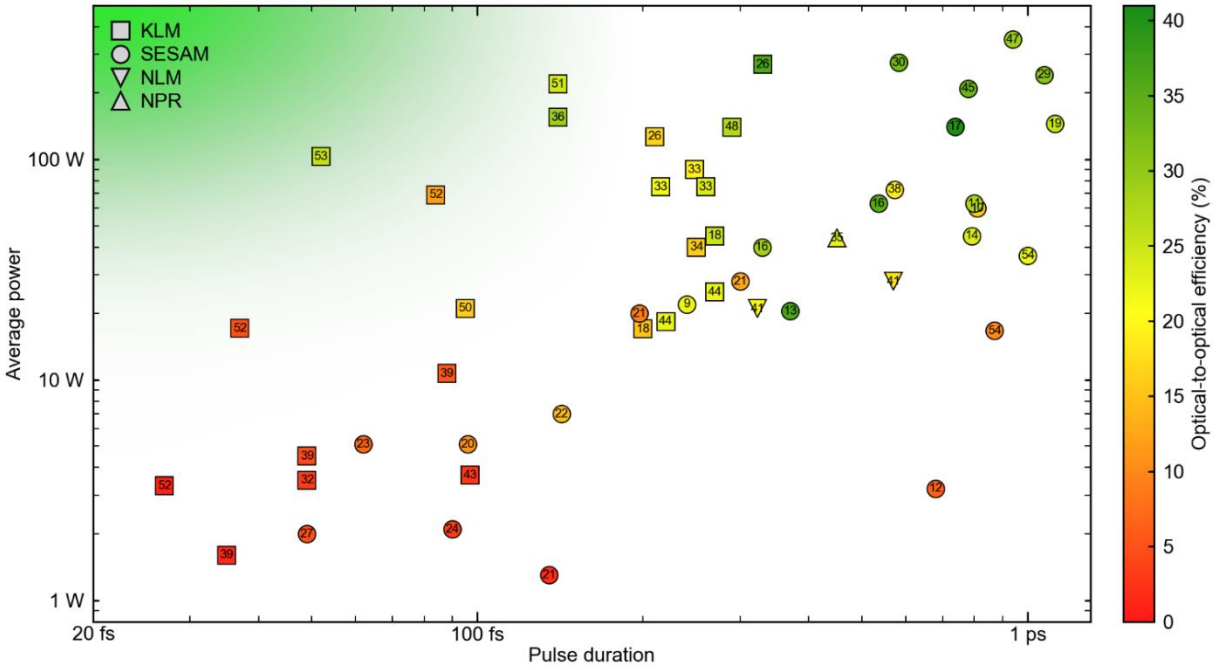

Figure 6. Overview of the optical-to-optical efficiency depicted by color with respect to average power and pulse duration. The highest optical-to-optical efficiencies of ~40% have been typically achieved by SESAM mode-locked lasers at > 500 fs pulse durations. At shorter pulse durations KLM lasers typically offer higher efficiencies than SESAM mode-locked lasers.

In contrast, KLM TDLs typically operate at lower optical-to-optical efficiencies but much shorter pulse durations, which distinguishes them from amplifier systems. As can be seen in Fig. 5, KLM TDLs have completely taken over the sub-100-fs domain since the last decade. The optical-to-optical efficiency of these lasers have been typically ranging between 10% to 30% at > 100 fs pulse durations but dropped significantly in the sub-100-fs domain as shown in Fig. 6. Recently, this limitation has been overcome by the demonstration of a SPM-broadened KLM TDL oscillator delivering 52-fs pulse duration with 26% optical-to-optical efficiency [53]. Thus, it is likely that more efficient TDL oscillators will soon operate in the sub-50-fs domain, which will also allow to increase their average power in this regime.

4. Peak power scaling and pulse compression

One of the most important parameters for many applications is the peak power of the driving laser, which rules the efficiency of many nonlinear processes. TDL oscillators are very interesting for scaling the peak power since the thin-disk gain medium does not pose a strong limitation in this sense. Several studies have investigated scaling of this parameter in TDL oscillators. In SESAM mode-locked lasers, the peak power is mainly determined by the design of the SESAM, mostly through the reflectivity rollover induced by two-photon absorption and by the gain bandwidth of the gain crystal [40]. In KLM TDL oscillators, the intra-cavity peak power has been shown to scale with the beam size inside the Kerr medium [26].

Toward high intra-cavity peak powers, a further challenge arises from the nonlinear response of the air inside the cavity. Several approaches have been proposed to mitigate this issue. The laser can be operated in a low-nonlinearity atmosphere such as helium [11] or the SPM can be canceled using a phase-mismatched second-harmonic crystal [45]. The most frequently employed method is, however, based on operating the laser in a vacuum environment [29–31,36,40,47,52], which also prevents the gas thermal lens induced by the multi-pass pumping scheme [89].

Figure 7 depicts the historical evolution of the highest peak power reached by TDL oscillators. Whereas SESAM mode-locked lasers had been continuously increasing their peak power up to 66 MW demonstrated in 2014 [29], KLM lasers have very rapidly surpassed this value in 2013 [25], three years after their first demonstration, and nowadays reach values of 100 MW [51,53]. It can be also noticed that most of the recent high-peak-power systems are operated in vacuum as indicated by the bell jar symbol around the markers, shown in Fig. 7.

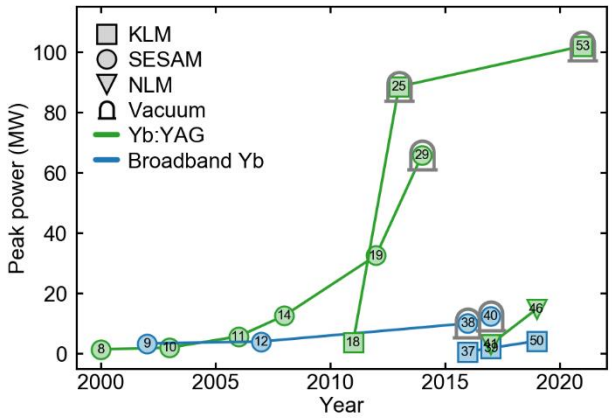

Figure 7. Historical evolution of the highest peak power achieved by TDL oscillators based on different mode-locking mechanisms. The bell jar symbol indicates systems operated in vacuum.

Further increase of the peak power can be achieved by nonlinear pulse compression that relies on SPM to induce spectral broadening. Driving this process in an anomaly dispersive medium can lead to self-compression of the pulse, whereas subsequent chirp removal is required for compression in normal-dispersive media. Both approaches have been pursued in numerous studies that are summarized in Fig. 8. The first compression experiments were based on micro-structured large-mode-area fibers [90,91] and reached ~30 fs pulse duration and 10-MW-level peak power. These were followed by very-large-mode-area rod-type gain fibers [92] generating 50-MW-level peak power and then by gas-filled hollow-core photonic crystal fibers [63,93] surpassing 100 MW peak power levering the scalability of the compression schemes. All experiments showed that the nearly transform-limited soliton pulses and the excellent beam quality of the TDL oscillators allow for high-quality pulse compression. Unfortunately, the average power generally remains limited to several tens of Watts for practical application due to the damage vulnerability of the fiber tips.
More recently, multi-pass cells were employed for nonlinear compression, both in the normal [94] and the net-anomalous dispersive regime [95]. Their high overall

transmission and their robustness against beam pointing instabilities allows for reliable operation at average powers well above the 100 W. The highest demonstrated peak power is close to 170 MW [96] in approximately 30 fs pulses. Compression into the few-cycle regime (≤10 fs at 1 µm) has been demonstrated as well using single- or multi-plate compressors to avoid the need for broadband, dispersion-engineered multi-pass cell mirrors [34,97].

Overall, nonlinearly compressed TDL oscillators generate peak power on the 100 MW-level, which already suffices for many nonlinear applications. Only for the efficient generation of high harmonics the peak power is still about an order of magnitude too low. In the future, this can change with the availability of oscillators directly emitting 100 MW peak power [51,53] combined with nonlinear compression in gas-based multi-pass cells, which support both few-cycle pulses and high average power [98,99].This allows envisioning GW-class sources suitable for high-harmonic generation in near future.

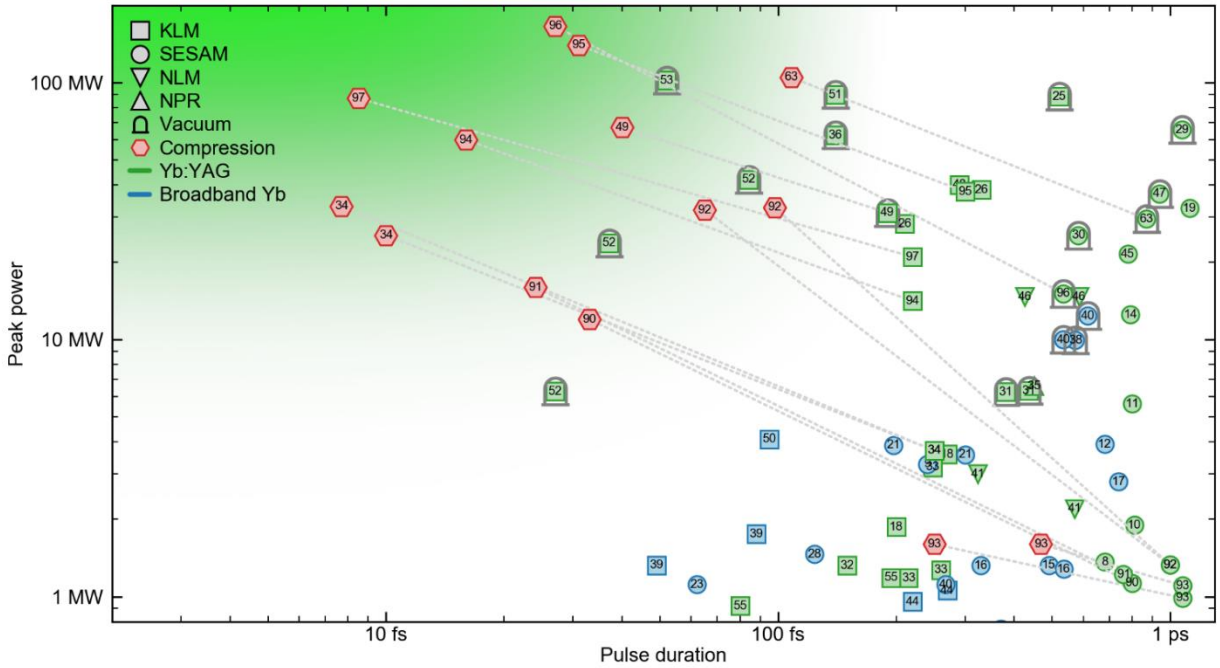

Figure 8. Overview of peak power and pulse duration of state-of-the-art TDL oscillators operating at sub-picosecond pulse duration. The red hexagon markers depict the parameters after nonlinear pulse compression [34,49,63,90–97]. The bell jar symbols indicate systems operated in vacuum. For references [34,97], the peak power was calculated based on the compression ratio, power efficiency and compression efficiency stated in the manuscripts, which is likely an overoptimistic estimate.

5. CEO frequency stabilization

An attractive application field of ultrafast oscillators is precision spectroscopy based on optical frequency combs. Here, the high average power and short pulse duration of TDL oscillators are especially attractive for efficient nonlinear conversion toward mid-infrared or extreme-ultraviolet frequencies, where directly emitting laser sources are not readily available. The key requirement for optical frequency-comb applications is the carrier-envelope offset frequency (f_{CEO}) stability of the source.

The most common way to access the f_{CEO} is using *f*-to-2*f* interferometry after coherent super-continuum generation [100]. Here, the low-frequency part of an octave-spanning optical spectrum is frequency doubled and interfered with the high-frequency part of the fundamental spectrum. The resulting optical beat note provides access to measuring the f_{CEO}. The f_{CEO} is affected by many parameters of the laser such as nonlinearity and dispersion providing wide range of options for an active stabilization. The most common method is modulation of the pump current. However, this method has a limitation for Yb-based lasers given by the long upper-state lifetime of the Yb-ion in the millisecond range. Correspondingly, the response of the f_{CEO} to a pump current modulation is limited to a few kilohertz range in bandwidth. An additional challenge of TDL oscillators compared to bulk lasers is the high amount of acoustical noise introduced by turbulent water cooling of the thin disk [34,65]. The high noise level increases the demand on the bandwidth of the control loop in order to cancel the noise. Many different modulation schemes have been investigated in order to stabilize the f_{CEO} of TDL oscillators which will be discussed in more detail in the following.

5.1. Pump current modulation

Regardless of the bandwidth limitation of the pump current modulation in Yb-based lasers, several studies have utilized this technique for f_{CEO} stabilization in TDL oscillators. The first f_{CEO}-stable TDL oscillator was demonstrated in 2013 [24]. The laser was a SESAM mode-locked Yb:CALGO TDL delivering 2 W of average power in 90-fs pulses. The octave-spanning supercontinuum spectrum was obtained by optical broadening in a highly nonlinear photonic-crystal fiber and the f_{CEO} was detected using a conventional *f*-to-2*f* interferometer. The f_{CEO} lock was implemented using the pump current modulation and resulted in a residual in-loop integrated phase noise of 120 mrad (1 Hz – 1 MHz).

Another challenge for the f_{CEO} stabilization over the pump current is the difficulty to modulate a high-power pump diode which generally involves custom-made electronics. An approach circumventing this issue was demonstrated in 2016, introducing dual wavelength pumping of a KLM Yb:YAG TDL [101]. This concept uses a high-power 940-nm pump diode for pumping the laser combined with a low-power 969-nm diode for fast f_{CEO} modulation. The difference in wavelength allows for applying a simple dichroic mirror to combine both pump beams. The octave-spanning supercontinuum spectrum was obtained by first compressing the 250-fs pulses down to 20-25 fs pulses in a large mode area fiber followed by multiple bounces on chirped mirrors and then further optical broadening in an all-normal-dispersion fiber and the f_{CEO} was detected using a conventional *f*-to-2*f* interferometer. The achieved residual in-loop integrated phase noise amounted to 390 mrad (1 Hz – 500 kHz) at 250 fs pulse duration and 45 W of average power.

A third demonstration of f_{CEO} stabilization modulating the pump current has been demonstrated for a KLM Yb:LuO TDL oscillator operating in a strongly SPM-broadened regime [102]. The laser generated 50-fs pulses at 4.4 W of average power and the f_{CEO} current-based lock resulted in a residual in-loop integrated phase noise of 197 mrad (1 Hz – 1 MHz). Also, in this result, the short pulse duration allowed to directly generate the coherent octave-spanning supercontinuum spectrum in a highly

nonlinear photonic-crystal fiber to detect the f_{CEO} using a conventional f-to-2f interferometer.

5.2. Intracavity AOM

A different approach to act on the f_{CEO} is based on modulating the intracavity losses. This can be achieved by placing an acousto-optic modulator (AOM) directly inside the cavity of the laser, as first demonstrated in 2015 [34]. This remarkable study utilized a nonlinearly compressed KLM TDL oscillator reaching a pulse duration of 7.7 fs at 6 W of average power. The AOM inside the cavity was capable of inducing up to 2% of losses, withstanding the average intracavity power of 280 W. The resulting residual in-loop integrated phase noise amounted to 180 mrad (1 Hz – 1 MHz). The out-of-loop measurement was also implemented in this work, revealing a value of 270 mrad, showing the importance of the out-of-loop measurement. The concept has been further scaled toward 100-W level in 2019, demonstrating 40-fs nonlinearly-compressed pulses at 105 W of average power and residual in-loop integrated phase noise of 90 mrad [49].

5.3. Depletion control

The most recently published method of f_{CEO} stabilization of a TDL oscillator is based on controlling the depletion of the gain through bouncing part of the laser output beam back over the disk [103]. The fraction of the laser output was controlled by an AOM and bounced 4 times over the disk depleting part of the available gain for the laser. This method is similar in its principle to pump current modulation and a similar control bandwidth can be expected. In this first study, the high free-running noise of the laser oscillator only allowed for a comparably poor stabilization with a residual integrated phase noise amounting to 1.5 rad (100 Hz to 500 kHz).

6. Applications

Over the last decade TDL oscillators have not only gained significant performance, but also reached sufficiently mature state of development to become driving sources for further experiments and applications.

6.1. High harmonic generation

One of the first applications of TDL oscillators clearly manifesting the importance of high repetition rate and short pulse duration was nonlinear conversion toward extreme ultraviolet (XUV) through high harmonic generation (HHG) in a noble gas target. Many applications such as photoelectron spectroscopy or XUV diffractive imaging have been relying on coherent XUV radiation delivered by large scale synchrotron facilities. HHG in a noble gas target is a lab-scale alternative which is constantly growing in popularity and finding more and more applications [104]. Historically, the biggest challenge of HHG systems has been the low conversion efficiency from the driving laser to the XUV light. The efficiency strongly increases with the peak power of the driving laser, while also benefiting from short pulse durations. Thus, HHG systems have been often driven by kilohertz-repetition-rate Ti:sapphire laser amplifiers. Unfortunately, some experiments such as photoelectron spectroscopy suffer from space-charge effects, meaning that when multiple photoelectrons are ejected by an XUV pulse from the sample, their trajectories are affected by their mutual coulomb interaction which limits the measurement resolution. In this case, lower-energy pulses emitting only a few

electrons at higher repetition rates are favored in order to maximize the resolution while allowing for short acquisition times. Regardless of space charge effects, the higher repetition rate is often useful for increasing the photon flux of these systems, benefiting most of the XUV applications. Compared to systems based on Ti:sapphire, Yb-based lasers are able to reach considerably higher average powers due to their lower quantum defect and well-developed high-power pump diodes. Hence, Yb-based lasers are much better suited for reaching the HHG required pulse energies at high repetition rates, enabling the transition from kilohertz- to megahertz-repetition rate HHG systems.

The first TDL driven HHG source was presented in 2015, based on a 70-W, 780-fs SESAM mode-locked oscillator operating at 2.4 MHz [63]. The laser output was nonlinearly compressed in a krypton filled HC-PCF fiber to 105 fs at 105 MW of peak power. HHG was obtained from a xenon gas target and reached photon energies up to 30 eV with an extracted XUV flux in a single harmonic of 0.18 nW. These were, however, rather modest values which have been surpassed by orders of magnitude by high-power Yb-based laser amplifier systems [105].

In the recent years, a new avenue for TDL oscillators has been opening up in the XUV realm. With the increasing capabilities of nonlinear pulse compression combined with the decreasing pulse duration of high average power KLM oscillators, there is a potential that these sources will reach single-cycle pulse duration in the near future. This would allow for generation of isolated attosecond pulses at megahertz repetition rates. Such a megahertz-rate isolated attosecond pulse source would highly benefit many applications in the attosecond domain, in particular attosecond streaking experiments [106]. Recently several major steps have been made in this direction. The demonstration of CEO stabilization of a 100-W class TDL oscillator [49] followed by another 100-MW class oscillator directly emitting 50-fs pulses [53] is highly promising. Especially, in combination with the advances in multi-pass cell bulk compression schemes, which have been routinely reaching sub-30-fs pulses at these power levels [94,96] and most recently even 8.5 fs [97]. Combining these recent results will likely provide a CEO-stable single-cycle 100-W-class laser source capable of generating isolated attosecond pulses at megahertz repetition rates.

6.2. Intra-oscillator high harmonic generation

A high potential of TDL oscillators is driving extreme nonlinear processes such as HHG directly inside the laser cavity since this enables the utilization of the very high intra-cavity peak powers. This concept is similar in its principle to femtosecond enhancement cavities [104,107]. In both concepts, the unconverted energy of the driving laser pulse is recycled inside the cavity, while increasing the available peak power by the enhancement factor of the cavity. In comparison to femtosecond enhancement cavities, the laser oscillator is a free-running system which does not require active phase lock and coherent coupling of fs-pulses into the enhancement cavity, thus, further simplifying the concept.

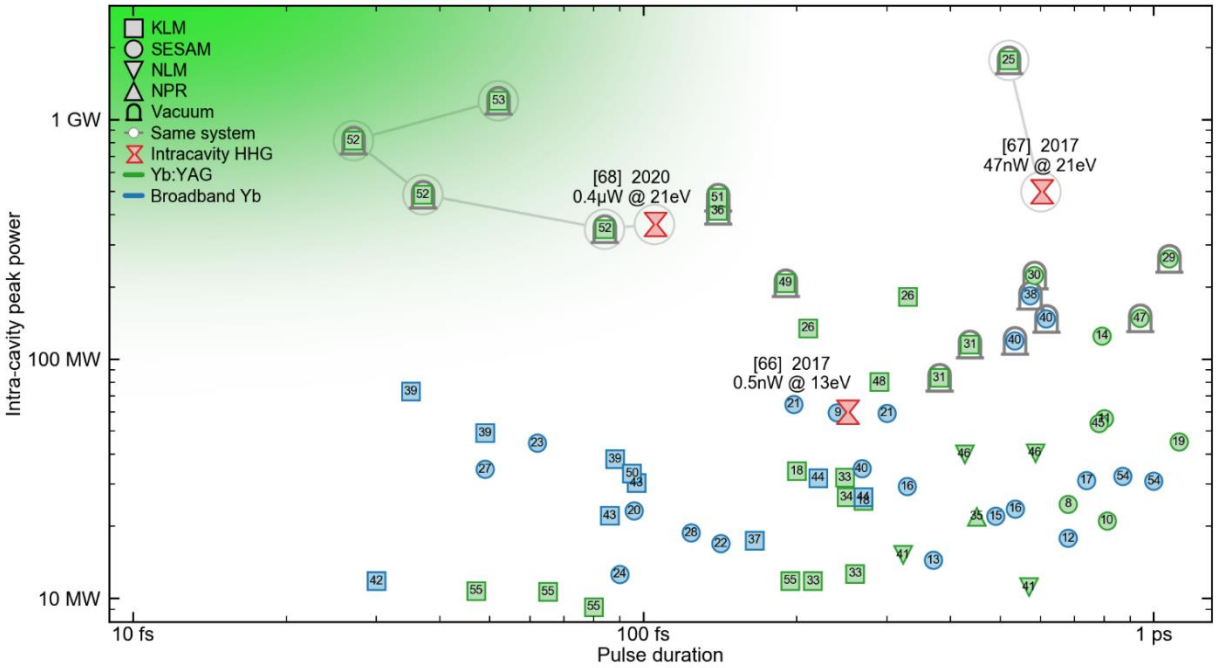

Figure 9. Overview of intracavity peak power with respect to pulse duration of state-of-the-art TDL oscillators operating at sub-picosecond pulse duration. The red hourglass symbols depict intra-oscillator HHG systems [66–68], labeled with the year and the generated XUV flux within the highest harmonic and its photon energy. The bell jar symbols indicate systems operated in vacuum. The gray connecting line indicates laser results, which were obtained with the systems developed for driving intra-oscillator HHG, showing that development of these systems has been also driving the progress in the TDL oscillator technology.

The high peak power and short pulse duration required for efficient HHG [108] makes TDL oscillators ideal candidates for this task. An overview of the intra-cavity peak power with respect to the pulse duration of TDL oscillators including intra-oscillator HHG systems (red hourglass markers) is shown in Fig. 9. The first HHG inside a TDL oscillator was demonstrated in 2017 [66]. The SESAM mode-locked Yb:LuO TDL operated at 320 W of average intra-cavity power, 255 fs pulse duration, and 17.4 MHz repetition rate, corresponding to 64 MW of intra-cavity peak power. The XUV average power generated in xenon was very modest in this first demonstration and amounted to only 0.5 nW in a single harmonic at 13 eV. This first demonstration was closely followed in the same year by a different system based on a KLM Yb:YAG TDL oscillator operating at 500 MW of intra-cavity peak power and 600 fs pulse duration at 3 MHz repetition rate [67]. The intra-oscillator HHG yielded an XUV flux of 47 nW at 21 eV generated in argon. The next intra-oscillator HHG system was published in 2021 [68]. The KLM TDL used Yb:YAG gain material and operated at 365 MW with 105 fs pulse duration at 11 MHz. HHG was driven in argon and the generated XUV photon flux at 30 eV amounted to 0.4 µW. This value has been recently increased to 10 µW by further optimization of the laser system [109].

The connecting line in Fig. 9 indicates the results obtained with the same laser systems developed for intra-oscillator HHG. It can be noticed that even much higher performance has been achieved by these lasers when not driving HHG. This can be attributed to the plasma effects inside the HHG gas target which typically limit the laser performance [68]. Without HHG, intra-cavity peak powers as high as 1.7 GW at 600 fs pulse duration [25] as well as 1.2 GW at 52 fs [53] have been shown, also at substantial output power of 150 W and 100 W, respectively, pushing the frontier of the whole TDL oscillator domain.

6.3. THz generation

The properties of mode-locked TDL oscillators also benefit frequency conversion toward long wavelength in the THz range. This potential has been recognized and discussed in detail in a review article in 2018 [110]. Analogically to HHG, THz generation typically suffer from low conversion efficiency ranging from 10^{-5} up to a few percent. Therefore, increasing the THz power available for the experiment also requires an increase in the driving laser power. In addition to the high average power, the short pulse duration of TDL oscillators provides a broad optical spectrum in the THz domain relevant for broadband spectroscopy applications.

Optical rectification in nonlinear crystals is particularly suitable for this purpose since it supports the high average powers delivered by TDLs. The first THz generation driven by a mode-locked TDL was published in 2018 [58]. The original demonstration used one of the simplest approaches of optical rectification in GaP in a collinear geometry. The generated THz radiation featured a broad spectrum extending up to 7 THz with an average power around 10 µW. The same concept has been power-scaled to 300 µW in 2019 [59] and to 1.3 mW later the same year [60]. In a narrowband regime, average terahertz power has been increased even further. Up to 66 mW was generated in lithium niobate driven by a TDL oscillator [61].

6.4. Dual-comb oscillators

Dual-comb spectroscopy is an extremely powerful tool for applications simultaneously requiring fast acquisition time and high spectral resolution [111]. Conventionally, the technology requires two optical frequency combs with slightly different line spacing, such as two fully stabilized mode-locked lasers operating at slightly different repetition rates. The spectroscopic information is obtained through heterodyne beating between the two combs.

A simplified alternative to fully-stabilized lasers is based on generating the two optical frequency combs from the same laser cavity in a free-running operation. Here, the noise of the unstabilized f_{CEO} and repetition rate of the two pulse trains is highly correlated and the common part of the noise cancels out in the beating process. This allows for short-term measurements within a time frame where the two pulse trains remain mutually stable, without the requirement for active stabilization. TDL oscillators are promising sources for this purpose since their high peak power allows for efficient nonlinear conversion toward MIR or UV wavelengths, which are of high interest for many spectroscopy applications [111,112].

The first steps on this path were made in 2019 [64] by the demonstration of the highest average power dual-comb laser based on a KLM TDL oscillator. The dual-comb cavity was based on splitting both end mirrors while the rest of the cavity components remained shared. The second demonstration of this concept came in 2020 based on polarization splitting [65]. The study showed that the stability of the free-running KLM TDL oscillator is sufficient for performing dual-comb spectroscopy within a 1-ms window in a proof-of-principle experiment measuring the absorption spectrum of acetylene gas. The acquisition time was limited by the uncorrelated noise in the laser mostly originating from water cooling of the disk. Longer acquisition times would likely require the development of a passive cooling of the thin disk. The suitability for high resolution measurements after nonlinear frequency conversion still needs to be demonstrated.

6.5. Field resolved spectroscopy

An advanced application utilizing a TDL oscillator as a driving source building upon the recent advances in this technology is a field-resolved MIR spectroscopy [57], published in 2020. The study uses a nonlinearly compressed TDL oscillator delivering 16 fs pulses at 60 W of average and 28 MHz repetition rate for driving intra-pulse difference frequency generation (DFG) toward MIR. The few-cycle pulse duration of the laser enables detection of the MIR light through electro-optic sampling (EOS) in the time domain, providing information directly about the electric field rather than its intensity. The measurement in the time domain allows for starting the acquisition after the passage of the MIR excitation pulse and sampling only the response of the sample. This endows the field-resolved spectroscopy with unique sensitivity and resolution and also broad tunability in the MIR range. The technology was shown to be highly suitable for fingerprinting of complex molecular ensembles such as human blood serum or in vivo transmission spectroscopy of intact strongly absorptive biological samples such as living cell cultures or even plant leaves. The unprecedented sensitivity and repeatability of the presented experiments proves the suitability of the TDL oscillators for driving demanding applications requiring short pulse durations high average powers and also stable long-term operation.

7. Conclusion

We have reviewed the recent development of ultrafast TDL oscillators. Over the last decade, we have observed a strong push toward short pulse duration. A lot of effort was focused on the development of broadband gain materials suitable for the thin-disk geometry. However, against expectations, the industrial standard of Yb:YAG has still remained the most successful candidate even for very short sub-100-fs pulses. It will be very interesting to see if this trend will continue in future or if Yb:YAG will be replaced by another candidate, since the development of broadband gain materials is still ongoing. Concerning power-scaling of TDL oscillators, a significant progress has been recently made by systems operated in vacuum. It will be equally interesting to see if these systems will be replaced by simpler approaches such as those based on helium atmosphere. Hand in hand with the improving performance of TDL oscillators came the development of nonlinear pulse compression techniques suitable for the high average powers and low pulse energies of these lasers. Nowadays few-cycle pulses are already routinely available from nonlinearly compressed TDL oscillators. With the fast development of both technologies, we will likely observe these sources entering the

single-cycle regime in the near future. In combination with CEO-frequency stabilization, this will likely allow TDL oscillators becoming reliable waveform-stable single-cycle sources with GW-level peak powers and megahertz repetition rates. Such sources will benefit many scientific applications particularly in the attosecond domain. Another important potential of ultrafast TDLs is driving extreme nonlinear processes such as HHG directly inside the laser oscillator, offering a way toward compact coherent XUV sources based on the commercially available and well-developed TDL technology.

Acknowledgements
Schweizerischer Nationalfonds zur Förderung der Wissenschaftlichen Forschung (200020_179146, 200020_200774, 206021_144970, 206021_170772, 206021_198176). H2020 European Research Council (ERC) "Efficient megahertz XUV light source" (279545), Starting Grant 2011.

References

[1] A. Giesen, H. Hügel, A. Voss, K. Wittig, U. Brauch, H. Opower, *Appl Phys B* **1994**, *58*, 365–372.
[2] S. Nagel, B. Metzger, D. Bauer, J. Dominik, T. Gottwald, V. Kuhn, A. Killi, T. Dekorsy, S.-S. Schad, *Opt. Lett.* **2021**, *46*, 965–968.
[3] T. Dietz, M. Jenne, D. Bauer, M. Scharun, D. Sutter, A. Killi, *Opt. Express* **2020**, *28*, 11415–11423.
[4] D. Petring, F. Schneider, N. Wolf, V. Nazery, in *Int. Congr. Appl. Lasers Electro-Opt.*, Laser Institute of America, Temecula, California, USA, **2008**, p. 206.
[5] K. Löffler, in *Handb. Laser Weld. Technol.*, (Eds: S. Katayama), Woodhead Publishing, **2013**, pp. 73–102.
[6] S.-S. Schad, C. Stolzenburg, K. Michel, D. Sutter, *Laser Tech. J.* **2014**, *11*, 49–53.
[7] T. Nubbemeyer, M. Kaumanns, M. Ueffing, M. Gorjan, A. Alismail, H. Fattahi, J. Brons, O. Pronin, H. G. Barros, Z. Major, T. Metzger, D. Sutter, F. Krausz, *Opt. Lett.* **2017**, *42*, 1381–1384.
[8] J. Aus der Au, G. J. Spühler, T. Südmeyer, R. Paschotta, R. Hövel, M. Moser, S. Erhard, M. Karszewski, A. Giesen, U. Keller, *Opt. Lett.* **2000**, *25*, 859–861.
[9] F. Brunner, T. Südmeyer, E. Innerhofer, F. Morier-Genoud, R. Paschotta, V. E. Kisel, V. G. Shcherbitsky, N. V. Kuleshov, J. Gao, K. Contag, A. Giesen, U. Keller, *Opt. Lett.* **2002**, *27*, 1162–1164.
[10] E. Innerhofer, T. Südmeyer, F. Brunner, R. Häring, A. Aschwanden, R. Paschotta, C. Hönninger, M. Kumkar, U. Keller, *Opt. Lett.* **2003**, *28*, 367–369.
[11] S. V. Marchese, T. Südmeyer, M. Golling, R. Grange, U. Keller, *Opt. Lett.* **2006**, *31*, 2728–2730.
[12] G. Palmer, M. Siegel, A. Steinmann, U. Morgner, *Opt. Lett.* **2007**, *32*, 1593–1595.
[13] S. V. Marchese, C. R. E. Baer, R. Peters, C. Kränkel, A. G. Engqvist, M. Golling, D. J. H. C. Maas, K. Petermann, T. Südmeyer, G. Huber, U. Keller, *Opt. Express* **2007**, *15*, 16966–16971.
[14] S. V. Marchese, C. R. E. Baer, A. G. Engqvist, S. Hashimoto, D. Maas, M. Golling, T. Südmeyer, U. Keller, *Opt. Express* **2008**, *16*, 6397–6407.

[15] G. Palmer, M. Schultze, M. Siegel, M. Emons, U. Bünting, U. Morgner, *Opt. Lett.* **2008**, *33*, 1608–1610.
[16] C. R. Baer, C. Kränkel, C. J. Saraceno, O. H. Heckl, M. Golling, T. Südmeyer, R. Peters, K. Petermann, G. Huber, U. Keller, *Opt. Lett.* **2009**, *34*, 2823–2825.
[17] C. R. E. Baer, C. Kränkel, C. J. Saraceno, O. H. Heckl, M. Golling, R. Peters, K. Petermann, T. Südmeyer, G. Huber, U. Keller, *Opt. Lett.* **2010**, *35*, 2302–2304.
[18] O. Pronin, J. Brons, C. Grasse, V. Pervak, G. Boehm, M.-C. Amann, V. L. Kalashnikov, A. Apolonski, F. Krausz, *Opt. Lett.* **2011**, *36*, 4746–4748.
[19] D. Bauer, I. Zawischa, D. H. Sutter, A. Killi, T. Dekorsy, *Opt. Express* **2012**, *20*, 9698–9704.
[20] C. J. Saraceno, O. H. Heckl, C. R. E. Baer, C. Schriber, M. Golling, K. Beil, C. Kränkel, T. Südmeyer, G. Huber, U. Keller, *Appl. Phys. B* **2012**, *106*, 559–562.
[21] S. Ricaud, A. Jaffres, K. Wentsch, A. Suganuma, B. Viana, P. Loiseau, B. Weichelt, M. Abdou-Ahmed, A. Voss, T. Graf, D. Rytz, C. Hönninger, E. Mottay, P. Georges, F. Druon, *Opt. Lett.* **2012**, *37*, 3984–3986.
[22] C. Saraceno, S. Pekarek, O. Heckl, C. Baer, C. Schriber, M. Golling, T. Südmeyer, K. Beil, C. Krankel, G. Huber, others, in *Adv. Solid-State Photonics*, Optical Society of America, **2012**, pp. AM2A-3.
[23] A. Diebold, F. Emaury, C. Schriber, M. Golling, C. J. Saraceno, T. Südmeyer, U. Keller, *Opt. Lett.* **2013**, *38*, 3842–3845.
[24] A. Klenner, F. Emaury, C. Schriber, A. Diebold, C. J. Saraceno, S. Schilt, U. Keller, T. Südmeyer, *Opt. Express* **2013**, *21*, 24770–24780.
[25] N. Kanda, A. A. Eilanlou, T. Imahoko, T. Sumiyoshi, Y. Nabekawa, M. Kuwata-Gonokami, K. Midorikawa, in *Adv. Solid State Lasers Congr.*, Optical Society of America, **2013**, pp. AF3A-8.
[26] J. Brons, V. Pervak, E. Fedulova, D. Bauer, D. Sutter, V. Kalashnikov, A. Apolonskiy, O. Pronin, F. Krausz, *Opt. Lett.* **2014**, *39*, 6442–6445.
[27] C. Schriber, L. Merceron, A. Diebold, F. Emaury, M. Golling, K. Beil, C. Kränkel, C. J. Saraceno, T. Südmeyer, U. Keller, in *Adv. Solid State Lasers*, Optical Society of America, **2014**, p. AF1A.4.
[28] C. Schriber, F. Emaury, A. Diebold, S. Link, M. Golling, K. Beil, C. Kränkel, C. J. Saraceno, T. Südmeyer, U. Keller, *Opt. Express* **2014**, *22*, 18979–18986.
[29] C. J. Saraceno, F. Emaury, C. Schriber, M. Hoffmann, M. Golling, T. Südmeyer, U. Keller, *Opt. Lett.* **2014**, *39*, 9–12.
[30] C. J. Saraceno, F. Emaury, O. H. Heckl, C. R. E. Baer, M. Hoffmann, C. Schriber, M. Golling, T. Südmeyer, U. Keller, *Opt. Express* **2012**, *20*, 23535–23541.
[31] A. A. Eilanlou, Y. Nabekawa, M. Kuwata-Gonokami, K. Midorikawa, *Jpn. J. Appl. Phys.* **2014**, *53*, 082701.
[32] J. Zhang, J. Brons, M. Seidel, V. Pervak, V. Kalashnikov, Z. Wei, A. Apolonski, F. Krausz, O. Pronin, in *Eur. Quantum Electron. Conf.*, Optical Society of America, **2015**, p. PD_A_1.
[33] J. Zhang, J. Brons, N. Lilienfein, E. Fedulova, V. Pervak, D. Bauer, D. Sutter, Z. Wei, A. Apolonski, O. Pronin, F. Krausz, *Opt. Lett.* **2015**, *40*, 1627–1630.
[34] O. Pronin, M. Seidel, F. Lücking, J. Brons, E. Fedulova, M. Trubetskov, V. Pervak, A. Apolonski, T. Udem, F. Krausz, *Nat. Commun.* **2015**, *6*, 6988.
[35] B. Borchers, C. Schäfer, C. Fries, M. Larionov, R. Knappe, in *Adv. Solid State Lasers*, Optical Society of America, **2015**, p. ATh4A.9.
[36] J. Brons, V. Pervak, D. Bauer, D. Sutter, O. Pronin, F. Krausz, *Opt. Lett.* **2016**, *41*, 3567–3570.

[37] B. Kreipe, J. Andrade, B. Deppe, C. Kränkel, U. Morgner, in *Conf. Lasers Electro-Opt.*, Optical Society of America, **2016**, p. SM1I.4.
[38] I. Graumann, A. Diebold, F. Emaury, B. Deppe, C. Kraenkel, C. Saraceno, U. Keller, in *Lasers Congr. 2016 ASSL LSC LAC*, Optical Society of America, **2016**, pp. ATu1A-3.
[39] C. Paradis, N. Modsching, V. J. Wittwer, B. Deppe, C. Kränkel, T. Südmeyer, *Opt. Express* **2017**, *25*, 14918–14925.
[40] I. J. Graumann, A. Diebold, C. G. E. Alfieri, F. Emaury, B. Deppe, M. Golling, D. Bauer, D. Sutter, C. Kränkel, C. J. Saraceno, C. R. Phillips, U. Keller, *Opt. Express* **2017**, *25*, 22519–22536.
[41] F. Saltarelli, A. Diebold, I. J. Graumann, C. R. Phillips, U. Keller, *Opt. Express* **2017**, *25*, 23254–23265.
[42] N. Modsching, C. Paradis, F. Labaye, M. Gaponenko, I. J. Graumann, A. Diebold, F. Emaury, V. J. Wittwer, T. Südmeyer, *Opt. Lett.* **2018**, *43*, 879–882.
[43] S. Kitajima, A. Shirakawa, H. Yagi, T. Yanagitani, *Opt. Lett.* **2018**, *43*, 5451–5454.
[44] J. Zhang, K. F. Mak, O. Pronin, *IEEE J. Sel. Top. Quantum Electron.* **2018**, *24*, 1–11.
[45] F. Saltarelli, A. Diebold, I. J. Graumann, C. R. Phillips, U. Keller, *Optica* **2018**, *5*, 1603.
[46] I. J. Graumann, F. Saltarelli, L. Lang, V. J. Wittwer, T. Südmeyer, C. R. Phillips, U. Keller, *Opt. Express* **2019**, *27*, 37349–37363.
[47] F. Saltarelli, I. J. Graumann, L. Lang, D. Bauer, C. R. Phillips, U. Keller, *Opt. Express* **2019**, *27*, 31465–31474.
[48] M. Poetzlberger, J. Zhang, S. Gröbmeyer, D. Bauer, D. Sutter, J. Brons, O. Pronin, *Opt. Lett.* **2019**, *44*, 4227–4230.
[49] S. Gröbmeyer, J. Brons, M. Seidel, O. Pronin, *Laser Photonics Rev.* **2019**, *13*, 1800256.
[50] N. Modsching, J. Drs, J. Fischer, C. Paradis, F. Labaye, M. Gaponenko, C. Kränkel, V. J. Wittwer, T. Südmeyer, *Opt. Express* **2019**, *27*, 16111–16120.
[51] S. Goncharov, K. Fritsch, O. Pronin, in *2021 Conf. Lasers Electro-Opt. Eur. Eur. Quantum Electron. Conf. OSA Tech. Dig. Opt. Soc. Am. 2021*, Munich, Germany, **2021**, p. cf_4_1.
[52] J. Drs, J. Fischer, N. Modsching, F. Labaye, V. J. Wittwer, T. Südmeyer, *Opt. Express* **2021**, *29*, 35929–35937.
[53] J. Fischer, J. Drs, N. Modsching, F. Labaye, V. J. Wittwer, T. Südmeyer, *Opt. Express* **2021**, *29*, 42075–42081.
[54] S. Tomilov, M. Hoffmann, J. Heidrich, B. Ö. Alaydin, M. Golling, Y. Wang, U. Keller, C. J. Saraceno, in *2021 Conf. Lasers Electro-Opt. Eur. Eur. Quantum Electron. Conf. CLEOEurope-EQEC*, **2021**, pp. 1–1.
[55] J. Zhang, M. Pötzlberger, Q. Wang, J. Brons, M. Seidel, D. Bauer, D. Sutter, V. Pervak, A. Apolonski, K. F. Mak, V. Kalashnikov, Z. Wei, F. Krausz, O. Pronin, *Ultrafast Sci.* **2022**, *2022*.
[56] T. Südmeyer, C. Kränkel, C. R. E. Baer, O. H. Heckl, C. J. Saraceno, M. Golling, R. Peters, K. Petermann, G. Huber, U. Keller, *Appl. Phys. B* **2009**, *97*, 281–295.
[57] I. Pupeza, M. Huber, M. Trubetskov, W. Schweinberger, S. A. Hussain, C. Hofer, K. Fritsch, M. Poetzlberger, L. Vamos, E. Fill, T. Amotchkina, K. V. Kepesidis, A. Apolonski, N. Karpowicz, V. Pervak, O. Pronin, F. Fleischmann, A. Azzeer, M. Žigman, F. Krausz, *Nature* **2020**, *577*, 52–59.

[58] C. Paradis, J. Drs, N. Modsching, O. Razskazovskaya, F. Meyer, C. Kränkel, C. J. Saraceno, V. J. Wittwer, T. Südmeyer, *Opt. Express* **2018**, *26*, 26377–26384.
[59] J. Drs, N. Modsching, C. Paradis, C. Kränkel, V. J. Wittwer, O. Razskazovskaya, T. Südmeyer, *JOSA B* **2019**, *36*, 3039–3045.
[60] F. Meyer, N. Hekmat, T. Vogel, A. Omar, S. Mansourzadeh, F. Fobbe, M. Hoffmann, Y. Wang, C. J. Saraceno, *Opt. Express* **2019**, *27*, 30340–30349.
[61] F. Meyer, T. Vogel, S. Ahmed, C. J. Saraceno, *Opt. Lett.* **2020**, *45*, 2494–2497.
[62] G. Barbiero, H. Wang, J. Brons, B.-H. Chen, V. Pervak, H. Fattahi, *J. Phys. B At. Mol. Opt. Phys.* **2020**, *53*, 6.
[63] F. Emaury, A. Diebold, C. J. Saraceno, U. Keller, *Optica* **2015**, *2*, 980–984.
[64] K. Fritsch, J. Brons, M. Iandulskii, K. F. Mak, Z. Chen, F. Krausz, N. Picqué, O. Pronin, in *Eur. Quantum Electron. Conf.*, **2019**, p. CA.5-2.
[65] N. Modsching, J. Drs, P. Brochard, J. Fischer, S. Schilt, V. J. Wittwer, T. Südmeyer, *Opt. Express* **2021**, *29*, 15104–15113.
[66] F. Labaye, M. Gaponenko, V. J. Wittwer, A. Diebold, C. Paradis, N. Modsching, L. Merceron, F. Emaury, I. J. Graumann, C. R. Phillips, C. J. Saraceno, C. Kränkel, U. Keller, T. Südmeyer, *Opt. Lett.* **2017**, *42*, 5170–5173.
[67] N. Kanda, T. Imahoko, K. Yoshida, A. Tanabashi, A. Amani Eilanlou, Y. Nabekawa, T. Sumiyoshi, M. Kuwata-Gonokami, K. Midorikawa, *Light Sci. Appl.* **2020**, *9*, 168.
[68] J. Fischer, J. Drs, F. Labaye, N. Modsching, V. Wittwer, T. Südmeyer, *Opt. Express* **2021**, *29*, 5833–5839.
[69] Y. Wang, S. Tomilov, C. J. Saraceno, *Adv. Opt. Technol.* **2021**, *10*, 247–261.
[70] R. Peters, C. Kränkel, S. T. Fredrich-Thornton, K. Beil, K. Petermann, G. Huber, O. H. Heckl, C. R. E. Baer, C. J. Saraceno, T. Südmeyer, U. Keller, *Appl. Phys. B* **2011**, *102*, 509–514.
[71] M. Larionov, J. Gao, S. Erhard, A. Giesen, K. Contag, V. Peters, E. Mix, L. Fornasiero, K. Petermann, G. Huber, J. A. der Au, G. J. Spühler, F. Brunner, R. Paschotta, U. Keller, A. A. Lagatsky, A. Abdolvand, N. V. Kuleshov, in *Adv. Solid-State Lasers*, Optica Publishing Group, **2001**, p. WC4.
[72] R. Peters, C. Kränkel, K. Petermann, G. Huber, *Opt. Express* **2007**, *15*, 7075.
[73] C. Kränkel, *IEEE J. Sel. Top. Quantum Electron.* **2015**, *21*, 250–262.
[74] C. Kränkel, A. Uvarova, É. Haurat, L. Hülshoff, M. Brützam, C. Guguschev, S. Kalusniak, D. Klimm, *Acta Crystallogr. Sect. B Struct. Sci. Cryst. Eng. Mater.* **2021**, *77*, 550–558.
[75] C. Kränkel, A. Uvarova, C. Guguschev, S. Kalusniak, L. Hülshoff, H. Tanaka, D. Klimm, *Opt. Mater. Express* **2022**, *12*, 1074–1091.
[76] S. Ricaud, A. Jaffres, P. Loiseau, B. Viana, B. Weichelt, M. Abdou-Ahmed, A. Voss, T. Graf, D. Rytz, M. Delaigue, E. Mottay, P. Georges, F. Druon, *Opt. Lett.* **2011**, *36*, 4134–4136.
[77] K. Hasse, T. Calmano, B. Deppe, C. Liebald, C. Kränkel, *Opt. Lett.* **2015**, *40*, 3552–3555.
[78] A. Greborio, A. Guandalini, J. Aus der Au, in *Proc SPIE*, (Eds: W. A. Clarkson, R. K. Shori), 8235, **2012**, p. 823511.
[79] F. Labaye, V. J. Wittwer, M. Hamrouni, N. Modsching, E. Cormier, E. Cormier, T. Südmeyer, *Opt. Express* **2022**, *30*, 2528–2538.
[80] U. Keller, *Appl. Phys. B* **2010**, *100*, 15–28.
[81] U. Keller, D. A. B. Miller, G. D. Boyd, T. H. Chiu, J. F. Ferguson, M. T. Asom, *Opt. Lett.* **1992**, *17*, 505.

[82] U. Keller, K. J. Weingarten, F. X. Kärtner, D. Kopf, B. Braun, I. D. Jung, R. Fluck, C. Hönninger, N. Matuschek, J. Aus der Au, *IEEE J. Sel. Top. Quantum Electron.* **1996**, *2*, 435–453.
[83] C. J. Saraceno, C. Schriber, M. Mangold, M. Hoffmann, O. H. Heckl, C. R. Baer, M. Golling, T. Südmeyer, U. Keller, *IEEE J. Sel. Top. Quantum Electron.* **2012**, *18*, 29–41.
[84] C. G. E. Alfieri, A. Diebold, F. Emaury, E. Gini, C. J. Saraceno, U. Keller, *Opt. Express* **2016**, *24*, 27587.
[85] A. Diebold, T. Zengerle, C. G. E. Alfieri, C. Schriber, F. Emaury, M. Mangold, M. Hoffmann, C. J. Saraceno, M. Golling, D. Follman, G. D. Cole, M. Aspelmeyer, T. Südmeyer, U. Keller, *Opt. Express* **2016**, *24*, 10512.
[86] D. E. Spence, P. N. Kean, W. Sibbett, *Opt. Lett.* **1991**, *16*, 42–44.
[87] P. F. Moulton, *J. Opt. Soc. Am. B* **1986**, *3*, 125–133.
[88] U. Keller, *Nature* **2003**, *424*, 831–838.
[89] A. Diebold, F. Saltarelli, I. J. Graumann, C. J. Saraceno, C. R. Phillips, U. Keller, *Opt. Express* **2018**, *26*, 12648–12659.
[90] T. Südmeyer, F. Brunner, E. Innerhofer, R. Paschotta, K. Furusawa, J. C. Baggett, T. M. Monro, D. J. Richardson, U. Keller, *Opt. Lett.* **2003**, *28*, 1951.
[91] E. Innerhofer, F. Brunner, S. V. Marchese, R. Paschotta, U. Keller, K. Furusawa, J. C. Baggett, T. M. Monro, D. J. Richardson, in *Adv. Solid-State Photonics*, Optical Society of America, **2005**, p. TuA3.
[92] C. J. Saraceno, O. H. Heckl, C. R. E. Baer, T. Südmeyer, U. Keller, *Opt. Express* **2011**, *19*, 1395.
[93] O. H. Heckl, C. J. Saraceno, C. R. E. Baer, T. Südmeyer, Y. Y. Wang, Y. Cheng, F. Benabid, U. Keller, *Opt. Express* **2011**, *19*, 19142–19149.
[94] K. Fritsch, M. Poetzlberger, V. Pervak, J. Brons, O. Pronin, *Opt. Lett.* **2018**, *43*, 4643.
[95] S. Gröbmeyer, K. Fritsch, B. Schneider, M. Poetzlberger, V. Pervak, J. Brons, O. Pronin, *Appl. Phys. B* **2020**, *126*, 159.
[96] C.-L. Tsai, F. Meyer, A. Omar, Y. Wang, A.-Y. Liang, C.-H. Lu, M. Hoffmann, S.-D. Yang, C. J. Saraceno, *Opt. Lett.* **2019**, *44*, 4115–4118.
[97] G. Barbiero, H. Wang, M. Graßl, S. Gröbmeyer, D. Kimbaras, M. Neuhaus, V. Pervak, T. Nubbemeyer, H. Fattahi, M. F. Kling, *Opt. Lett.* **2021**, *46*, 5304–5307.
[98] M. Müller, J. Buldt, H. Stark, C. Grebing, J. Limpert, *Opt. Lett.* **2021**, *46*, 2678–2681.
[99] S. Hädrich, E. Shestaev, M. Tschernajew, F. Stutzki, N. Walther, F. Just, M. Kienel, I. Seres, P. Jójárt, Z. Bengery, B. Gilicze, Z. Várallyay, Á. Börzsönyi, M. Müller, C. Grebing, A. Klenke, D. Hoff, G. G. Paulus, T. Eidam, J. Limpert, *Opt. Lett.* **2022**, *47*, 1537–1540.
[100] H. R. Telle, G. Steinmeyer, A. E. Dunlop, J. Stenger, D. H. Sutter, U. Keller, *Appl. Phys. B* **1999**, *69*, 327–332.
[101] M. Seidel, J. Brons, F. Lücking, V. Pervak, A. Apolonski, T. Udem, O. Pronin, *Opt. Lett.* **2016**, *41*, 1853–1856.
[102] N. Modsching, C. Paradis, P. Brochard, N. Jornod, K. Gürel, C. Kränkel, S. Schilt, V. J. Wittwer, T. Südmeyer, *Opt. Express* **2018**, *26*, 28461–28467.
[103] J. R. C. Andrade, N. Modsching, A. Tajalli, C. M. Dietrich, S. Kleinert, F. Placzek, B. Kreipe, S. Schilt, V. J. Wittwer, T. Sudmeyer, U. Morgner, *IEEE Photonics J.* **2020**, *12*, 1–9.
[104] I. Pupeza, C. Zhang, M. Högner, J. Ye, *Nat. Photonics* **2021**, 1–12.

[105] S. Hädrich, M. Krebs, A. Hoffmann, A. Klenke, J. Rothhardt, J. Limpert, A. Tünnermann, *Light Sci. Appl.* **2015**, *4*, e320.
[106] F. Krausz, M. Ivanov, *Rev. Mod. Phys.* **2009**, *81*, 163–234.
[107] A. K. Mills, T. J. Hammond, M. H. C. Lam, D. J. Jones, *J. Phys. B At. Mol. Opt. Phys.* **2012**, *45*, 142001.
[108] S. Hädrich, J. Rothhardt, M. Krebs, S. Demmler, A. Klenke, A. Tünnermann, J. Limpert, *J. Phys. B At. Mol. Opt. Phys.* **2016**, *49*, 172002.
[109] J. Drs, J. Fischer, F. Labaye, N. Modsching, V. J. Wittwer, T. Südmeyer, in *Adv. Solid State Lasers*, Optical Society of America, **2021**, p. ATh3A.2.
[110] C. J. Saraceno, *J. Opt.* **2018**, *20*, 044010.
[111] N. Picqué, T. W. Hänsch, *Nat. Photonics* **2019**, *13*, 146–157.
[112] V. Schuster, C. Liu, R. Klas, P. Dominguez, J. Rothhardt, J. Rothhardt, J. Limpert, B. Bernhardt, *Opt. Express* **2021**, *29*, 21859–21875.

Research Article | Vol. 27, No. 11 | 27 May 2019 | OPTICS EXPRESS 16111
Optics EXPRESS

Sub-100-fs Kerr lens mode-locked Yb:Lu_2O_3 thin-disk laser oscillator operating at 21 W average power

NORBERT MODSCHING,[1,*] JAKUB DRS,[1] JULIAN FISCHER,[1] CLÉMENT PARADIS,[1] FRANÇOIS LABAYE,[1] MAXIM GAPONENKO,[1] CHRISTIAN KRÄNKEL,[2] VALENTIN J. WITTWER,[1] AND THOMAS SÜDMEYER[1]

[1]*Laboratoire Temps-Fréquence (LTF), Institut de Physique, Université de Neuchâtel, Avenue de Bellevaux 51, 2000 Neuchâtel, Switzerland*
[2]*Center for Laser Materials, Leibniz-Institut für Kristallzüchtung, Max-Born-Str. 2, 12489 Berlin, Germany*
**norbert.modsching@unine.ch*

Abstract: We investigate power-scaling of a Kerr lens mode-locked (KLM) Yb:Lu_2O_3 thin-disk laser (TDL) oscillator operating in the sub-100-fs pulse duration regime. Employing a scheme with higher round-trip gain by increasing the number of passes through the thin-disk gain element, we increase the average power by a factor of two and the optical-to-optical efficiency by a factor of almost three compared to our previous sub-100-fs mode-locking results. The oscillator generates pulses with a duration of 95 fs at 21.1 W average power and 47.9 MHz repetition rate. We discuss the cavity design for continuous-wave and mode-locked operation and the estimation of the focal length of the Kerr lens. Unlike to usual KLM TDL oscillators, an operation at the edge of the stability zone in continuous-wave operation is not required. This work shows that KLM TDL oscillators based on the gain material Yb:Lu_2O_3 are an excellent choice for power-scaling of laser oscillators in the sub-100-fs regime, and we expect that such lasers will soon operate at power levels in excess of hundred watts.

© 2019 Optical Society of America under the terms of the OSA Open Access Publishing Agreement

1. Introduction

High-power ultrafast laser systems operating at MHz repetition rates are a versatile tool for numerous applications in science and industry [1]. Compared to amplifiers, oscillators generate usually close to transform-limited pulses in fundamental TEM_{00} mode operation without pre- or post-pulses and feature low noise levels, suitable for carrier-envelope-offset frequency stabilization. However, the currently achieved power levels decrease strongly as function of the minimum achieved pulse duration. In the last decade, numerous studies have been targeting to increase the achievable power levels of ultrafast laser oscillators operating in the sub-100-fs regime [2–4]. Sub-100-fs bulk oscillators based on Ti:sapphire are currently limited to 3.5 W of average power [5] (Fig. 1). In comparison, sub-100-fs oscillators based on Yb-doped bulk gain materials operate at a reduced quantum defect, enabling up to 12.5 W of average power [6]. However, even in this case thermal effects in the bulk gain material are the most severe challenge for further increase of the average power.

The thin-disk geometry is advantageous for further power increase of sub-100-fs laser oscillators, because it reduces the thermal effects in the gain material during laser operation [7]. Various techniques have been applied for efficient mode-locking of thin-disk laser (TDL) oscillators, e.g. by saturable absorber mirrors (SESAMs) [8], nonlinear polarization rotation [9], nonlinear mirror mode-locking [10] and Kerr lens mode-locking [11]. Among those techniques, the shortest pulse duration of a TDL oscillator was achieved by Kerr lens mode-locking [12].

#362282 https://doi.org/10.1364/OE.27.016111
Journal © 2019 Received 14 Mar 2019; revised 4 May 2019; accepted 6 May 2019; published 22 May 2019

Optics EXPRESS

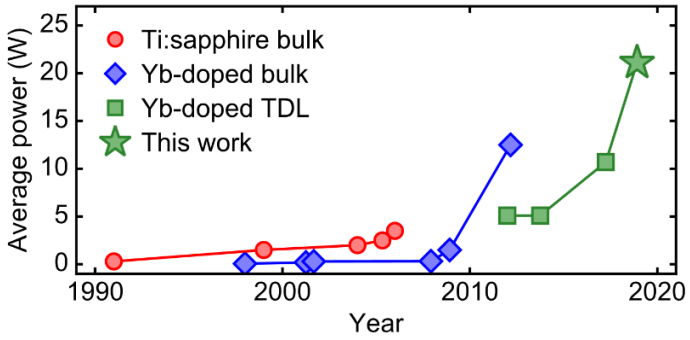

Fig. 1. Progress of the average power of ultrafast solid-state laser oscillators operating in the sub-100-fs pulse duration regime (Ti:sapphire [5,13], Yb-doped bulk [6,13–15], Yb-doped thin-disk laser (TDL) [16–18]).

In order to expand high-power operation of ultrafast TDL oscillators into the sub-100-fs regime [2], mode-locking of various broadband Yb-doped gain materials was investigated by several research groups [19–24]. The first TDL oscillators achieving sub-100-fs pulse durations were based on the broadband gain materials Yb:$LuScO_3$ and Yb:CALGO. Up to 5.1 W average power were demonstrated with an optical-to-optical efficiency amounting to 11% [16,17] (Table 1). Although their distorted crystalline structure is beneficial for a broad gain bandwidth, the resulting reduced thermal conductivity as well as the crystal quality of the available disks are limiting factors for achieving higher average powers. Currently, the highest average power of any ultrafast TDL oscillator based on disordered gain materials is limited to 28 W with 300-fs pulses [24].

Table 1. Selection of state-of-the-art ultrafast Yb-based laser oscillators.[a]

Type	Gain material	P_{ave}	τ_{pulse}	η_{eff}	Reference
Bulk	Yb:CALGO	12.5 W	94 fs	20%	[6]
Bulk	Yb:CALGO	3.3 W	45 fs	16%	[25]
TDL	Yb:$LuScO_3$	5.1 W	96 fs	11%	[16]
TDL	Yb:CALGO	5.1 W	62 fs	7%	[17]
TDL	Yb:YAG	155 W	140 fs	29%	[26]
TDL	Yb:YAG	3.5 W	49 fs	3.5%	[27,28]
TDL	Yb:Lu_2O_3	10.7 W	88 fs	5.8%	[18]
TDL	Yb:Lu_2O_3	21.1 W	95 fs	16.2%	This work

[a]P_{ave}: average power; τ_{pulse}: pulse duration; η_{eff}: optical-to-optical efficiency; TDL, thin-disk laser.

Ultrafast TDL oscillators based on the most mature gain material Yb:YAG have already reached average powers of 275 W, but operating at several hundred femtoseconds of pulse duration [29,30]. Kerr lens mode-locked (KLM) TDL oscillators demonstrated laser operation with 140-fs pulses at 155 W of average power and an optical-to-optical efficiency of 29% by fully exploiting the emission bandwidth of Yb:YAG [26]. Even shorter pulse durations of 49 fs were achieved by inserting nonlinear crystals for the generation of additional spectral components by self-phase modulation (SPM) in the cavity of a KLM Yb:YAG TDL oscillators. However, in this case the laser performance was limited to 3.5 W of average power at an optical-to-optical efficiency of 3.5% [27,28]. A gain material for high-power laser operation, which directly supports sub-100-fs pulse durations is Yb:Lu_2O_3. Yb:Lu_2O_3 provides a 60% broader emission bandwidth than Yb:YAG supporting the generation of 86-fs pulses at an even better thermal conductivity [2]. Although the gain material is still at an early stage of development, its suitability for high-power laser operation was already demonstrated by an ultrafast SESAM mode-locked TDL oscillator reaching 141 W of average power, albeit at pulse durations of several hundred femtoseconds [31]. In 2017, we demonstrated a KLM TDL oscillator fully

Optics EXPRESS

exploiting the emission bandwidth of Yb:Lu_2O_3. The laser operated at 10.7 W of average power in 88-fs pulses with a modest optical-to-optical efficiency of 5.8% [18].

In this work, we investigate the impact of higher round-trip gain on the average power and the optical-to-optical efficiency of a sub-100-fs KLM Yb:Lu_2O_3 TDL oscillator. Folding the standing-wave cavity two times on the disk enabled an increase of the average output power by a factor of two and the optical-to-optical efficiency by a factor of three compared to our previous result [18]. We demonstrate that using this approach TDL oscillators based on the gain material Yb:Lu_2O_3 are suitable for the generation of sub-100-fs pulses at high average power with optical-to-optical efficiencies that are comparable to Yb-doped bulk oscillators (Table 1).

2. Cavity design

The performance of the Yb:Lu_2O_3 disk in continuous-wave (CW) operation and previous mode-locking results are published in [18]. Compared to these results, the presented cavity is modified by folding the standing-wave cavity a second time on the disk (Fig. 2). A second folding of the cavity on the disk is commonly used in high-power KLM TDL oscillators [26,30]. In this configuration, the gain propagation length of the laser beam per cavity round-trip amounts to the eightfold of the gain crystal thickness, resulting in a higher round-trip gain.

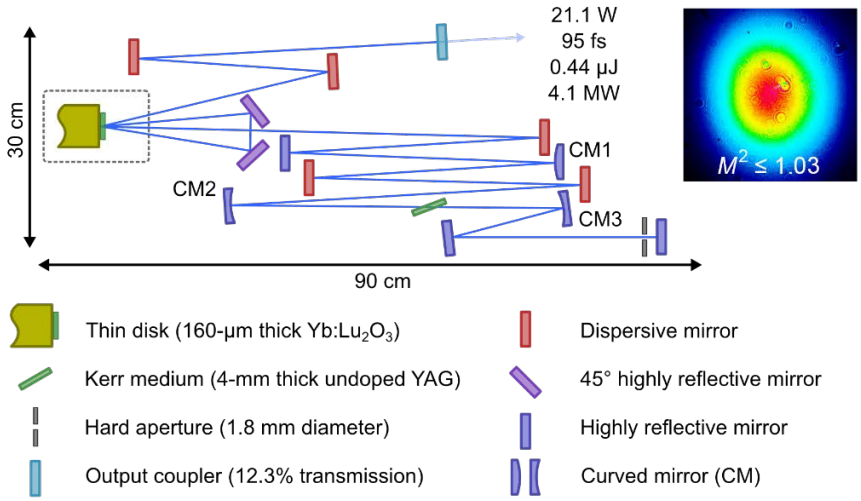

Fig. 2. Schematic of the Kerr lens mode-locked Yb:Lu_2O_3 thin-disk laser oscillator. (inset) Beam profile in mode-locked operation and M^2 beam quality factor. CM1, convex radius of curvature (ROC) of 2 m; CM2 and CM3, concave ROC of 250 mm.

Higher round-trip gain in the oscillator cavity enables laser operation at higher total cavity losses and, thus, the operation at a higher output coupler transmission (T_{OC}). Considering a constant intracavity performance, an increase in the T_{OC} should result in an increase of the output performance. However, higher round-trip gain also causes stronger gain narrowing which can reduce the spectral bandwidth and might prevent an exploitation of the gain bandwidth. The gain spectrum of Yb:Lu_2O_3 features a peak at a central wavelength of around 1033 nm with a full width at half maximum (FWHM) bandwidth of around 13 nm [Fig. 5(a)] [2,32]. Both parameters are nearly constant with the inversion level. Therefore, effects on the spectral gain properties for laser operation at a different inversion level can be neglected.

The mode radius in the cavity is calculated based on a formalism of ray transfer matrices for Gaussian beams (Fig. 3). We restrict the discussion to the sagittal plane which experiences a stronger Kerr lens due to the smaller beam radius in the Kerr medium (KM). The different mode radii in tangential and sagittal plane originate from the Brewster's angle under which the

Optics EXPRESS

KM is placed. In mode-locked operation, the additional Kerr lens changes the mode radius compared to the CW operation.

The focal length of the Kerr lens (f_{KM}) is estimated for a given intracavity peak power by an iterative optimization routine. In the simplified model, f_{KM} is considered as a single lens in the center of the KM. In the routine, the cavity is calculated for an initially guessed focal length $f_{KM,guess}$. For a stable cavity, the mode radius in the KM (w_{KM}) is retrieved and a resulting averaged focal length of the lens in the Kerr medium ($f_{KM,calc}$) is calculated based on

$$f_{KM,calc}^{-1} = \frac{4n_2 d_{KM,eff}}{\pi w_{KM}^4} \cdot P_{peak,IC} \quad ,$$

where n_2 is the nonlinear refractive index of the KM, $d_{KM,eff}$ is the effective thickness of the KM under Brewster's angle, and $P_{peak,IC}$ is the intracavity peak power [33]. A stable solution for f_{KM} can be found by an iterative optimization routine minimizing the difference between $f_{KM,guess}$ and $f_{KM,calc}$ for a given intracavity peak power. Once a stable solution is found, it enables an estimation of the mode radius in mode-locked operation (Fig. 3). In the presented cavity are two design aspects considered. First, the mode radius has to decrease at the position of the hard aperture (HA) to form a fast saturable absorber for self-amplitude modulation. Second, the mode radii at the position of the disk (DISK1, DISK2), have to increase for an optimized overlap with the pump spot. This increase affects the optical-to-optical efficiency and creates an additional soft-aperture self-amplitude modulation.

For efficient laser operation, the mode radius on the disk in mode-locked operation has to fit to the pump spot on the disk. An 80% overlap with the pump spot diameter of 2.8 mm was evaluated for highest optical-to-optical efficiency of the fundamental-mode in CW operation [18] (Fig. 3). The different mode radii on the disk originate from the concave 2.1 m radius of curvature of the disk. For improved overlap of both mode radii on the disk (DISK1, DISK2) the free space propagation distance between them (length b) was minimized, using two highly reflective mirrors optimized for 45° angle of incidence (Fig. 2). In contrast to our previous mode-locking results, a slightly elliptical beam profile is observed (inset of Fig. 2). We attributed the ellipticity to the larger angle of incidence on the disk of 9°.

Unlike to usual KLM TDL oscillators [11,34], an operation at the edge of the stability zone in CW operation is not required. Typically, KLM TDL oscillators are first optimized for fundamental-mode CW laser operation in the center of the stability zone and adjusted mode radius on the disk. Then, a 4-*f* imaging section is introduced into the cavity via two curved mirrors to create an intracavity focus without influencing the behavior of the laser in CW operation. The Kerr medium is placed in the vicinity of the intracavity focus for the formation of the Kerr lens in mode-locked operation. By increasing the distance between the curved mirrors, the cavity is shifted towards the edge of the stability zone in CW operation to promote Kerr lens mode-locking. In contrast, our cavity design has not been optimized for CW operation. The curved mirrors CM2 and CM3 form an intracavity focus without serving the purpose of a 4-*f* imaging section leading to different cavity dynamics. This allows for tailoring the mode size on the disk by adjusting the length e between CM2 and CM3 (Fig. 4). During the experimental optimization of the mode-locking performance for highest average power at sub-100-fs pulse durations the length e, the position and thickness of the KM, the HA diameter, the T_{OC} and the introduced group delay dispersion (GDD) were adapted.

Optics EXPRESS

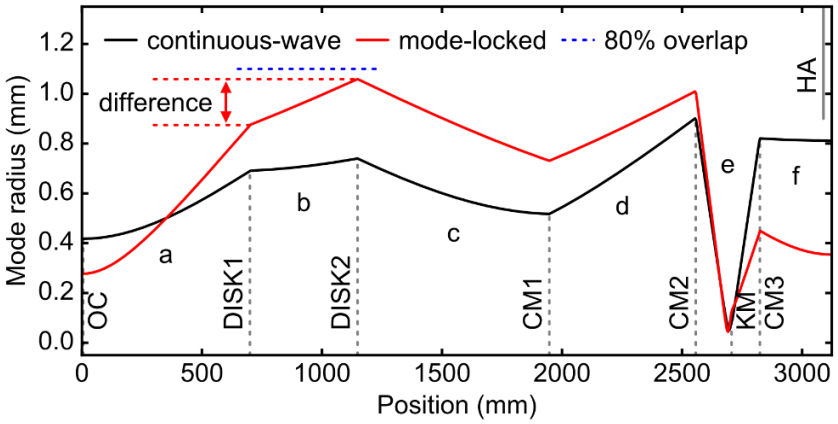

Fig. 3. Cavity design in continuous-wave and mode-locked operation shown for the sagittal plane. The mode radius is defined as the $1/e^2$ decay of the maximal intensity. In mode-locked operation, the effect of the Kerr lens in the Kerr medium (KM) is estimated for an intracavity peak power of 33 MW. Gray dotted lines indicate the position of the cavity components. In mode-locked operation, the mode radius on the disk (DISK1, DISK2) targets an 80% overlap with the pump spot (blue dotted). The different mode radii on the disk (red dotted) originate from the ROC of the disk. Cavity lengths in the simulation are a = 700 mm; b = 448 mm; c = 799 mm; d = 610 mm; e = 267mm; f = 300 mm. The distance between curved mirror CM2 and the KM is 149 mm. The hard aperture (HA, gray solid) is placed 30 mm before the cavity end mirror. In the experimental setup, the uncertainty of each length measurement towards the disk is ± 3 mm. The uncertainty of each length measurement between all other cavity components is ± 1 mm. OC, output coupler.

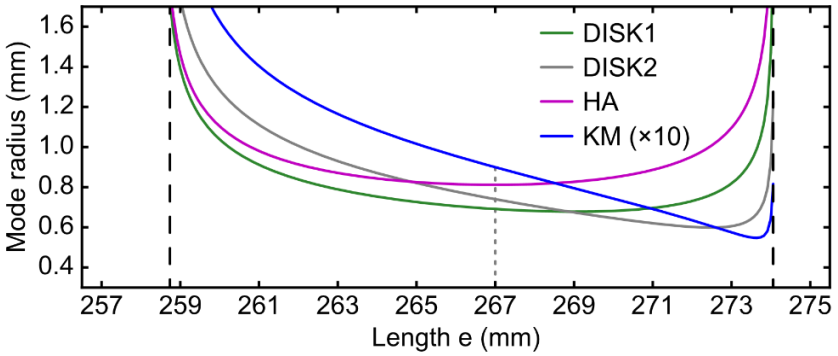

Fig. 4. Impact of the distance between the curved mirrors CM2 and CM3 in CW operation on the mode radii on the disk (DISK1; DISK2), in the Kerr medium (KM) and on the hard aperture (HA). Vertical black dashed lines indicate the edge of the stability zone for a stable cavity. The gray dotted line indicates the length e after the cavity optimization.

3. Performance in mode-locked operation

For mode-locked operation, −5400 fs^2 of GDD per cavity roundtrip are introduced by five dispersive mirrors (Fig. 2) at a T_{OC} of 12.3%. A 4 mm thick undoped YAG plate acts as KM and the diameter of the HA is 1.8 mm. The mode radii in the KM in CW operation were estimated by the cavity calculation to be 90 µm × 165 µm in sagittal and tangential plane, respectively. The start-up of the mode-locked operation follows the same procedure utilized in our initial laser result [18]. In the presented configuration, the formation of a single soliton in the cavity is achieved by setting the pump power to 160 W and knocking on the laser table. Afterwards, the pump power is reduced to 130 W to suppress a CW breakthrough visible in the

Optics EXPRESS

optical spectrum. As Kerr lens mode-locking features discrete stable solutions for the pulse formation, residual energy is often extracted by CW lasing.

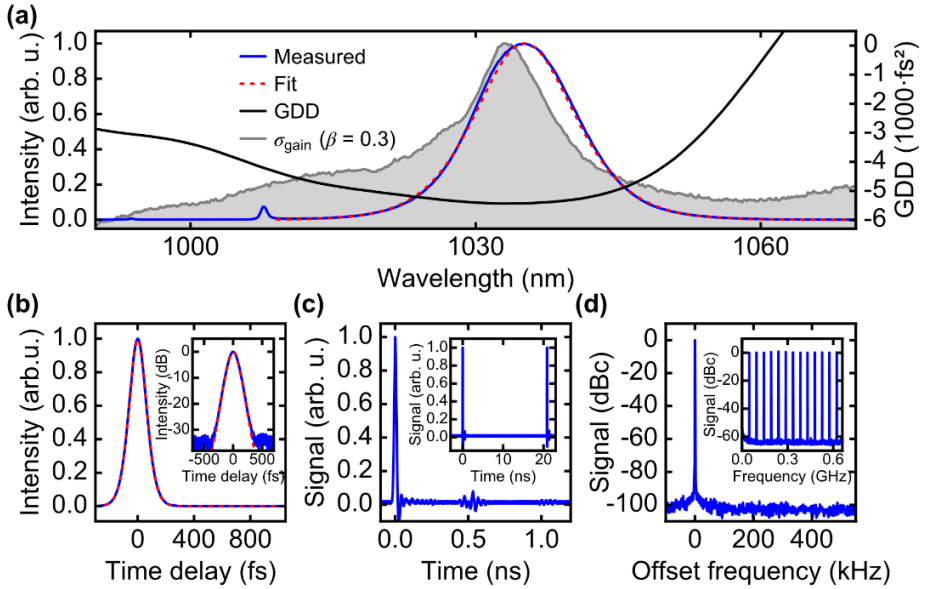

Fig. 5. (a) Optical spectrum of the laser output with sech^2 fit for soliton pulses, introduced group delay dispersion (GDD) per cavity roundtrip, and normalized gain cross-section of Yb:Lu_2O_3 for an inversion level β of 0.3 as reference (data taken from [2]). (b) Autocorrelation trace of the 95-fs pulses with sech^2 fit (measured in blue solid line and fit in red dotted line) in linear and (inset) logarithmic scale. (c) Sampling oscilloscope trace for 1 ns and (inset) 20 ns. (d) Radio-frequency spectrum of the fundamental repetition-rate frequency at 47.9 MHz and (inset) its harmonics at 100 Hz and 1 kHz resolution bandwidth, respectively.

In this configuration, the oscillator generates 95-fs pulses at an average output power of 21.1 W. The generated peak power is estimated to be 4.1 MW for soliton pulses at 0.44 µJ of pulse energy. The optical spectrum of the generated pulses [Fig. 5(a)] is centered at a wavelength of 1035.1 nm with a FWHM bandwidth of 12.3 nm. It is in good agreement with the sech^2 fit for soliton pulses. In comparison, the normalized spectrum of the gain cross-sections of Yb:Lu_2O_3 is plotted for an inversion level β of 0.3. Compared to the gain cross-sections, the central wavelength of the optical spectrum is shifted by 2 nm towards longer wavelengths. The shift is a result of the reflectivity and dispersion of the cavity components.

The pulse duration of 95 fs is measured by intensity autocorrelation [Fig. 5(b)] and has an ideal sech^2 shape for soliton pulses down to the measurement noise floor of –32 dB. The time-bandwidth product of 0.325 is close to the transform limit and 1.04 times the ideal value for sech^2 pulses. Single pulse operation was proven by a 180-ps scan with the autocorrelator and by observing the pulse train with an 18.5-ps-rise-time photodetector on a 40-GHz sampling oscilloscope [Fig. 5(c)]. Fluctuations at 0.5 ns and 1.0 ns are electronic reflections. The radio-frequency spectrum measured at the fundamental repetition frequency of 47.9 MHz shows no side peaks down to the measurement noise floor of –100 dBc and modulation-free higher harmonics confirm clean mode-locking [Fig. 5(d)]. The beam quality factor M^2 was measured to be ≤ 1.03. A summary of the parameters in mode-locked operation is given in Table 2.

For long-term operation, the pump power was slightly reduced to 126 W, decreasing the average power by 5% to 20.0 W. This suppressed a CW breakthrough that appeared during the warm-up of the system after several minutes. During a one-hour measurement in this condition, the average power and pulse duration showed no drift and fluctuated by less than 0.3% rms (Fig. 6).

Optics EXPRESS

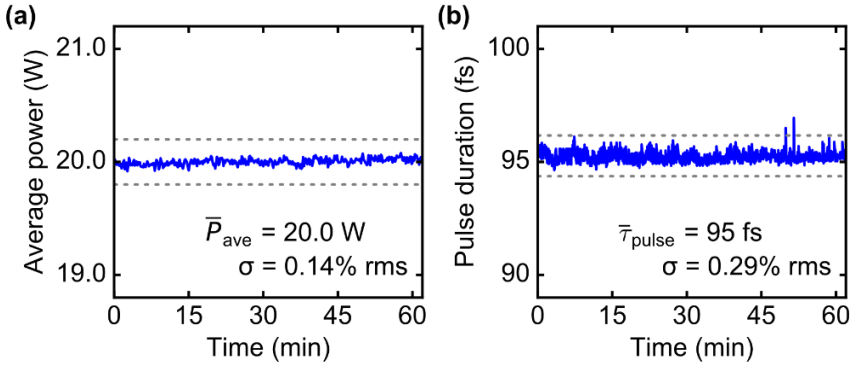

Fig. 6. (a) Average power and (b) pulse duration during a stability measurement of one hour. Corresponding averaged values are given with the root mean square (rms) error (σ). Gray dotted lines indicate the ± 1% margins of the average value.

Table 2. Summary of the mode-locking performance of the KLM Yb:Lu_2O_3 TDL oscillator for a single and double folding of the cavity on the disk.[a]

	Single folding	Double folding	Com-parison		Single folding	Double folding	Com-parison
$w_{KM,CW}$	90 µm × 150 µm	90 µm × 165 µm	≈	E_{pulse}	0.18 µJ	0.44 µJ	2 × ↑
τ_{FWHM}	88 fs	95 fs	≈	$P_{peak,\,IC}$	39 MW	33 MW	≈
$N_{Disk,RT}$	4	8	2 × ↑	$E_{pulse,\,IC}$	3.9 µJ	3.6 µJ	≈
P_{ave}	10.7 W	21.1 W	2 × ↑	$P_{ave,\,IC}$	233 W	172 W	26% ↓
η_{eff}	5.8%	16.2%	3 × ↑	f_{rep}	61 MHz	47.9 MHz	21% ↓
T_{OC}	4.6%	12.3%	3 × ↑	GDD_{RT}	–2200 fs^2	–5400 fs^2	2 × ↑
P_{peak}	1.8 MW	4.1 MW	2 × ↑	d_{KM}	2 mm	4 mm	2 × ↑
				$\lambda_{central}$	1037.6 nm	1035.1 nm	

[a]$w_{KM,CW}$: mode radius in the Kerr medium in continuous-wave operation; τ_{FWHM}: FWHM pulse duration; N_{Disk}: number of passes through the disk per cavity round-trip; P_{ave}: average power; η_{eff}: optical-to-optical efficiency; T_{OC}: output coupler transmission; P_{peak}: peak power; E_{pulse}: pulse energy; IC: intracavity; f_{rep}: repetition rate; GDD_{RT}: introduced group delay dispersion per cavity round-trip; d_{KM}: thickness of the Kerr medium; $\lambda_{central}$: central wavelength; ≈: comparable; ↑: increase; ↓: decrease.

The performance of the oscillator is compared to previous mode-locking results achieved with folding the cavity once on the disk (Table 2) [18]. In both configurations, the mode size in the KM in CW operation and the pulse duration are similar.

Doubling the number of passes through the disk per cavity round-trip enabled an increase of the average output power by a factor of two. Optical-to-optical efficiency and output coupler transmission were increased by a factor of almost three to 16.2% and 12.3%, respectively. Although peak power and pulse energy increased, the corresponding intracavity values remained comparable. This observation agrees with the geometrical scaling law of KLM TDLs [30] which relates the achievable intracavity peak power to the mode size in the KM in CW operation. As consequence of a similar intracavity peak power ($P_{peak,IC} \approx 0.88 \cdot E_{pulse,IC} / \tau_{FWHM}$), the 26% decrease in intracavity average power can be attributed to the reduced repetition rate ($E_{pulse,IC} = P_{ave} / T_{OC} \cdot f_{rep}$). The two times larger amount of introduced GDD per round-trip compensates for the stronger SPM (γ_{SPM}) in the two times thicker YAG KM plate ($E_{pulse,IC} \approx 2 \cdot 1.76 \cdot |GDD| / \gamma_{SPM} \cdot \tau_{FWHM}$). The stronger SPM is attributed to be required for the compensation of the gain narrowing caused by the increased T_{OC} to maintain the spectral bandwidth. The central wavelength is slightly shifted by 2 nm towards the gain peak in the cross sections of Yb:Lu_2O_3 at 1033 nm, which may contribute to the increased laser efficiency. We suggest that the different central wavelengths originate from the slightly different dispersion profiles of the dispersive mirrors used in both lasers.

Optics EXPRESS

4. Conclusion and outlook

We demonstrated a KLM Yb:Lu_2O_3 TDL oscillator generating 95-fs pulses at 21.1 W average power. By folding the cavity two times on the disk, the average power was increased by a factor of two with an almost three times higher optical-to-optical efficiency of 16.2%, compared to our previous result [18]. We showed that KLM TDL oscillators based on the gain material Yb:Lu_2O_3 are suitable for the generation of sub-100-fs pulses at high average power with optical-to-optical efficiencies that are comparable to Yb-doped bulk oscillators. The presented TDL oscillator has been used as single-stage driving laser for broadband THz generation via optical rectification in GaP [35]. In this case, high-power laser operation with sub-100-fs pulse duration was beneficial for the generated THz spectral bandwidth that expanded up to 5 THz at 0.3 mW of THz average power.

The average power of SESAM mode-locked Yb:Lu_2O_3 TDL oscillators was scaled from initially 20 W up to 141 W [31,36]. We anticipate that similar power-scaling should be feasible for sub-100-fs KLM Yb:Lu_2O_3 TDL oscillators. We expect that further power-scaling of sub-100-fs KLM Yb:Lu_2O_3 TDL oscillators can be achieved by scaling the intracavity peak power via adapting the mode size in the Kerr medium [30], enlarging the pump spot diameter on the disk [7] and by further increasing the number of passes through the disk. By this, we anticipate that sub-100-fs KLM Yb:Lu_2O_3 TDL oscillators operating at more than hundred watt of average power are within reach.

Funding

Swiss National Science Foundation (SNSF) (179146, 170772, 144970); German Ministry of Education and Research (BMBF) (13N14192).

Acknowledgements

The authors thank Olga Razskazovskaya (Université de Neuchâtel, Switzerland) for the fabrication of optical coatings and helpful discussions.

Experimental results presented in this work are open-access available under DOI: http://doi.org/10.23728/b2share.b5900f02cd3147cfa9f23c51f539f1d8

References

1. D. T. Reid, C. M. Heyl, R. R. Thomson, R. Trebino, G. Steinmeyer, H. H. Fielding, R. Holzwarth, Z. Zhang, P. Del'Haye, T. Südmeyer, G. Mourou, T. Tajima, D. Faccio, F. J. M. Harren, and G. Cerullo, "Roadmap on ultrafast optics," J. Opt. **18**(9), 093006 (2016).
2. T. Südmeyer, C. Kränkel, C. R. E. Baer, O. H. Heckl, C. J. Saraceno, M. Golling, R. Peters, K. Petermann, G. Huber, and U. Keller, "High-power ultrafast thin disk laser oscillators and their potential for sub-100-femtosecond pulse generation," Appl. Phys. B **97**(2), 281–295 (2009).
3. H. Zhao and A. Major, "Megawatt peak power level sub-100 fs Yb:KGW oscillators," Opt. Express **22**(25), 30425–30431 (2014).
4. U. Keller, "Ultrafast solid-state laser oscillators: a success story for the last 20 years with no end in sight," Appl. Phys. B **100**(1), 15–28 (2010).
5. S. Dewald, T. Lang, C. D. Schröter, R. Moshammer, J. Ullrich, M. Siegel, and U. Morgner, "Ionization of noble gases with pulses directly from a laser oscillator," Opt. Lett. **31**(13), 2072–2074 (2006).
6. A. Greborio, A. Guandalini, and J. Aus der Au, "Sub-100 fs pulses with 12.5-W from Yb:CALGO based oscillators," in Proc. SPIE, (2012), paper 823511.
7. A. Giesen, H. Hügel, A. Voss, K. Wittig, U. Brauch, and H. Opower, "Scalable concept for diode-pumped high-power solid-state lasers," Appl. Phys. B. **58**(5), 365–372 (1994).
8. J. Aus der Au, G. J. Spühler, T. Südmeyer, R. Paschotta, R. Hövel, M. Moser, S. Erhard, M. Karszewski, A. Giesen, and U. Keller, "16.2-W average power from a diode-pumped femtosecond Yb:YAG thin disk laser," Opt. Lett. **25**(11), 859–861 (2000).
9. B. Borchers, C. Schäfer, C. Fries, M. Larionov, and R. Knappe, "Nonlinear polarization rotation mode-locking via phase-mismatched type I SHG of a thin disk femtosecond laser," in Advanced Solid State Lasers (Optical Society of America, 2015), paper ATh4A.9.
10. F. Saltarelli, A. Diebold, I. J. Graumann, C. R. Phillips, and U. Keller, "Modelocking of a thin-disk laser with the frequency-doubling nonlinear-mirror technique," Opt. Express **25**(19), 23254–23266 (2017).

Optics EXPRESS

11. O. Pronin, J. Brons, C. Grasse, V. Pervak, G. Boehm, M.-C. Amann, V. L. Kalashnikov, A. Apolonski, and F. Krausz, "High-power 200 fs Kerr-lens mode-locked Yb:YAG thin-disk oscillator," Opt. Lett. **36**(24), 4746–4748 (2011).
12. N. Modsching, C. Paradis, F. Labaye, M. Gaponenko, I. J. Graumann, A. Diebold, F. Emaury, V. J. Wittwer, and T. Südmeyer, "Kerr lens mode-locked Yb:CALGO thin-disk laser," Opt. Lett. **43**(4), 879–882 (2018).
13. U. Keller, *Ultrafast Solid-State Lasers*, Landolt-Börnstein. Laser Physics and Applications. Subvolume B: Laser Systems. Part I (Springer, 2007).
14. M. Tokurakawa, A. Shirakawa, K. Ueda, H. Yagi, S. Hosokawa, T. Yanagitani, and A. A. Kaminskii, "Diode-pumped 65 fs Kerr-lens mode-locked Yb^{3+}:Lu_2O_3 and nondoped Y_2O_3 combined ceramic laser," Opt. Lett. **33**(12), 1380–1382 (2008).
15. M. Tokurakawa, A. Shirakawa, K. Ueda, H. Yagi, M. Noriyuki, T. Yanagitani, and A. A. Kaminskii, "Diode-pumped ultrashort-pulse generation based on Yb^{3+}:Sc_2O_3 and Yb^{3+}:Y_2O_3 ceramic multi-gain-media oscillator," Opt. Express **17**(5), 3353–3361 (2009).
16. C. J. Saraceno, O. H. Heckl, C. R. E. Baer, C. Schriber, M. Golling, K. Beil, C. Kränkel, T. Südmeyer, G. Huber, and U. Keller, "Sub-100 femtosecond pulses from a SESAM modelocked thin disk laser," Appl. Phys. B **106**(3), 559–562 (2012).
17. A. Diebold, F. Emaury, C. Schriber, M. Golling, C. J. Saraceno, T. Südmeyer, and U. Keller, "SESAM mode-locked Yb:$CaGdAlO_4$ thin disk laser with 62 fs pulse generation," Opt. Lett. **38**(19), 3842–3845 (2013).
18. C. Paradis, N. Modsching, V. J. Wittwer, B. Deppe, C. Kränkel, and T. Südmeyer, "Generation of 35-fs pulses from a Kerr lens mode-locked Yb:Lu_2O_3 thin-disk laser," Opt. Express **25**(13), 14918–14925 (2017).
19. C. R. E. Baer, C. Kränkel, O. H. Heckl, M. Golling, T. Südmeyer, R. Peters, K. Petermann, G. Huber, and U. Keller, "227-fs pulses from a mode-locked Yb:$LuScO_3$ thin disk laser," Opt. Express **17**(13), 10725–10730 (2009).
20. G. Palmer, M. Schultze, M. Siegel, M. Emons, U. Bünting, and U. Morgner, "Passively mode-locked Yb:KLu(WO_4)_2 thin-disk oscillator operated in the positive and negative dispersion regime," Opt. Lett. **33**(14), 1608–1610 (2008).
21. F. Brunner, T. Südmeyer, E. Innerhofer, F. Morier-Genoud, R. Paschotta, V. E. Kisel, V. G. Shcherbitsky, N. V. Kuleshov, J. Gao, K. Contag, A. Giesen, and U. Keller, "240-fs pulses with 22-W average power from a mode-locked thin-disk Yb:$KY(WO_4)_2$ laser," Opt. Lett. **27**(13), 1162–1164 (2002).
22. O. H. Heckl, C. Kränkel, C. R. E. Baer, C. J. Saraceno, T. Südmeyer, K. Petermann, G. Huber, and U. Keller, "Continuous-wave and modelocked Yb:YCOB thin disk laser: first demonstration and future prospects," Opt. Express **18**(18), 19201–19208 (2010).
23. C. J. Saraceno, O. H. Heckl, C. R. E. Baer, M. Golling, T. Südmeyer, K. Beil, C. Kränkel, K. Petermann, G. Huber, and U. Keller, "CW and Modelocked Operation of an Yb:(Sc,Y,Lu)2O3 Thin-disk Laser," in CLEO:2011 - Laser Applications to Photonic Applications (Optical Society of America, 2011), paper CWP1.
24. S. Ricaud, A. Jaffres, K. Wentsch, A. Suganuma, B. Viana, P. Loiseau, B. Weichelt, M. Abdou-Ahmed, A. Voss, T. Graf, D. Rytz, C. Hönninger, E. Mottay, P. Georges, and F. Druon, "Femtosecond Yb:$CaGdAlO_4$ thin-disk oscillator," Opt. Lett. **37**(19), 3984–3986 (2012).
25. S. Manjooran and A. Major, "Diode-pumped 45 fs Yb:CALGO laser oscillator with 1.7 MW of peak power," Opt. Lett. **43**(10), 2324–2327 (2018).
26. J. Brons, V. Pervak, D. Bauer, D. Sutter, O. Pronin, and F. Krausz, "Powerful 100-fs-scale Kerr-lens mode-locked thin-disk oscillator," Opt. Lett. **41**(15), 3567–3570 (2016).
27. J. Zhang, J. Brons, M. Seidel, V. Pervak, V. Kalashnikov, Z. Wei, A. Apolonski, F. Krausz, and O. Pronin, "49-fs Yb:YAG thin-disk oscillator with distributed Kerr-lens mode-locking," in European Quantum Electronics Conference (Optical Society of America, 2015), paper PD_A_1.
28. J. Brons, "High-power femtosecond laser-oscillators for applications in high-field physics," Dissertation, Ludwig-Maximilians-Universität München (2017).
29. C. J. Saraceno, F. Emaury, O. H. Heckl, C. R. E. Baer, M. Hoffmann, C. Schriber, M. Golling, T. Südmeyer, and U. Keller, "275 W average output power from a femtosecond thin disk oscillator operated in a vacuum environment," Opt. Express **20**(21), 23535–23541 (2012).
30. J. Brons, V. Pervak, E. Fedulova, D. Bauer, D. Sutter, V. Kalashnikov, A. Apolonskiy, O. Pronin, and F. Krausz, "Energy scaling of Kerr-lens mode-locked thin-disk oscillators," Opt. Lett. **39**(22), 6442–6445 (2014).
31. C. R. E. Baer, C. Kränkel, C. J. Saraceno, O. H. Heckl, M. Golling, R. Peters, K. Petermann, T. Südmeyer, G. Huber, and U. Keller, "Femtosecond thin-disk laser with 141 W of average power," Opt. Lett. **35**(13), 2302–2304 (2010).
32. C. Kränkel, "Rare-earth-doped sesquioxides for diode-pumped high-power lasers in the 1-, 2-, and 3-µm spectral range," IEEE J. Sel. Top. Quantum Electron. **21**(1), 250–262 (2015).
33. S. Yefet and A. Pe'er, "A Review of Cavity Design for Kerr Lens Mode-Locked Solid-State Lasers," Appl. Sci. (Basel) **3**(4), 1–31 (2015).
34. J. Brons, O. Pronin, M. Seidel, V. Pervak, D. Bauer, D. Sutter, V. L. Kalashnikov, A. Apolonskiy, and F. Krausz, "120 W, 4 µJ from a purely Kerr-lens mode-locked Yb:YAG thin-disk oscillator," in Advanced Solid-State Lasers Congress (Advanced Solid-State Lasers Congress, G. Huber and P. Moulton, eds., OSA Technical Digest (online), 2013), paper AF3A.4.

Optics EXPRESS

35. J. Drs, N. Modsching, C. Paradis, C. Kränkel, V. Wittwer, O. Razskazovskaya, and T. Südmeyer, "Optical rectification of ultrafast Yb-lasers: Pushing power and bandwidth of THz generation in GaP," Opt. Express. submitted.
36. S. V. Marchese, C. R. E. Baer, R. Peters, C. Kränkel, A. G. Engqvist, M. Golling, D. J. H. C. Maas, K. Petermann, T. Südmeyer, G. Huber, and U. Keller, "Efficient femtosecond high power Yb:Lu_2O_3 thin disk laser," Opt. Express **15**(25), 16966–16971 (2007).

213.55.220.185 {ts '2021-12-04 17:01:53'}

Research Article | Vol. 29, No. 22 / 25 Oct 2021 / Optics Express 35929
Optics EXPRESS

Sub-30-fs Yb:YAG thin-disk laser oscillator operating in the strongly self-phase modulation broadened regime

JAKUB DRS,* JULIAN FISCHER, NORBERT MODSCHING, FRANÇOIS LABAYE, VALENTIN J. WITTWER, AND THOMAS SÜDMEYER

Laboratoire Temps-Fréquence (LTF), Institut de Physique, Université de Neuchâtel, Avenue de Bellevaux 51, 2000 Neuchâtel, Switzerland
*jakub.drs@unine.ch

Abstract: We experimentally investigate the limits of pulse duration in a Kerr-lens mode-locked Yb:YAG thin-disk laser (TDL) oscillator. Thanks to its excellent mechanical and optical properties, Yb:YAG is one of the most used gain materials for continuous-wave and pulsed TDLs. In mode-locked operation, its 8-nm wide gain bandwidth only directly supports pulses with a minimum duration of approximately 140 fs. For achieving shorter pulses, a Kerr-lens mode-locked TDL oscillator can be operated in the strongly self-phase modulation (SPM) broadened regime. Here, the spectral bandwidth of the oscillating pulse exceeds the available gain bandwidth by generating additional frequencies via SPM inside the Kerr medium. In this work, we study and compare different laser configurations in the strongly SPM-broadened regime. Starting with a configuration providing 84-fs pulses at 69 W average power at 17 MHz repetition rate, we reduce the pulse duration by optimizing various mode-locking parameters. One crucial parameter is the dispersion control which was provided by in-house-developed dispersive mirrors produced by ion-beam sputtering (IBS). We discuss trade-offs in average power, pulse duration, efficiency, and intra-cavity peak power. For the configuration operating at the highest SPM-broadening, we achieve a minimum pulse duration of 27 fs, which represents the shortest pulse duration directly generated by any ultrafast TDL oscillator. The corresponding full width at half maximum (FWHM) spectral bandwidth exceeds more than five times the FWHM gain bandwidth. The average output power of 3.3 W is moderate for ultrafast TDL oscillators, but higher than other Yb-based laser oscillators operating at this pulse duration. Additionally, the corresponding intra-cavity peak power of 0.8 GW is highly attractive for implementing intra-cavity extreme nonlinear optical interactions such as high harmonic generation.

© 2021 Optical Society of America under the terms of the OSA Open Access Publishing Agreement

1. Introduction

Ultrafast lasers have revolutionized many scientific fields [1]. For applications relying on few-cycle pulses, Ti:sapphire lasers have been the workhorse. But since the last decade, also Yb-based lasers have started entering this domain, gradually reaching shorter and shorter pulse durations. Currently, pulses below 18 fs have been demonstrated directly generated by an Yb-based bulk laser oscillator [2,3]. The properties of Yb-doped gain materials, in particular, the low quantum defect and the pumping wavelength compatible with efficient laser diodes, make these lasers much better suited for high-power applications otherwise inaccessible to the Ti:sapphire technology. On the other hand, decreasing the pulse duration of Yb-based lasers is much more challenging because of the narrower gain bandwidth compared to Ti:sapphire.

A successful laser technology specifically designed for Yb-doped materials is the thin-disk laser (TDL) [4]. Thanks to the thin-disk geometry allowing for extremely efficient cooling and very large beam sizes in the gain material, ultrafast TDL oscillators [5] can handle the highest

#440196 https://doi.org/10.1364/OE.440196
Journal © 2021 Received 11 Aug 2021; revised 4 Oct 2021; accepted 6 Oct 2021; published 18 Oct 2021

Optics EXPRESS

average and peak intra-cavity powers among all mode-locked laser oscillator technologies [6]. As such, they can serve as a single-stage alternative to laser amplifier systems directly delivering clean transform limited soliton pulses at excellent beam quality and megahertz repetition rates. Ultrafast TDL oscillators have demonstrated output powers up to 350 W in 1-ps pulses [7] or 150 W in 140-fs pulses [8]. Moreover, the high intra-cavity performance of TDL oscillators makes this technology an excellent candidate for driving nonlinear frequency conversion directly inside the laser cavity such as intra-oscillator high harmonic generation (HHG) [9].

Decreasing the pulse duration of the TDL oscillators has been an important goal since more than a decade [10]. Up to nowadays, it has been mostly believed that short pulse durations (<100 fs) require broadband gain materials. A lot of effort has been, thus, invested into mode-locking studies using disks based on various broadband Yb-doped gain materials such as Yb:$LuScO_3$ [11], Yb:Sc_2O_3 [12], Yb:CALGO [13,14], and Yb:Lu_2O_3 [15,16]. Unfortunately, despite the fact that most of these materials have been very useful in the bulk geometry, in the thin-disk, they have not yet been particularly successful. The main limitation seems to be either the not yet sufficient crystal growth quality required for production of high-quality disks, or the inferior thermal properties and the lower gain of these materials, which did not yet allow to fully harness their potential in the thin-disk geometry for high-power operation. The highest average power achieved by a TDL oscillator using these materials in the sub-100-fs regime has been so far limited to ~20 W [16]. This can be also identified from Fig. 1 showing an overview of state-of-the-art TDL oscillators based on different Yb-doped materials. Here, the broadband, but much less commonly available gain materials depicted in red, clearly dominate the left part of the graph corresponding to short pulse durations. But one can also clearly identify the trade-off between pulse duration and average power which is strongly decreasing for shorter pulses. On the other hand, the Yb:YAG gain material depicted by the green markers represents the well-developed industrial standard for high-power applications. High-quality disks are commercially available and are suitable for several hundred watts of output power. Unfortunately, its moderate gain bandwidth of ~8-nm full width at half maximum (FWHM) directly supports only a pulse duration down to ~140 fs. In 2015, it has been shown that the pulse duration of an Yb:YAG TDL oscillator can be decreased beyond this limit by utilizing a distributed Kerr-lens mode-locking (KLM) scheme [17]. The laser emitted 49-fs pulses at 3.5 W of average power and 3.5% optical-to-optical efficiency. Here the shorter pulse duration was achieved by operating the laser oscillator in the self-phase modulation (SPM) broadened regime, where the frequencies outside of the gain bandwidth are generated by intra-cavity SPM inside the Kerr medium, as also shown in [18]. The operation in the SPM-broadened regime, however, still follows the standard soliton mode-locking scheme, where the phase shift induced by SPM is compensated by the one from anomalous dispersion and combined with saturable losses resulting in a stable roundtrip soliton solution.

In our study, we further exploit the strongly SPM-broadened regime using a KLM Yb:YAG TDL oscillator. We show three laser configurations operating at 84 fs with 69 W of average power, 37 fs with 17 W, and 27 fs with 3.3 W, by far exceeding the performance achieved with broadband Yb-doped gain materials as shown by the star markers in Fig. 1. We further discuss the trade-off between different parameters of our laser operating in the strongly SPM-broadened regime in a comprehensive table and show the dispersion profile introduced by our in-house developed dispersive mirrors. The 27-fs configuration represents the shortest pulse duration of any TDL oscillator [14] and the corresponding intra-cavity peak power of ~0.8 GW is extremely promising for intra-oscillator HHG. This demonstrates that at the current state of development, the most promising direction toward high-power short-pulse TDL oscillators is still using commercially available Yb:YAG disks, while operating the KLM laser in the strongly SPM-broadened regime.

We expect being able to further increase the output power of our laser toward the 100-W level at a few tens of femtoseconds. This together with the clean $sech^2$-shaped optical spectrum and excellent beam quality, inherent to laser oscillators, should make our TDL oscillator an excellent

Optics EXPRESS

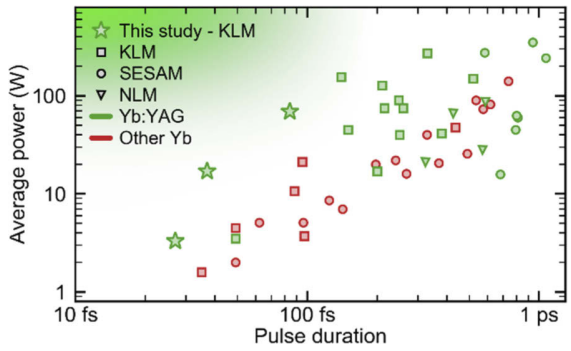

Fig. 1. Overview of various Yb-based TDL oscillators operating at >1 W of average power and <1-ps pulse duration. The color code depicts Yb:YAG in green and other more broadband Yb-doped gain materials in red. Different mode-locking mechanisms are indicated by the markers: squares - Kerr-lens mode-locking (KLM), circles - semiconductor saturable absorber mirror (SESAM) mode-locking, triangles - nonlinear mirror mode-locking (NLM). The targeted area of shortest pulse duration and highest average power is highlighted by the green shaded area. The references for the graph can be found in [9].

candidate for subsequent nonlinear pulse compression toward single-cycle pulses. This will highly benefit various experiments, particularly in the domain of attosecond science.

2. Experimental setup

The TDL oscillator setup is depicted in Fig. 2. The whole system, originally designed for driving intra-oscillator HHG [19], is housed in a vacuum chamber with a footprint of 0.8×1.6 m^2 and operates at ~100 mbar of pressure. The cavity design is inspired by the power-scaling approach for KLM TDLs presented in [20]. The laser cavity is built around a commercial TDL head from TRUMPF GmbH designed for 36 passes of the pump through a ~100-µm-thick Yb:YAG disk. The disk is optically pumped by a 2-kW, 969-nm volume-Bragg-grating-stabilized fiber-coupled diode from DILAS Diodenlaser GmbH. The cavity is folded twice over the disk, increasing the gain per cavity roundtrip. For KLM of the TDL oscillator [21], a sapphire plate at the Brewster's angle is placed in the vicinity of an intra-cavity focus created by two concave mirrors (CM1, CM2) with 1-m radius of curvature (RoC). A water-cooled copper hard aperture is placed close to one laser end mirror. Several dispersive mirrors (DM) introduce a negative group delay dispersion (GDD), balancing the positive dispersion of the Kerr and gain medium and the SPM. The optical coatings of the mirrors have been designed and grown inhouse in our ion-beam sputtering coating facility. Mode-locked operation in vacuum is initialized by shaking one of the cavity mirrors mounted on a piezo stage. The second cavity end mirror serves as an output coupler. An imaging cavity extension consisting of two focusing mirrors (CM3, CM4) is introduced into the output coupling arm of the laser, originally intended for creating a tight focus at an HHG gas target. One of the tight focus mirrors (CM3) is placed on a motorized linear stage, allowing for fine-tuning of the laser cavity during the mode-locked operation. The stage can be moved within ~1-mm travel range between a position where the laser easily mode-locks to a position of highest laser performance. The cavity, however, remains stable for all positions even with negligible Kerr effect in the case of continuous-wave operation.

Due to the presence of the tight focus, our laser requires vacuum environment for its operation. In ambient air, the intensity in the focus would exceed the air ionization level and the plasma formation would prevent stable mode-locked operation. On the other hand, a common issue of

Optics EXPRESS

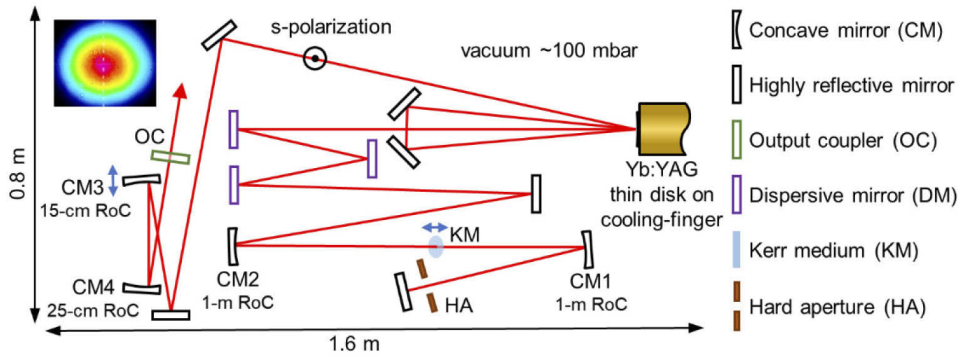

Fig. 2. Schematic of the Kerr-lens mode-locked Yb:YAG TDL oscillator with a double pass on the disk. An imaging cavity extension with concave 15-cm and 25-cm RoC mirrors creates a tight-focus which can be used for an HHG gas target. CM3 is mounted on a translation stage that allows for fine tuning of the cavity during laser operation from a position where it is easy to mode-lock to a position of highest laser performance. The inset shows the beam profile of the 27-fs laser configuration during mode-locked operation.

optical systems operated in vacuum is the deposition of carbon on the optics experiencing high intensities such as the Kerr medium inside the laser [22]. As a compromise between both effects, we selected a vacuum level of 100 mbar. At this pressure, the SPM and dispersion induced by air are still negligible compared to the other cavity components.

3. Experimental results

The here presented results correspond to two individual experiments. The first one, performed in 2020, was focused on increasing the average power in the sub-100-fs regime, yielding 69 W of average power at 84-fs pulse duration. Unfortunately, during this experiment, our fiber for pump power delivery suffered a damage due to insufficient cooling of the collimation unit in the vacuum environment. Since we have not yet fully resolved this issue with the pump delivery, we have decreased the pump spot diameter on the disk in order to reduce the required pump power for the second experiment targeting for shortest pulse duration. Additionally, we have optimized the dispersion in the detection line to compensate for the transmissive elements (output coupler, vacuum window, telescope lenses). We have also switched from p- to s-polarization by turning the Brewster's angle Kerr medium by 90° in order to benefit from the flatter dispersion profile of our 45° angle of incidence cavity mirrors in s-polarization. For all experiments, we have limited ourselves to a pump intensity of ~6 kW/cm^2 to prevent damage of the disk.

Each of the presented laser configuration was individually experimentally optimized. The degrees of freedom for the optimization included the GDD introduced by the DMs, thickness and position of the sapphire plate used as a Kerr medium, the size of the hard aperture, output-coupling rate, the position of the detuning stage of the CM3, and the pump power. A set of semi-empirical scaling rules can be formulated to aid with the optimization process:

- The pulse duration scales approximately linearly with the introduced GDD down to the point where the laser does not mode-lock anymore.
- Decreasing the thickness of the Kerr medium increases the intra-cavity peak power, but also leads to an increased pulse duration.

Optics EXPRESS

- Moving the Kerr medium further away from the intra-cavity focus towards the CM2 improves the intra-cavity peak power but increases the difficulty to initiate mode-locking of the laser.

The position of CM3 is initially adjusted for easiest mode-locking and later allows for elimination of the continuous-wave lasing break-through which otherwise appears at higher pump powers, preventing a further pump increase. The size of the hard aperture has a minor influence, since the size of the beam can be tuned using the position of the CM3, but typically has a weak optimum depending on the laser configuration.

The experimental results of the laser configurations are summarized in Fig. 3 and Table 1. The 84-fs and 37-fs configuration were optimized for highest output power at an introduced total negative GDD per cavity roundtrip of -6000 fs^2 and -1500 fs^2, respectively. The 84-fs configuration allows for stable mode-locking up to an output coupling rate of 12% and the 37-fs configuration up to 5%, resulting in an average power of 69 W and 17 W, respectively. The required pump power of 580 W and 350 W leads to optical-to-optical efficiencies of 12% and 4.9%. Both configurations feature relatively clean $sech^2$ soliton spectra with FWHM bandwidths of 16.5 nm and 29.5 nm, clearly exceeding the 8-nm gain bandwidth of Yb:YAG. The bump in the optical spectra at 1030 nm corresponds to the position of the peak of the Yb:YAG gain profile and is a commonly seen feature in TDL oscillators operating in the strongly SPM-broadened regime [15,17].

Table 1. Mode-locking performance and parameters for the presented laser configurations at pulse durations of 84 fs, 37 fs, 29 fs, and 27 fs.

Configuration	84 fs	37 fs	29 fs	27 fs
Output power (W)	69	17.1	2.5	3.3
Peak power (MW)	42	23.8	4.5	6.3
Pulse energy (µJ)	3.6	0.91	0.13	0.18
Central wavelength (nm)	1029.0	1029.4	1028.4	1028.0
FWHM bandwidth (nm)	16.5	29.5	34.2	39.8
Time-bandwidth product	0.392	0.309	0.281	0.307
Relative deviation of TBP from $sech^2$	1.25	0.98	0.89	0.97
Introduced GDD per roundtrip (fs^2)	-6000	-1500	-900	-900
Intra cavity peak power (MW)	350	477	587	820
Kerr medium distance from CM2 (mm)	560	545	545	548
Repetition rate (MHz)	17.3	17.1	17.1	17.1
Output coupling rate (%)	12	5.0	0.77	0.77
Pump power (W)	580	350	150	315
Pump-spot diameter (mm)	4.0	2.9	2.9	2.9
Optical-to-optical efficiency (%)	12	4.9	1.7	1.1
Hard aperture diameter (mm)	3.6	4.0	4.2	4.2
Sapphire plate thickness (mm)	4	2	2	2
Laser polarization	p	s	s	s

The 27-fs and 29-fs configurations are optimized for the shortest pulse duration. For this purpose, we selected a low output-coupling rate of 0.77% and further reduced the introduced total roundtrip GDD to -900 fs^2. The 27-fs is a rather extreme configuration of the laser. It requires a pump power of 350 W, which is more than 2 × higher compared to the 29-fs one [Table 1]. The only other difference between both configurations is the slightly different position of the Kerr medium, which was moved during the mode-locked operation by ~3 mm out of the

Optics EXPRESS

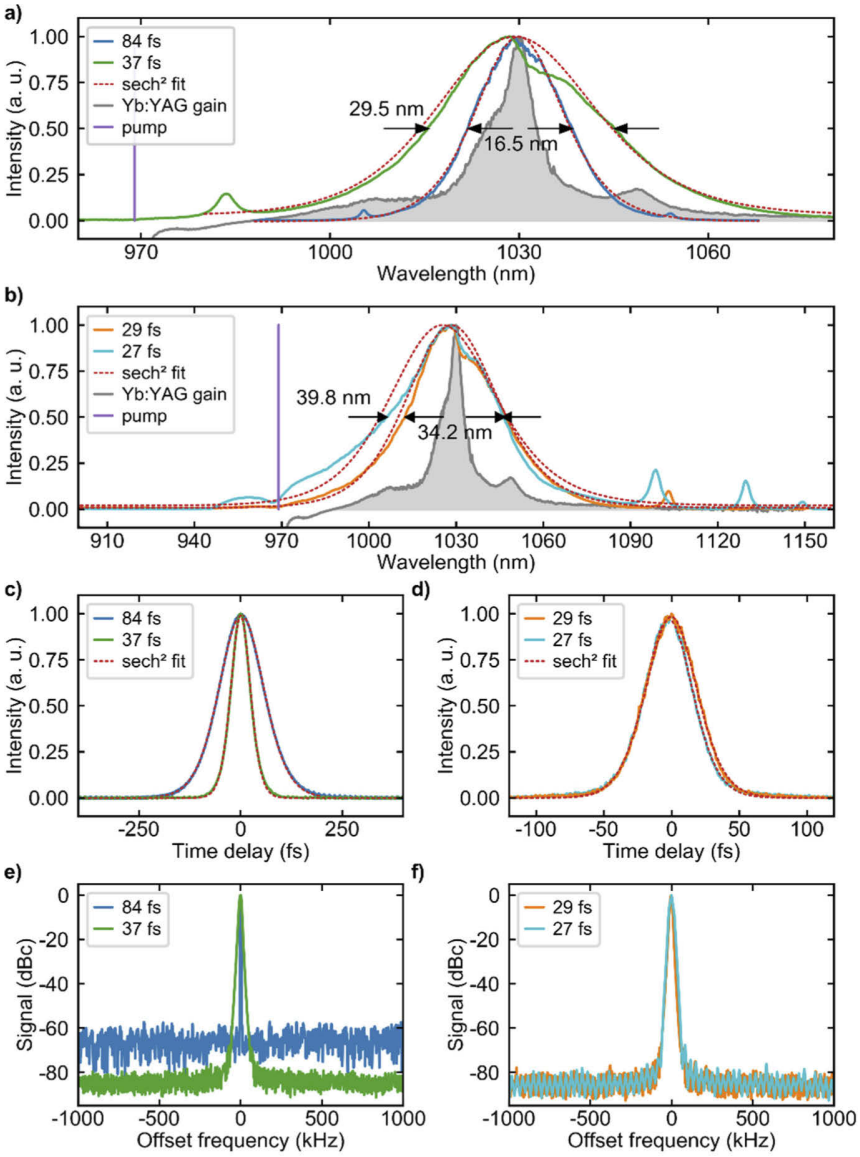

Fig. 3. a) and b) Optical spectra of the laser output with least-squares fits of sech^2 soliton pulses and normalized gain cross-section of Yb:YAG at an inversion level of 0.3. The pump wavelength of 969 nm is depicted by the purple line. c) and d) Intensity autocorrelation traces with fits for sech^2 soliton pulses. e) and f) Radio-frequency (RF) spectrum of the fundamental repetition-rate at 17.1 MHz measured at 10-kHz resolution bandwidth. The 84-fs laser configuration was characterized using a different RF analyzer at 3-kHz resolution bandwidth using a higher-bandwidth photodiode, thus, the noise level of this measurement is slightly higher than the others.

Optics EXPRESS

focus. At this extreme performance, the 39.8-nm FWHM optical spectrum deviates from the ideal sech^2 shape and clearly extends towards shorter wavelength even beyond the 969-nm pump wavelength [Fig. 3(b)]. The dip at the pump wavelength can be attributed to the reabsorption of the spectral components, originally generated by the SPM in the Kerr medium, inside the Yb:YAG gain material. On the other hand, the 29-fs configuration is much more relaxed. It requires only 150 W of pump power leading to an optical-to-optical efficiency of 1.7%. The 34.2-nm FWHM optical spectrum follows closer the ideal sech^2 shape. Nevertheless, we achieve a slightly too low time-bandwidth-product (TBP) of 0.281 (0.89× ideal sech^2). We attribute this deviation to the gain bump in the optical spectrum artificially narrowing its FWHM.

Single-pulse operation was verified for each configuration by a 180-ps autocorrelator scan and by observing the pulse train on a 40-GHz sampling oscilloscope with an 18.5-ps-rise-time photodetector. The radio-frequency spectra [Fig. 3(e), (f)] measured at the fundamental repetition frequency of 17.1 MHz show no side peaks down to the measurement noise floor indicating stable mode-locking.

4. Introduced group delay dispersion

One of the key challenges in shortening the pulse duration is the optimization of the introduced GDD for a flat profile over a broad spectral range. For the results presented here, the introduced GDD per cavity roundtrip by the DMs is shown in Fig. 4 in comparison to the corresponding optical spectra in shaded colors. The coatings of the dispersive mirrors were designed and

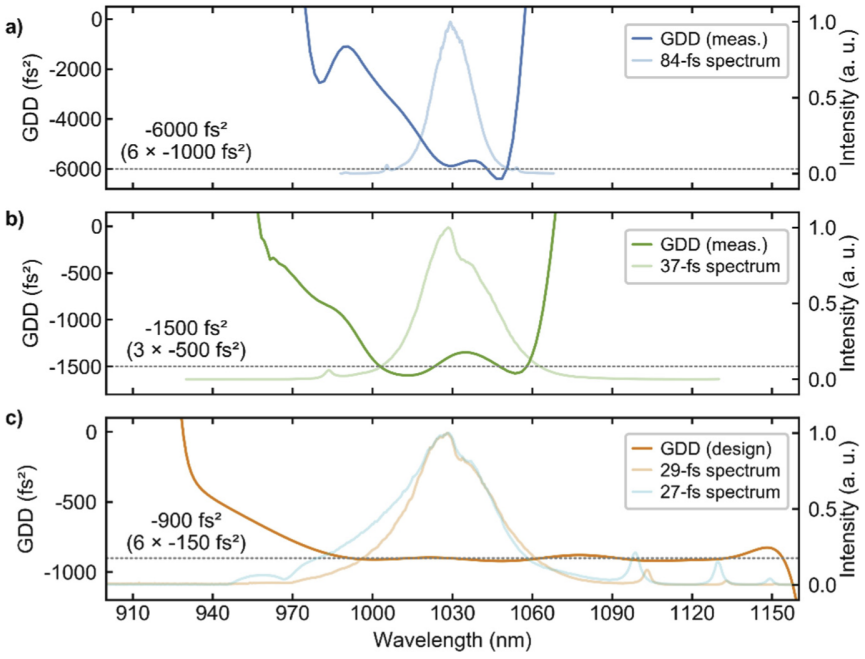

Fig. 4. Total introduced GDD of the DMs per cavity roundtrip for the four presented laser configurations in comparison to the corresponding optical spectrum. The nominal values are indicated by the horizontal dotted lines. For a) and b) the dispersion profile of the dispersive mirrors used in the 84-fs and 37-fs laser configuration was obtained by measuring the single-bounce GDD of a DM with an in-house developed white-light interferometer and multiplied by the number of bounces per cavity roundtrip. c) The introduced GDD of the 29-fs and 27-fs laser configuration is based on the design of the DMs.

Optics EXPRESS

manufactured inhouse in our ion-beam sputtering coating facility. For the 84-fs and 37-fs configuration, the dispersion profile of the DMs was measured utilizing a home-build white-light interferometer and multiplied by the number of bounces per cavity roundtrip. In the shortest-pulse configurations, the flat dispersion range of the DMs exceeded the spectral coverage of the white-light interferometer restricting us to rely on the design parameters. As can be seen exemplarily in the 84-fs configuration, the flat dispersion range is truncated by a gradually rising edge towards shorter wavelengths and a steep edge towards longer wavelengths, a common feature in the here applied double-resonant Gires-Tournois- Interferometer (GTI) type dispersive mirror design. While towards shorter pulse durations, the total amount of introduced negative GDD was decreased, the flat dispersion profile had to be extended over a broader spectral range to support a broader optical spectrum. This was realized in a chirped-mirror-type dispersive mirror design. In the trade-off between the GDD per bounce and the spectral width of the flat dispersion profile, the GDD per bounce had to be reduced. It amounted for the 84-fs configuration to $6 \times$ -1000 fs^2, for the 37-fs configuration to $3 \times$ -500 fs^2, and for the 27-fs / 29-fs configuration to $6 \times$ -150 fs^2. A further reduction of the introduced GDD to -750 fs^2 ($5 \times$ -150 fs^2) resulted repeatably in strong Q-switching and a damage in the Kerr medium.

Towards shorter pulse durations, we observe the expansion of the optical spectrum only towards shorter wavelengths. We attribute the limitation at the longer wavelength side to the unknown optical coatings of the thin disk. We expect shorter pulse durations within reach by optimization of all optical coatings including the coatings of the thin disk.

5. Conclusion

We have presented the experimental investigation of a KLM TDL oscillator based on commercially available Yb:YAG gain material operating in the strongly SPM-broadened regime. We have discussed the optimization of the introduced negative group delay dispersion that enabled generating pulses as short as 27 fs, corresponding to the shortest pulse duration of any ultrafast TDL oscillator [14]. Independent of the gain material, we considerably exceed the average power in comparison to previous sub-100-fs TDL oscillators of similar pulse duration [14–17]. This result is particularly important for the original purpose of our laser of driving intra-oscillator HHG [23], where short pulse durations strongly benefit the phase-matching of the XUV light [24]. We also expect being able to increase the output power of the laser well above the 100-W level at a few tens of femtoseconds pulse duration. Thanks to the clean soliton spectrum and excellent beam quality, the laser output should be ideally suited for further nonlinear pulse compression into the single-cycle regime within a single compression stage [25–27]. The ultrashort megahertz-repetition-rate pulses will be beneficial for experiments in the attosecond domain. Additionally, the laser output should be simultaneously available with the intra-oscillator HHG generated XUV light, offering a compact solution for pump-probe experiments. We expect even shorter pulse durations within reach by the optimization of the optical coatings including the coatings of the thin disk.

Funding. Schweizerischer Nationalfonds zur Förderung der Wissenschaftlichen Forschung (200020_179146, 200020_200774, 206021_144970, 206021_170772, 206021_198176).

Disclosures. The authors declare that there are no conflicts of interest related to this article.

Data availability. Data underlying the results presented in this paper are available in Ref. [28]

References

1. D. T. Reid, C. M. Heyl, R. R. Thomson, R. Trebino, G. Steinmeyer, H. H. Fielding, R. Holzwarth, Z. Zhang, P. Del'Haye, T. Südmeyer, G. Mourou, T. Tajima, D. Faccio, F. J. M. Harren, and G. Cerullo, "Roadmap on ultrafast optics," J. Opt. **18**(9), 093006 (2016).
2. Y. Wang, X. Su, Y. Xie, F. Gao, S. Kumar, Q. Wang, C. Liu, B. Zhang, B. Zhang, and J. He, "17.8 fs broadband Kerr-lens mode-locked Yb:CALGO oscillator," Opt. Lett. **46**(8), 1892–1895 (2021).

Optics EXPRESS

3. J. Ma, F. Yang, W. Gao, X. Xiaodong, X. Jun, D. Shen, and D. Tang, "Sub-five-optical-cycle pulse generation from a Kerr-lens mode-locked Yb:$CaYAlO_4$ laser," Opt. Lett. **46**(10), 2328 (2021).
4. A. Giesen, H. Hügel, A. Voss, K. Wittig, U. Brauch, and H. Opower, "Scalable concept for diode-pumped high-power solid-state lasers," Appl. Phys. B **58**(5), 365–372 (1994).
5. J. Aus der Au, G. J. Spühler, T. Südmeyer, R. Paschotta, R. Hövel, M. Moser, S. Erhard, M. Karszewski, A. Giesen, and U. Keller, "16.2-W average power from a diode-pumped femtosecond Yb:YAG thin disk laser," Opt. Lett. **25**(11), 859–861 (2000).
6. C. J. Saraceno, D. Sutter, T. Metzger, and M. Abdou Ahmed, "The amazing progress of high-power ultrafast thin-disk lasers," J. Eur. Opt. Soc.-Rapid Publ. **15**(1), 15 (2019).
7. F. Saltarelli, I. J. Graumann, L. Lang, D. Bauer, C. R. Phillips, and U. Keller, "Power scaling of ultrafast oscillators: 350-W average-power sub-picosecond thin-disk laser," Opt. Express **27**(22), 31465–31474 (2019).
8. J. Brons, V. Pervak, D. Bauer, D. Sutter, O. Pronin, and F. Krausz, "Powerful 100-fs-scale Kerr-lens mode-locked thin-disk oscillator," Opt. Lett. **41**(15), 3567–3570 (2016).
9. F. Labaye, M. Gaponenko, N. Modsching, P. Brochard, C. Paradis, S. Schilt, V. J. Wittwer, and T. Südmeyer, "XUV sources based on intra-oscillator high harmonic generation with thin-disk lasers: Current status and prospects," IEEE J. Sel. Top. Quantum Electron. **25**(4), 1–19 (2019).
10. T. Südmeyer, C. Kränkel, C. R. E. Baer, O. H. Heckl, C. J. Saraceno, M. Golling, R. Peters, K. Petermann, G. Huber, and U. Keller, "High-power ultrafast thin disk laser oscillators and their potential for sub-100-femtosecond pulse generation," Appl. Phys. B **97**(2), 281–295 (2009).
11. C. J. Saraceno, O. H. Heckl, C. R. E. Baer, C. Schriber, M. Golling, K. Beil, C. Kränkel, T. Südmeyer, G. Huber, and U. Keller, "Sub-100 femtosecond pulses from a SESAM modelocked thin disk laser," Appl. Phys. B **106**(3), 559–562 (2012).
12. C. Schriber, F. Emaury, A. Diebold, S. Link, M. Golling, K. Beil, C. Kränkel, C. J. Saraceno, T. Südmeyer, and U. Keller, "Dual-gain SESAM modelocked thin disk laser based on Yb:Lu_2O_3 and Yb:Sc_2O_3," Opt. Express **22**(16), 18979–18986 (2014).
13. A. Diebold, F. Emaury, C. Schriber, M. Golling, C. J. Saraceno, T. Südmeyer, and U. Keller, "SESAM mode-locked Yb:$CaGdAlO_4$ thin disk laser with 62 fs pulse generation," Opt. Lett. **38**(19), 3842–3845 (2013).
14. N. Modsching, C. Paradis, F. Labaye, M. Gaponenko, I. J. Graumann, A. Diebold, F. Emaury, V. J. Wittwer, and T. Südmeyer, "Kerr lens mode-locked Yb:CALGO thin-disk laser," Opt. Lett. **43**(4), 879–882 (2018).
15. C. Paradis, N. Modsching, V. J. Wittwer, B. Deppe, C. Kränkel, and T. Südmeyer, "Generation of 35-fs pulses from a Kerr lens mode-locked Yb:Lu_2O_3 thin-disk laser," Opt. Express **25**(13), 14918–14925 (2017).
16. N. Modsching, J. Drs, J. Fischer, C. Paradis, F. Labaye, M. Gaponenko, C. Kränkel, V. J. Wittwer, and T. Südmeyer, "Sub-100-fs Kerr lens mode-locked Yb:Lu_2O_3 thin-disk laser oscillator operating at 21 W average power," Opt. Express **27**(11), 16111–16120 (2019).
17. J. Zhang, J. Brons, M. Seidel, V. Pervak, V. Kalashnikov, Z. Wei, A. Apolonski, F. Krausz, and O. Pronin, "49-fs Yb:YAG thin-disk oscillator with distributed Kerr-lens mode-locking," in *European Quantum Electronics Conference* (Optical Society of America, 2015), paper PD_A_1.
18. M. Tokurakawa, A. Shirakawa, K. Ueda, H. Yagi, S. Hosokawa, T. Yanagitani, and A. A. Kaminskii, "Diode-pumped 65 fs Kerr-lens mode-locked Yb^{3+}:Lu_2O_3 and nondoped Y_2O_3 combined ceramic laser," Opt. Lett. **33**(12), 1380–1382 (2008).
19. J. Fischer, J. Drs, F. Labaye, N. Modsching, V. Wittwer, and T. Südmeyer, "Intra-oscillator high harmonic generation in a thin-disk laser operating in the 100-fs regime," Opt. Express **29**(4), 5833–5839 (2021).
20. J. Brons, V. Pervak, E. Fedulova, D. Bauer, D. Sutter, V. Kalashnikov, A. Apolonskiy, O. Pronin, and F. Krausz, "Energy scaling of Kerr-lens mode-locked thin-disk oscillators," Opt. Lett. **39**(22), 6442–6445 (2014).
21. O. Pronin, J. Brons, C. Grasse, V. Pervak, G. Boehm, M.-C. Amann, V. L. Kalashnikov, A. Apolonski, and F. Krausz, "High-power 200 fs Kerr-lens mode-locked Yb:YAG thin-disk oscillator," Opt. Lett. **36**(24), 4746–4748 (2011).
22. A. A. Eilanlou, Y. Nabekawa, M. Kuwata-Gonokami, and K. Midorikawa, "Femtosecond laser pulses in a Kerr lens mode-locked thin-disk ring oscillator with an intra-cavity peak power beyond 100 MW," Jpn. J. Appl. Phys. **53**(8), 082701 (2014).
23. F. Labaye, M. Gaponenko, V. J. Wittwer, A. Diebold, C. Paradis, N. Modsching, L. Merceron, F. Emaury, I. J. Graumann, C. R. Phillips, C. J. Saraceno, C. Kränkel, U. Keller, and T. Südmeyer, "Extreme ultraviolet light source at a megahertz repetition rate based on high-harmonic generation inside a mode-locked thin-disk laser oscillator," Opt. Lett. **42**(24), 5170–5173 (2017).
24. S. Hädrich, J. Rothhardt, M. Krebs, S. Demmler, A. Klenke, A. Tünnermann, and J. Limpert, "Single-pass high harmonic generation at high repetition rate and photon flux," J. Phys. B: At., Mol. Opt. Phys. **49**(17), 172002 (2016).
25. M. Müller, J. Buldt, H. Stark, C. Grebing, and J. Limpert, "Multipass cell for high-power few-cycle compression," Opt. Lett. **46**(11), 2678–2681 (2021).
26. S. Gröbmeyer, K. Fritsch, B. Schneider, M. Poetzlberger, V. Pervak, J. Brons, and O. Pronin, "Self-compression at 1 µm wavelength in all-bulk multi-pass geometry," Appl. Phys. B **126**(10), 159 (2020).
27. C.-L. Tsai, F. Meyer, A. Omar, Y. Wang, A.-Y. Liang, C.-H. Lu, M. Hoffmann, S.-D. Yang, and C. J. Saraceno, "Efficient nonlinear compression of a mode-locked thin-disk oscillator to 27 fs at 98 W average power," Opt. Lett. **44**(17), 4115–4118 (2019).
28. J. Drs, Sub-30-fs Yb:YAG thin-disk laser oscillator operating in the strongly self-phase modulation broadened regime, EUDAT (2021), http://doi.org/10.23728/b2share.42d04391fbcf47f7b0ddde764f18f270.

213.55.220.185 (s 2021-12-04 17:02:52)

Research Article | Vol. 29, No. 25 / 6 Dec 2021 / Optics Express 42075
Optics EXPRESS

Efficient 100-MW, 100-W, 50-fs-class Yb:YAG thin-disk laser oscillator

JULIAN FISCHER,* JAKUB DRS, NORBERT MODSCHING, FRANÇOIS LABAYE, VALENTIN J. WITTWER, AND THOMAS SÜDMEYER

Laboratoire Temps-Fréquence (LTF), Institut de Physique, Université de Neuchâtel, Avenue de Bellevaux 51, 2000 Neuchâtel, Switzerland
julian.fischer@unine.ch

Abstract: We demonstrate an efficient 102-MW peak power, 103-W average power, Kerr-lens mode-locked thin-disk laser (TDL) oscillator generating 52-fs pulses at 17.1-MHz repetition rate. The TDL is based on an Yb:YAG disk and operates in the strongly self-phase-modulation (SPM) broadened regime. In this regime, the spectral bandwidth of the oscillating pulse exceeds the available gain bandwidth by generating additional frequency components via SPM in the Kerr medium inside the laser cavity. At an optical-to-optical efficiency of 26%, our oscillator delivers a more than six times higher average power compared to any 50-fs-class laser oscillator. Compared to previous 100-W-class high-power laser oscillators, we reach this performance in a more than two times shorter pulse duration at a comparable optical-to-optical efficiency. Our TDL delivers the highest peak power of any ultrafast laser oscillator. The short pulse duration combined with high average power and peak power makes the presented TDL oscillator an attractive source for high field science and nonlinear optics.

© 2021 Optica Publishing Group under the terms of the Optica Open Access Publishing Agreement

1. Introduction

Ultrafast lasers have enabled nonlinear frequency conversion processes such as high harmonic generation (HHG), optical parametric amplification (OPA), or THz generation, providing coherent light at a wide range of photon energies [1,2]. Many experiments relying on these technologies such as multidimensional spectroscopy or pump probe measurements strongly benefit from high repetition rates allowing for shorter acquisition times. This has stimulated the development of megahertz-repetition-rate laser systems over the last decade. The resulting need for higher average powers has caused a shift from a Ti:sapphire to an Yb-based laser technology. Due to the low quantum defect and availability of efficient diode pumping, ultrafast Yb-based laser amplifier systems can reach kilowatts of average power at sub-picosecond pulse durations and megahertz repetition rates. Up to 10.4 kW at 254 fs and 80 MHz have already been demonstrated using twelve coherently combined fiber laser amplifiers [3], 620 W at 640 fs and 20 MHz using an Innoslab amplifier [4], and 1.9 kW at 1 ps and 400 kHz based on a multi-pass thin-disk amplifier [5]. The high average power, however, comes at the expense of a longer pulse duration, typically >200 fs, due to the gain bandwidth of most common Yb-doped gain materials.

Another successful approach allowing for short pulses from Yb-based gain materials is ultrafast thin-disk laser (TDL) oscillators. Thanks to the thin-disk geometry, they can operate at high peak and average powers, while keeping the favorable properties inherent to laser oscillators. TDL oscillators provide transform-limited soliton pulses without temporal pre or post features and excellent beam quality at megahertz repetition rates and can thus be used as a single-stage alternative to laser amplifier systems. The output pulses are directly suited for nonlinear frequency conversion [6] as well as for few-cycle pulse compression [7,8]. Figure 1 shows an overview of ultrafast TDL oscillators with respect to peak power and pulse duration based on the two most common mode-locking techniques. While semiconductor saturable absorber mirror (SESAM)

#442833 https://doi.org/10.1364/OE.442833
Journal © 2021 Received 27 Sep 2021; revised 18 Nov 2021; accepted 18 Nov 2021; published 2 Dec 2021

Optics EXPRESS

mode-locked TDLs have been historically well-suited for delivering the highest average powers (currently up to 350 W), they only provide these power levels at >500-fs pulse durations, limiting the achievable peak power [9–11]. On the other hand, Kerr-lens mode-locked (KLM) TDLs have been particularly successful in delivering shorter pulse durations at high average power, enabling a higher peak power. Recently, 90 MW of peak power were presented in 140-fs pulses and 220 W of average power [12]. However, even for KLM TDLs, a clear trade-off between peak power and pulse duration can be observed for sub-100-fs pulse durations [Fig. 1].

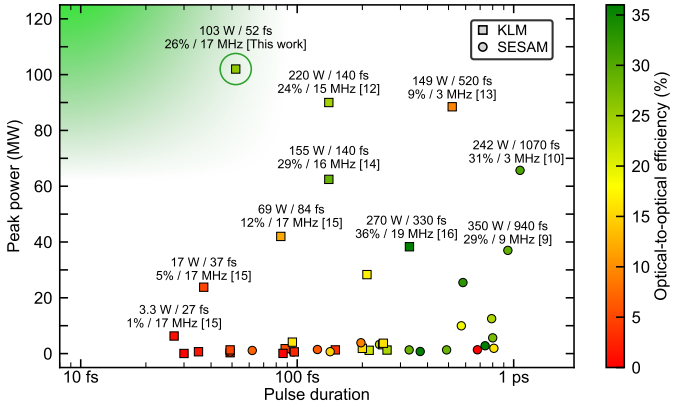

Fig. 1. Overview of sub-ps KLM and SESAM mode-locked thin-disk laser oscillators based on Yb-doped gain materials. Mode-locking techniques are distinguished by the symbol. KLM: Kerr-lens mode-locking; SESAM: semiconductor saturable absorber mirror. The most outstanding performances are labeled with average power, pulse duration, optical-to-optical efficiency, and repetition rate. The result presented in this manuscript is highlighted with the green circle. The green shaded area represents the favored region of laser operation at shortest pulse duration and highest peak power. References: [9,10,12–16].

As we have recently shown in [15], so far the most promising direction towards sub-100-fs pulse durations at high peak powers is based on operating a KLM Yb:YAG TDL oscillator in the strongly self-phase modulation (SPM) broadened regime. In this regime, additional frequency components outside of the gain bandwidth are generated by excessive SPM in the Kerr medium inside the laser cavity. We have demonstrated the shortest pulse duration of a TDL oscillator corresponding to 27 fs at 3.3-W average power and 6-MW peak power, but only with 1% of optical-to-optical efficiency ("efficiency" in the following). We have also shown 84-fs pulses at 69 W and 42 MW, however, even here the efficiency was still only 12%, limiting the achievable average and peak power.

Whereas our previous result was optimized for shortest pulse duration, in this work, we optimized our KLM Yb:YAG TDL operating in the SPM-broadened regime towards increased output performance, i.e. highest peak power, and efficiency. At 103 W of average output power with 52-fs pulses, our TDL delivers 102 MW of peak power at 26% efficiency. The peak power is the highest delivered by any ultrafast laser oscillator [12,13]. Compared to previous 100-W-class ultrafast TDL oscillators, we reach this performance range in a more than two times shorter pulse duration while maintaining a comparable efficiency [9–12,14].

2. Experimental setup

The setup of the KLM TDL oscillator is shown in Fig. 2. The oscillator is housed in a vacuum chamber with a footprint of 0.8×1.6 m^2 and operates at a pressure of around 1 mbar. The laser

Optics EXPRESS

is built using a commercially available TDL head (Trumpf GmbH) designed for 36 passes of the pump. An Yb:YAG disk with a thickness of ~100-µm and ~20-m concave radius of curvature (RoC) is used. The disk is optically pumped on a 2.9-mm diameter pump spot at a wavelength of 969 nm with a fiber-coupled wavelength-stabilized pump diode (Dilas Diodenlaser GmbH). The pump system is capable of delivering up to 2 kW of pump average power, but we limited ourselves to a maximum pump power of 400 W, resulting in a pump intensity of ~6 kW/cm^2 on the disk, to prevent the risk of damaging the disk.

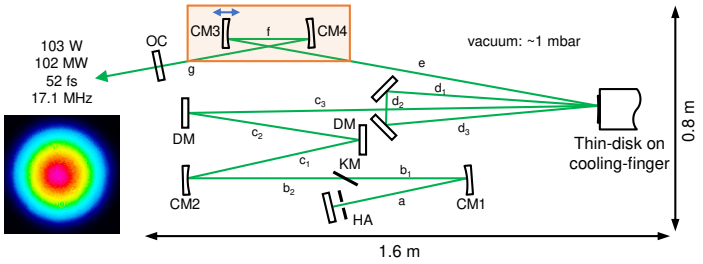

Fig. 2. Schematic of the Kerr-lens mode-locked Yb:YAG thin-disk laser oscillator with double pass over the disk. The orange box highlights the tight focus created between two curved mirrors, CM3 and CM4, which has been implemented for intra-oscillator high harmonic generation. As indicated by the double arrow, CM3 is mounted on a translation stage used for fine-tuning of the laser cavity during mode-locked operation. The inset shows the beam profile of the laser output in mode-locked operation when the laser generates 52-fs pulses at 103-W average power. HA: hard aperture; CM1 and CM2: concave mirror with 1-m radius of curvature (RoC); KM: Kerr medium; DM: dispersive mirror; CM3 and CM4: concave mirror with 150-mm and 250-mm RoC; OC: output coupler. Cavity lengths: a = 520 mm; b_1 = 475 mm; b_2 = 550 mm; c_1+c_2+c_3 = 3455 mm; d_1+d_2+d_3 = 1545 mm; e = 1780mm; f = ~200 mm; g = 250 mm.

The laser cavity is folded twice over the disk for higher roundtrip gain. Following the standard scheme of Kerr-lens mode-locking for TDLs [17], a wedged (30 arcmin) 1-mm-thick *c*-cut sapphire plate acts as the Kerr medium which is placed under Brewster's angle in the vicinity of a first intracavity focus created by two concave mirrors, CM1 and CM2, with 1-m RoC. A water-cooled copper plate with a 4.4-mm diameter hole serves as a hard aperture for the fast-saturable loss. The Kerr medium is purged with oxygen from both sides to prevent contamination during laser operation, for example through carbon deposition in vacuum. Two -500-fs^2 dispersive mirrors (DM) in folding configuration introduce a total negative group delay dispersion (GDD) of -2000 fs^2 per cavity roundtrip. The corresponding spectral profile of the GDD is shown in Fig. 3(a), which was obtained by measuring the GDD of the DMs with an in-house developed white-light interferometer and multiplied by the number of bounces per cavity roundtrip. The TDL setup has been originally designed for intra-oscillator HHG [18] and the output coupling arm of the oscillator thus contains an extension intended to create a tight focus for HHG. It consists of two concave mirrors with a RoC of 150 mm (CM3) and 250 mm (CM4) leading to an estimated tight focus of ~20-µm radius in mode-locked operation. Due to the tight focus, operation of the TDL strictly requires vacuum. In ambient air, the intensity in the focus would exceed the air ionization level and the plasma formation would prevent mode-locking. CM3 is placed on a motorized linear stage, allowing to tune the laser cavity from a position where it is easy to start the mode-locking operation to a position of improved intracavity and output performance. Before mode-locking can be initialized, the distance between CM3 and CM4 is slightly increased in order to decrease the beam size on the aperture, facilitating the onset of mode-locking. Mode-locked operation is initiated by shaking one of the cavity mirrors

Optics EXPRESS

through a piezo actuator. After mode-locking is started, the pump power is decreased until the continuous-wave (cw) breakthrough otherwise visible in the optical spectrum disappears. Then, the pump power is again slowly increased while at the same time the distance between CM3 and CM4 is decreased, increasing the beam size on the hard aperture. This procedure allows operation of the TDL at maximum pump power without the appearance of a cw-breakthrough. Between the mode-locking starting position and the final, high-power operation position, the linear stage is moved by less than 1 mm, resulting in a ~20% decrease in pulse duration and a peak power increase by a factor of ~2 while the pump power is also increased by a factor of ~2. The cavity remains stable for cw-operation in all configurations. Further details about the optimization of the TDL regarding, e.g., the hard aperture size or the thickness of the Kerr medium are given in our recent publication [15]. The cavity end mirror after the tight focus serves as an output coupler with a transmission (T_{OC}) of 8.5%.

To increase the thermal stability of the laser system in vacuum, the cavity is built on a water-cooled breadboard and most of the mirror mounts are water-cooled. The optical coatings of the dispersive and highly reflective mirrors have been designed inhouse and grown in our ion-beam sputtering coating facility.

3. Experimental results

Table 1 summarizes the laser parameters and mode-locking performance of our TDL. The oscillator delivers an output power of 103 W, a peak power of 102 MW, and pulse energy of 5.5 µJ at a pulse duration of 52 fs. These parameters correspond to an intracavity peak and intracavity average power of 1.2 GW and 1.2 kW, respectively. The pump power of 400 W leads to an efficiency of 26%. This efficiency is for the first time comparable to the efficiency of other 100-W-class high-power TDLs operating with significantly longer pulses [9–12,14].

Table 1. Laser parameters and corresponding mode-locking performance of our TDL oscillator.

Laser parameter	Value	Laser parameter	Value
Output coupler transmission	8.5%	Pulse energy	5.5 µJ
Introduced roundtrip GDD	-2000 fs^2	Intracavity peak power	1.2 GW
Hard aperture diameter	4.4 mm	Intracavity average power	1.2 kW
Pump power	400 W	Pulse duration	52 fs
Output power	103 W	Central wavelength	1027.3 nm
Optical-to-optical efficiency	26%	FWHM bandwidth	21.4 nm
Peak power	102 MW	Repetition rate	17.1 MHz

Figure 3(a) shows the optical spectrum of the output pulses together with the normalized gain cross-section of Yb:YAG at an inversion level of 0.3. The optical spectrum is centered at a wavelength of 1027.3 nm. The central wavelength is blue-shifted by ~2 nm, away from the gain peak of Yb:YAG at 1030 nm. With a full width at half maximum (FWHM) bandwidth of 21.4 nm, the optical spectrum exceeds the ~8-nm FHWM gain bandwidth of Yb:YAG more than twice, indicating operation of the TDL in the strongly SPM-broadened regime [15,19,20]. Despite a small shoulder at the longer wavelength side, a feature that is commonly observed for TDL oscillators operating in the SPM-broadened regime [15,19,20], the $sech^2$ fit agrees well with the shape expected for soliton pulses. Also, the intensity autocorrelation of the 52-fs pulses is in excellent agreement with the fit for soliton pulses [Fig. 3(b)]. We achieve an ideal time-bandwidth product of 0.315, indicating the generation of transform-limited soliton pulses. The radio-frequency spectrum measured at the fundamental repetition frequency of 17.1 MHz shows no side peaks [Fig. 3(c)]. Modulation-free higher harmonics confirm clean mode-locking [inset of Fig. 3(c)]. We confirmed single pulse operation by a 180-ps scan in the autocorrelator

Optics EXPRESS

and by observing the pulse train with an 18.5-ps-rise-time photodetector on a 40-GHz sampling oscilloscope [Fig. 3(d)]. The output pulses feature an excellent fundamental mode Gaussian beam profile [inset of Fig. 2].

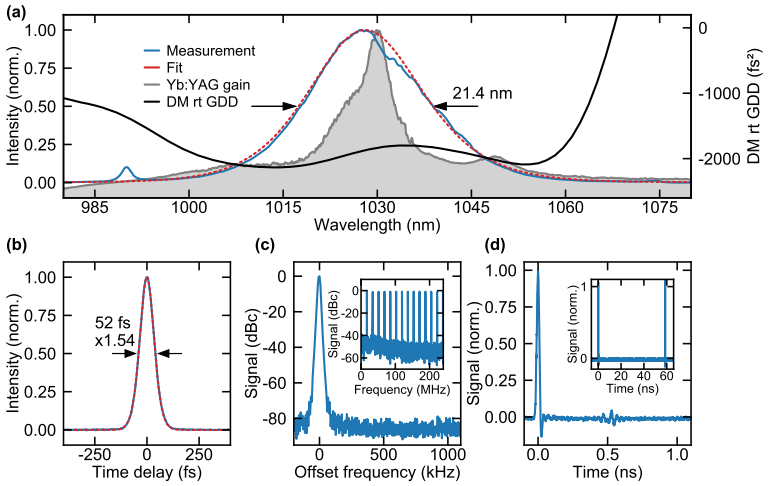

Fig. 3. Characterization of the Kerr-lens mode-locked Yb:YAG thin-disk laser oscillator. (a) Normalized optical spectrum of the laser output with sech^2 fit. In addition, the normalized Yb:YAG gain cross section at an inversion level of 0.3 (data taken from [22]) and the total group delay dispersion (GDD) introduced by the dispersive mirrors (DM) per cavity round-trip (rt) are shown. (b) Intensity autocorrelation trace with fit for soliton pulses. (c) Radio-frequency (RF) spectrum of the fundamental repetition rate (f_{rep}) at 17.1 MHz measured with 10-kHz resolution bandwidth (RBW). The inset shows the RF-spectrum of the higher f_{rep} harmonics measured with 30-kHz RBW. (d) Sampling oscilloscope trace for 1-ns and 70-ns (inset) time window.

Within our pump power restriction of 400 W (~6 kW/cm^2) set to prevent damage of the disk, we were not able to mode-lock the laser at a T_{OC} higher than 8.5%. We expect that higher pump intensities of ~10 kW/cm^2 [16,21] should allow for mode-locking at a T_{OC} above 10% and a corresponding performance improvement. High-power operation of our TDL is currently limited to a few minutes by the overheating of the non-water-cooled connector of the pump-delivery fiber in the vacuum environment. After changing to a water-cooled fiber, we expect long-term operability.

4. Conclusion and outlook

We have demonstrated an efficient 102-MW peak power, 103-W average power KLM TDL oscillator generating 52-fs pulses at 17.1-MHz repetition rate. The TDL oscillator is based on Yb:YAG gain material and operates in the strongly SPM-broadened regime at an efficiency of 26%. Our average output power is more than six times higher than any previous 50-fs-class laser oscillator [15,19,20]. Furthermore, we achieve the highest peak power delivered by any ultrafast laser oscillator [12,13]. Compared to previous 100-W-class high-power TDL oscillators, we reach this performance range in a more than two times shorter pulse duration while maintaining a comparable efficiency [9–12,14]. The clean soliton pulses with excellent beam quality and high peak power are well suited for broadband THz generation [23] or oscillator-driven HHG [24].

Additionally, the output of our TDL oscillator is very suitable for consecutive temporal pulse compression. Whereas efficient compression starting from several hundred femtoseconds down

Optics EXPRESS

to few-cycle pulses is already feasible [7,25–27], the compression often comes with reduced pulse contrast as well as limited beam quality and thus remains a challenging task. Thanks to our clean 52-fs soliton pulses and assuming a compression ratio of ten for a single compression stage [8,28,29], we expect being able to reach few-cycle pulse durations within a single instead of the typically at least two required cascaded temporal compression stages. This would make our source an excellent choice for applications requiring few-cycle pulses at high pulse contrast, excellent beam quality, and MHz repetition rates. After carrier-envelope phase stabilization of the TDL operating in the SPM-broadened regime [30], even applications in the single-cycle regime could be addressed.

Since the thin-disk concept is power scalable and we have not encountered any physical limitation, we expect that further power-scaling is feasible and that 50-fs-class TDL oscillators operating at several hundred megawatts of peak power are within reach.

Funding. Schweizerischer Nationalfonds zur Förderung der Wissenschaftlichen Forschung (200020_179146, 200020_200774, 206021_144970, 206021_170772, 206021_198176).

Disclosures. The authors declare that there are no conflicts of interest related to this article.

Data availability. Data underlying the results presented in this paper are available in Ref. [31].

References

1. D. T. Reid, C. M. Heyl, R. R. Thomson, R. Trebino, G. Steinmeyer, H. H. Fielding, R. Holzwarth, Z. Zhang, P. Del'Haye, T. Südmeyer, G. Mourou, T. Tajima, D. Faccio, F. J. M. Harren, and G. Cerullo, "Roadmap on ultrafast optics," J. Opt. **18**(9), 093006 (2016).
2. P. U. Jepsen, D. G. Cooke, and M. Koch, "Terahertz spectroscopy and imaging – Modern techniques and applications," Laser Photonics Rev. **5**(1), 124–166 (2011).
3. M. Müller, C. Aleshire, A. Klenke, E. Haddad, F. Légaré, A. Tünnermann, and J. Limpert, "10.4 kW coherently combined ultrafast fiber laser," Opt. Lett. **45**(11), 3083–3086 (2020).
4. P. Russbueldt, T. Mans, J. Weitenberg, H. D. Hoffmann, and R. Poprawe, "Compact diode-pumped 1.1 kW Yb:YAG Innoslab femtosecond amplifier," Opt. Lett. **35**(24), 4169–4171 (2010).
5. T. Dietz, M. Jenne, D. Bauer, M. Scharun, D. Sutter, and A. Killi, "Ultrafast thin-disk multi-pass amplifier system providing 1.9 kW of average output power and pulse energies in the 10 mJ range at 1 ps of pulse duration for glass-cleaving applications," Opt. Express **28**(8), 11415–11423 (2020).
6. C. Paradis, J. Drs, N. Modsching, O. Razskazovskaya, F. Meyer, C. Kränkel, C. J. Saraceno, V. J. Wittwer, and T. Südmeyer, "Broadband terahertz pulse generation driven by an ultrafast thin-disk laser oscillator," Opt. Express **26**(20), 26377–26384 (2018).
7. C.-L. Tsai, F. Meyer, A. Omar, Y. Wang, A.-Y. Liang, C.-H. Lu, M. Hoffmann, S.-D. Yang, and C. J. Saraceno, "Efficient nonlinear compression of a mode-locked thin-disk oscillator to 27 fs at 98 W average power," Opt. Lett. **44**(17), 4115–4118 (2019).
8. O. Pronin, M. Seidel, F. Lücking, J. Brons, E. Fedulova, M. Trubetskov, V. Pervak, A. Apolonski, T. Udem, and F. Krausz, "High-power multi-megahertz source of waveform-stabilized few-cycle light," Nat. Commun. **6**(1), 6988 (2015).
9. F. Saltarelli, I. J. Graumann, L. Lang, D. Bauer, C. R. Phillips, and U. Keller, "Power scaling of ultrafast oscillators: 350-W average-power sub-picosecond thin-disk laser," Opt. Express **27**(22), 31465–31474 (2019).
10. C. J. Saraceno, F. Emaury, C. Schriber, M. Hoffmann, M. Golling, T. Südmeyer, and U. Keller, "Ultrafast thin-disk laser with 80 µJ pulse energy and 242 W of average power," Opt. Lett. **39**(1), 9–12 (2014).
11. C. J. Saraceno, F. Emaury, O. H. Heckl, C. R. E. Baer, M. Hoffmann, C. Schriber, M. Golling, T. Südmeyer, and U. Keller, "275 W average output power from a femtosecond thin disk oscillator operated in a vacuum environment," Opt. Express **20**(21), 23535–23541 (2012).
12. S. Goncharov, K. Fritsch, and O. Pronin, "100 MW Thin-Disk Oscillator," in 2021 *Conference on Lasers and Electro-Optics Europe and European Quantum Electronics Conference, OSA Technical Digest* (Optical Society of America, 2021), paper cf_4_1.
13. N. Kanda, A. A. Eilanlou, T. Imahoko, T. Sumiyoshi, Y. Nabekawa, M. Kuwata-Gonokami, and K. Midorikawa, "High-Pulse-Energy Yb:YAG Thin Disk Mode-Locked Oscillator for Intra-Cavity High Harmonic Generation," in Advanced Solid State Lasers Congress (Optical Society of America, 2013), paper AF3A-8.
14. J. Brons, V. Pervak, D. Bauer, D. Sutter, O. Pronin, and F. Krausz, "Powerful 100-fs-scale Kerr-lens mode-locked thin-disk oscillator," Opt. Lett. **41**(15), 3567–3570 (2016).
15. J. Drs, J. Fischer, N. Modsching, F. Labaye, V. J. Wittwer, and T. Südmeyer, "Sub-30-fs Yb:YAG thin-disk laser oscillator operating in the strongly self-phase modulation broadened regime," Opt. Express **29**(22), 35929–35937 (2021).
16. J. Brons, V. Pervak, E. Fedulova, D. Bauer, D. Sutter, V. Kalashnikov, A. Apolonskiy, O. Pronin, and F. Krausz, "Energy scaling of Kerr-lens mode-locked thin-disk oscillators," Opt. Lett. **39**(22), 6442–6445 (2014).

Optics EXPRESS

17. O. Pronin, J. Brons, C. Grasse, V. Pervak, G. Boehm, M.-C. Amann, V. L. Kalashnikov, A. Apolonski, and F. Krausz, "High-power 200 fs Kerr-lens mode-locked Yb:YAG thin-disk oscillator," Opt. Lett. **36**(24), 4746–4748 (2011).
18. J. Fischer, J. Drs, F. Labaye, N. Modsching, V. Wittwer, and T. Südmeyer, "Intra-oscillator high harmonic generation in a thin-disk laser operating in the 100-fs regime," Opt. Express **29**(4), 5833–5839 (2021).
19. C. Paradis, N. Modsching, V. J. Wittwer, B. Deppe, C. Kränkel, and T. Südmeyer, "Generation of 35-fs pulses from a Kerr lens mode-locked Yb:Lu_2O_3 thin-disk laser," Opt. Express **25**(13), 14918–14925 (2017).
20. J. Zhang, J. Brons, M. Seidel, V. Pervak, V. Kalashnikov, Z. Wei, A. Apolonski, F. Krausz, and O. Pronin, "49-fs Yb:YAG thin-disk oscillator with distributed Kerr-lens mode-locking," in *European Quantum Electronics Conference* (Optical Society of America, 2015), paper PD_A_1.
21. J. Brons, "High-power femtosecond laser-oscillators for applications in high-field physics," Dissertation, Ludwig-Maximilians-Universität München (2017).
22. T. Südmeyer, C. Kränkel, C. R. E. Baer, O. H. Heckl, C. J. Saraceno, M. Golling, R. Peters, K. Petermann, G. Huber, and U. Keller, "High-power ultrafast thin disk laser oscillators and their potential for sub-100-femtosecond pulse generation," Appl. Phys. B **97**(2), 281–295 (2009).
23. C. J. Saraceno, "Mode-locked thin-disk lasers and their potential application for high-power terahertz generation," J. Opt. **20**(4), 044010 (2018).
24. S. Hädrich, J. Rothhardt, M. Krebs, S. Demmler, A. Klenke, A. Tünnermann, and J. Limpert, "Single-pass high harmonic generation at high repetition rate and photon flux," J. Phys. B At. Mol. Opt. Phys. **49**(17), 172002 (2016).
25. C. Grebing, M. Müller, J. Buldt, H. Stark, and J. Limpert, "Kilowatt-average-power compression of millijoule pulses in a gas-filled multi-pass cell," Opt. Lett. **45**(22), 6250–6253 (2020).
26. Y.-G. Jeong, R. Piccoli, D. Ferachou, V. Cardin, M. Chini, S. Hädrich, J. Limpert, R. Morandotti, F. Légaré, B. E. Schmidt, and L. Razzari, "Direct compression of 170-fs 50-cycle pulses down to 1.5 cycles with 70% transmission," Sci. Rep. **8**(1), 11794 (2018).
27. G. Barbiero, H. Wang, M. Graßl, S. Gröbmeyer, D. Kimbaras, M. Neuhaus, V. Pervak, T. Nubbemeyer, H. Fattahi, and M. F. Kling, "Efficient nonlinear compression of a thin-disk oscillator to 8.5 fs at 55 W average power," Opt. Lett. **46**(21), 5304–5307 (2021).
28. K. F. Mak, M. Seidel, O. Pronin, M. H. Frosz, A. Abdolvand, V. Pervak, A. Apolonski, F. Krausz, J. C. Travers, and P. St. J. Russell, "Compressing μJ-level pulses from 250 fs to sub-10 fs at 38-MHz repetition rate using two gas-filled hollow-core photonic crystal fiber stages," Opt. Lett. **40**(7), 1238–1241 (2015).
29. R. Klas, A. Kirsche, M. Gebhardt, J. Buldt, H. Stark, S. Hädrich, J. Rothhardt, and J. Limpert, "Ultra-short-pulse high-average-power megahertz-repetition-rate coherent extreme-ultraviolet light source," PhotoniX **2**, 4 (2021).
30. N. Modsching, C. Paradis, P. Brochard, N. Jornod, K. Gürel, C. Kränkel, S. Schilt, V. J. Wittwer, and T. Südmeyer, "Carrier-envelope offset frequency stabilization of a thin-disk laser oscillator operating in the strongly self-phase modulation broadened regime," Opt. Express **26**(22), 28461–28467 (2018).
31. J. Fischer, "Efficient 100-MW, 100-W, 50-fs-class Yb:YAG thin-disk laser oscillator,"*EUDAT* (2021).

213.55.220.185 {ts '2021-12-04 17:02:18'}

3 High harmonic generation inside thin-disk laser oscillators

Placing a noble gas target directly inside the cavity of a high-power thin-disk laser (TDL) oscillator, is a recent single-stage approach for building megahertz repetition rate coherent extreme-ultraviolet light (XUV) sources. A further introduction to the topic including an overview of other approaches for table-top coherent XUV sources is given in section 3.1. High harmonic generation (HHG) in a noble gas target is a process strongly depending on the peak intensity of the driving laser system. An important step for increasing the XUV output of any HHG system is thus the improvement of the peak power of the driving laser system. Furthermore, a short pulse duration of ideally only a few tens of femtosecond is required to suppress detrimental plasma effects negatively affecting the phase matching of the generated high harmonics [1]. The main focus for scaling the XUV output power of the HHG system developed in this thesis was thus the scaling of the intra-cavity peak power of the driving TDL oscillator. An overview of the progress of intra-cavity peak power against pulse duration is shown in Fig. 3.1. A clear trade-off of the two parameters could be observed prior to this thesis and intra-cavity peak powers of >100 MW were only achieved at >140 fs pulse durations. The initial semiconductor saturable absorber mirror (SESAM) mode-locked Yb:Lu_2O_3 TDL oscillator developed for intra-oscillator HHG in this research group in 2017 reached an intra-cavity peak power of only 64 MW at 264 fs pulse duration [2]. In a first step, the peak power of the system was increased to 170 MW while simultaneously reducing the pulse duration to 90 fs by changing from SESAM to Kerr lens mode-locking (KLM) [3]. The change of the gain material from Yb:Lu_2O_3 to commercially available Yb:YAG enabled further intra-cavity peak power scaling from here. Surprisingly, the narrower 8-nm FWHM gain bandwidth of Yb:YAG, directly supporting only ∼140-fs pulses, did not restrict the generation of several times shorter pulses by the in this thesis developed KLM TDL oscillator.[1] Shorter pulses were enabled by operating the TDL oscillator in the regime of strong intra-cavity self-phase

[1] Compared to Yb:YAG, Yb:Lu_2O_3 directly supports the generation of ∼90-fs pulses within its 13-nm FWHM gain bandwidth.

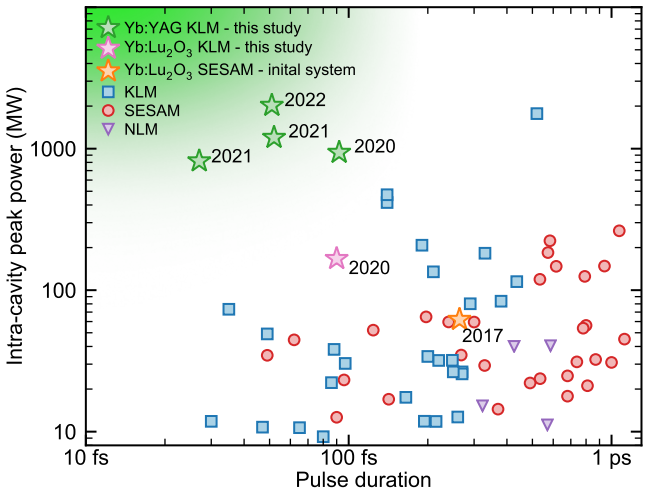

Figure 3.1: Overview of intra-cavity peak power against pulse duration for different TDL oscillators. The favored direction of the development towards highest intra-cavity peak power and shortest pulse duration is highlighted by the green shaded corner. Selected results are labeled by year of publication. The marker symbol emphasizes the employed mode-locking technique. KLM: Kerr lens mode-locking; SESAM: semiconductor saturable absorber mirror; NLM: non-linear mirror. The orange star marker shows the laser performance of the initial intra-oscillator HHG system based on a SESAM mode-locked Yb:Lu_2O_3 TDL developed in this research group in 2017 [2]. The pink star marker shows the performance after upgrading the initial Yb:Lu_2O_3 system from 2017 from SESAM to KLM [3]. The green star markers show the results based on a KLM Yb:YAG TDL oscillator (section 2.3, section 2.4, and [4, 5]).

modulation (SPM) where additional frequency components are generated via SPM in the Kerr medium inside the laser oscillator (section 2.3). Up to 0.9 GW at 92 fs pulse duration were achieved with the KLM Yb:YAG TDL oscillator in 2020 [4]. The intra-cavity performance was further improved thereafter, leading to the demonstration of 2 GW intra-cavity peak power, which is the highest intra-cavity peak power delivered by any ultrafast laser oscillator [5]. At 51 fs pulse duration, the latter system operated with an intra-cavity average power of 2 kW [5]. Despite reaching the highest intra-cavity peak power, also the shortest pulse duration of any ultrafast TDL oscillator amounting to 27 fs at an intra-cavity peak power of 0.8 GW was achieved (section 2.3). With this result, even shortest pulses generated by TDL oscillators based on significantly more broadband gain materials such as Yb:CALGO were surpassed [6].

Figure 3.2 shows the progress of the out-coupled XUV flux delivered by the intra-oscillator HHG source developed during this thesis in comparison to other state-of-the-art megahertz repetition rate XUV sources. The initial system of HHG inside a TDL oscillator in 2017 delivered an out-coupled XUV average power of less than 0.1 nW in a single harmonic at 13 eV. A first major result was achieved in 2021 when ∼60 nW were out-coupled at 30 eV after changing the 2017 system from SESAM to KLM and from Yb:Lu_2O_3 to Yb:YAG (section 3.1). Up to this point, the XUV out-coupling of all intra-oscillator HHG systems was based on a sapphire plate placed under Brewster's angle for the fundamental wavelength. As described in section 3.2, the challenge of this out-coupling mechanism is that it only supports the out-coupling of XUV light with energies around 25 eV with relatively sharp drops in XUV reflectivity towards higher and lower photon energies. Hence, finding a broadband and efficient XUV out-coupler presents another major challenge besides the intra-cavity peak

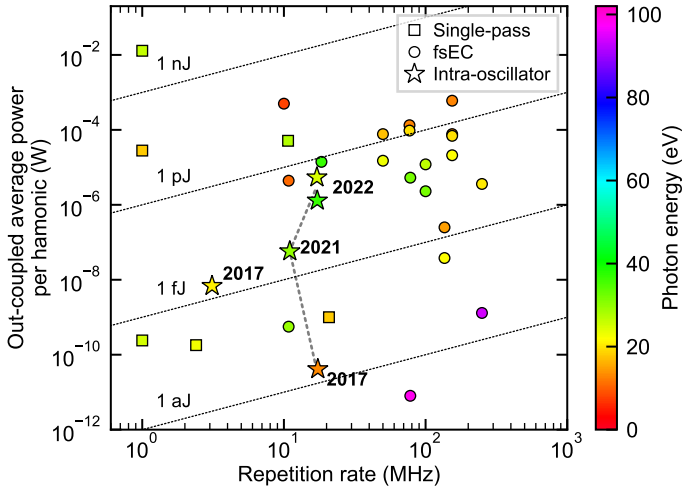

Figure 3.2: Overview of megahertz repetition rate XUV sources based on single-pass, femtosecond enhancement cavity (fsEC), and intra-oscillator HHG. The plot shows the out-coupled XUV average power per harmonic against the repetition rate and the color code represents the photon energy of the out-coupled XUV radiation. For single-pass HHG, an XUV out-coupling efficiency of 100% is assumed. Intra-oscillator sources are labeled by year. The dashed line indicates the progress of the here presented system: 2017: initial demonstration in this research group using a SESAM Yb:Lu_2O_3 TDL [2]; 2021: KLM Yb:YAG TDL with sapphire Brewster's plate XUV out-coupling (section 3.1); 2022: KLM Yb:YAG TDL with coated grazing-incidence plate XUV out-coupling (section 3.2).

power scaling of the driving oscillator. Out-coupling of intra-cavity generated high harmonics by a coated grazing-incidence plate (GIP) was proposed by [7] and enables more broadband XUV out-coupling while simultaneously increasing the XUV out-coupling efficiency. The during this thesis developed coated GIP features a broadband XUV out-coupling efficiency of >25% for photon energies ranging from 10 to 60 eV and presents the first intra-cavity implementation of the coated GIP XUV out-coupling mechanism (section 3.2). The coated GIP out-coupling combined with a further improvement of the KLM Yb:YAG TDL performance, enabled increasing the out-coupled XUV average power to 1.3 µW in a single harmonic at 37 eV in argon and 5.4 µW at 25 eV in xenon (section 3.2). Compared to the result from 2017, the out-coupled average XUV power has been increased by more than four orders of magnitude while simultaneously scaling the photon energy from 13 eV up to 37 eV. As shown by Fig. 3.2, the most recent intra-oscillator HHG result achieved during this thesis approaches the state-of-the-art out-coupled XUV average power levels of femtosecond enhancement cavities (fsEC) operating at comparable photon energies.

References

1. Hädrich, S., Rothhardt, J., Krebs, M., Demmler, S., Klenke, A., Tünnermann, A. & Limpert, J. Single-pass high harmonic generation at high repetition rate and photon flux. *Journal of Physics B: Atomic, Molecular and Optical Physics* **49**, 172002 (2016).

2. Labaye, F., Gaponenko, M., Wittwer, V. J., Diebold, A., Paradis, C., Modsching, N., Merceron, L., Emaury, F., Graumann, I. J., Phillips, C. R., Saraceno, C. J., Kränkel, C., Keller, U. & Südmeyer, T. Extreme ultraviolet light source at a megahertz repetition rate based on high-harmonic generation inside a mode-locked thin-disk laser oscillator. *Optics Letters* **42**, 5170 (2017).

3. Fischer, J., Drs, J., Labaye, F., Modsching, N., Kränkel, C., Wittwer, V. J. & Südmeyer, T. *Intra-Oscillator High Harmonic Generation in a ~100-fs Kerr-Lens Mode-Locked Thin-Disk Laser* in *Conference on Lasers and Electro-Optics 2020* (Optica Publishing Group, 2020), paper SF3H.3.

4. Fischer, J., Drs, J., Labaye, F., Modsching, N., Wittwer, V. J. & Südmeyer, T. *Intra-Oscillator High Harmonic Generation in a ~100-fs Kerr-Lens Mode-Locked Yb:YAG Thin-Disk Laser* in *Laser Congress 2020 (ASSL, LAC)* (Optica Publishing Group, 2020), paper AF3A.2.

5. Fischer, J., Drs, J., Labaye, F., Modsching, N., Müller, M., Wittwer, V. J. & Südmeyer, T. *High Harmonic Generation Inside Thin-Disk Laser Oscillators – An Efficient and Single-Stage XUV Source* in *Optica High-brightness Sources and Light-driven Interactions Congress 2022* (Optica Publishing Group, 2022), paper HW2B.3.

6. Modsching, N., Paradis, C., Labaye, F., Gaponenko, M., Graumann, I. J., Diebold, A., Emaury, F., Wittwer, V. J. & Südmeyer, T. Kerr lens mode-locked Yb:CALGO thin-disk laser. *Optics Letters* **43**, 879 (2018).

7. Pronin, O., Pervak, V., Fill, E., Rauschenberger, J., Krausz, F. & Apolonski, A. Ultrabroadband efficient intracavity XUV output coupler. *Optics Express* **19**, 10232 (2011).

Research Article | Vol. 29, No. 4 / 15 February 2021 / Optics Express 5833
Optics EXPRESS

Intra-oscillator high harmonic generation in a thin-disk laser operating in the 100-fs regime

JULIAN FISCHER,* JAKUB DRS, FRANÇOIS LABAYE, NORBERT MODSCHING, VALENTIN J. WITTWER, AND THOMAS SÜDMEYER

Laboratoire Temps-Fréquence (LTF), Institut de Physique, Université de Neuchâtel, Avenue de Bellevaux 51, 2000 Neuchâtel, Switzerland
julian.fischer@unine.ch

Abstract: We demonstrate that Kerr lens modelocking is well-suited for operating an ultrafast thin-disk laser with intra-oscillator high harmonic generation (HHG) in the 100-fs pulse duration regime. Exploiting nearly the full emission bandwidth of the gain material Yb:YAG, we generate 105-fs pulses with an intracavity peak power of 365 MW and an intracavity average power of 470 W. We drive HHG in argon with a peak intensity of ~$7{\cdot}10^{13}$ W/cm^2 at a repetition rate of 11 MHz. Extreme-ultraviolet (XUV) light is generated up to the 31st harmonic order (H31) at 37 eV, with an average power of ~0.4 µW in H25 at 30 eV. This work presents a considerable increase in performance of XUV sources based on intra-oscillator HHG and confirms that this approach is a promising technology for simple and portable XUV sources at MHz repetition rates.

© 2021 Optical Society of America under the terms of the OSA Open Access Publishing Agreement

1. Introduction

High harmonic generation (HHG) driven by ultrafast laser pulses in a noble gas target is the most common method for tabletop coherent extreme-ultraviolet (XUV) light sources. Driving this highly nonlinear process requires peak intensities in the range of 10^{13} - 10^{15} W/cm^2. Such high intensities are traditionally achieved using chirped pulse amplifier (CPA) systems based on Ti:sapphire bulk lasers. Due to thermal effects in the bulk gain material, these systems are limited in average power and typically operate with low kilohertz repetition rates in a single-pass configuration. The progress towards megahertz repetition rate XUV sources is of high scientific and technical interest, because it can strongly reduce acquisition times in imaging and pump-probe experiments, overcome limiting space-charge effects in photoelectron spectroscopy [1–4], and enable XUV frequency combs for spectroscopy applications [5,6].

Compared to Ti:sapphire based systems, Yb-based solid-state laser systems are much better suited for reaching the high pulse energies necessary for HHG combined with high repetition rates due to the lower quantum defect, the therefore lower thermal effects, and the more efficient direct diode pumping scheme. High-power fiber CPA systems have been achieving considerable success in this domain [7–9]. In 2015, an average power level of 50 µW in a single harmonic order at 28 eV and 10.7-MHz repetition rate was demonstrated [8]. This performance was reached with a driving laser that was based on the coherent combination of fiber chirped pulse amplification channels followed by a nonlinear temporal pulse compression in a gas filled photonic crystal fiber.

Another successful approach for HHG at megahertz repetition rates is based on placing the HHG gas target inside a passive femtosecond enhancement cavity (fsEC) [6,10], where the pulse enhancement provides sufficiently high intracavity peak power, even when operating at repetition rates of several hundred-megahertz. Because of the resonant enhancement, the power requirements of the driving laser are considerably reduced. Using this technology, XUV photon energies up to 94 eV with 1.3-nW average power in a single harmonic order at 250-MHz repetition

#414444 https://doi.org/10.1364/OE.414444
Journal © 2021 Received 12 Nov 2020; revised 11 Jan 2021; accepted 12 Jan 2021; published 9 Feb 2021

Optics EXPRESS

rate were demonstrated [11]. A record XUV average power of ~2 mW in a single harmonic at 13 eV and 77-MHz repetition rate was reported in 2018 [12]. However, the experimental realization of fsECs is challenging: coherent coupling of ultrafast pulses into a high-finesse optical resonator containing the HHG process is very demanding. For example, the system presented in [12] operated at an enhancement factor of ~200. In order to reach such enhancement factors, total cavity roundtrip losses have to be lower than 1%, making fsECs very sensitive to any kind of losses. This presents a constraint for the achievable enhancement and the implementation of efficient XUV output coupling methods, which often add further losses.

The high peak and average powers required for efficient HHG are also achievable inside ultrafast mode-locked thin-disk laser (TDL) oscillators, opening the potential for single-stage XUV sources. Placing the gas target directly inside the cavity of a TDL oscillator simplifies the overall experimental setup, requiring neither coherent coupling into an actively stabilized external fsEC nor temporal pulse compression. The available gain per cavity roundtrip strongly reduces the sensitivity to cavity losses compared to fsECs. In high-power TDL oscillators, the gain can be further increased with the number of passes over the disk. For instance, with a double pass on the disk, the roundtrip gain can compensate for output coupling rates of about 15%, while still exploiting the full available gain bandwidth [13,14]. This allows for the implementation of efficient XUV output coupling mechanisms that introduce significant losses for the circulating intracavity pulse, such as a pierced mirror with an increased diameter of the through hole [15,16].

In a proof-of-principle experiment in 2017, we demonstrated intra-oscillator HHG in xenon, driven inside a 255-fs semiconductor saturable absorber mirror (SESAM) mode-locked Yb:Lu_2O_3 TDL [17]. We generated XUV radiation up to the 17th harmonic (H17) at 20 eV with an average power of ~0.55 nW in H11 at 13 eV. In the same year, another demonstration of intra-oscillator HHG based on a Kerr lens mode-locked (KLM) Yb:YAG TDL was reported in [18] and recently published in more detail in [19]. The system operated with a pulse duration of 610 fs at a peak power of 445 MW and a repetition rate of 3.1 MHz. XUV light was generated in neon up to 52 eV (H43) and in argon with an average power of 47 nW in H17 at 20 eV.

In this work, we present intra-oscillator HHG at significantly improved performance. We use a 105-fs KLM Yb:YAG TDL operating at 365 MW of intracavity peak power and 11-MHz repetition rate. We generate XUV in argon with up to 37 eV (H31) with an average power of ~0.4 µW in H25 at 30 eV. Figure 1 shows a comparison of our system to other ultrafast high intracavity peak power TDLs together with the evolution of the intra-oscillator HHG driving systems. The desired parameter range for efficient HHG is depicted by the green shaded corner, corresponding to gigawatt level peak powers and tens of femtosecond pulse duration [4,25].

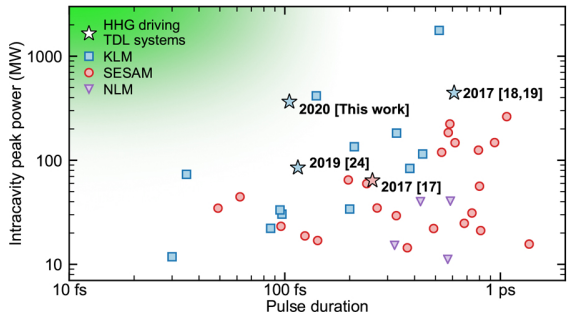

Fig. 1. Overview of ultrafast TDL oscillators based on SESAM, KLM, or nonlinear-mirror (NLM) modelocking with more than 10 MW of intracavity peak power. Stars with year show the evolution of HHG driving TDLs. The modelocking mechanism of HHG TDLs is indicated in the color code (blue for KLM; red for SESAM). References in [14,17–24].

Optics EXPRESS

However, a tradeoff between intracavity peak power and pulse duration for TDL oscillators utilizing different modelocking techniques can clearly be identified. The nearly instantaneous response of the Kerr effect and the high damage threshold of the components currently favor KLM for the combination of short pulse durations and high intracavity peak powers, making this approach most promising for intra-oscillator HHG.

2. Experimental setup

The TDL setup for intra-oscillator HHG is housed in a vacuum chamber with a footprint of 0.8×1.6 m^2 as shown in Fig. 2. The cavity design is based on the power-scaling approach for KLM TDLs presented in [26]. The laser is built using a commercially available TDL head designed for 36 passes of the pump through a ~100-µm thick Yb:YAG disk in order to achieve a high pump absorption. The disk is optically pumped at 969 nm with a fiber-coupled pump-diode on a 4.2-mm diameter pump spot. The diode delivers an average power up to 2 kW, but in the here described experiments, we only used a maximum pump power of 380 W. The cavity is folded twice over the disk, increasing the gain per cavity round trip. For KLM, an anti-reflection coated undoped 1-mm thick YAG plate is placed in the vicinity of an intracavity focus created by two concave mirrors (CM1, CM2) with 1-m radius of curvature (RoC). A water-cooled copper plate with a 3.6-mm diameter hole serves as hard aperture. Four dispersive mirrors introduce a total cavity roundtrip dispersion of -7000 fs^2. Mode-locked operation in vacuum is initialized by shaking one of the cavity mirrors mounted on a piezo stage. The cavity is extended by a telescope consisting of two concave mirrors (CM3, CM4) with RoC of 2 m and 3 m, respectively. One cavity end mirror serves as an output coupler with a transmission of 0.77%.

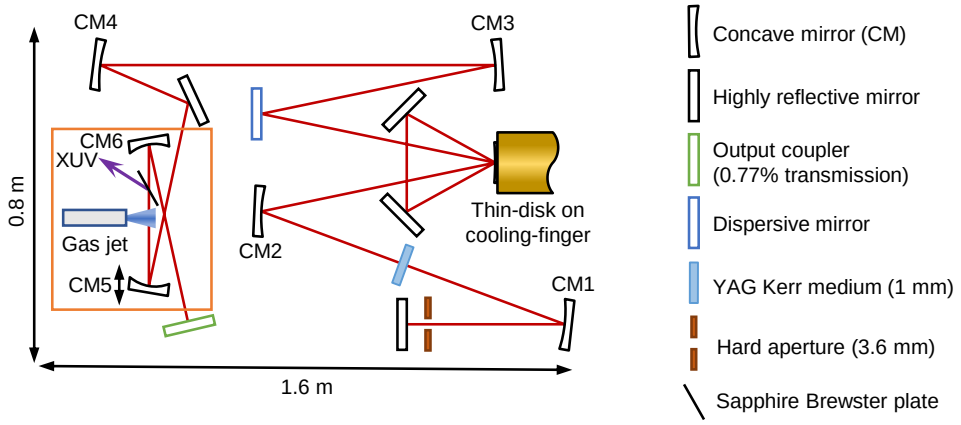

Fig. 2. Schematic of the Kerr lens mode-locked Yb:YAG thin-disk laser with a double pass on the disk and 4f-extension with tight-focus for HHG, which is indicated with an orange box. CM1 and CM2, RoC of 1 m; CM3, RoC of 2 m; CM4, RoC of 3 m; CM5 and CM6, RoC of 200 mm.

A 4f-extension consisting of two concave mirrors (CM5, CM6) with 200-mm RoC inserted in the output-coupling arm of the cavity creates a tight focus required to reach the high peak intensities for HHG. CM5 is placed on a piezo stage with a total travel range of 500 µm for fine-tuning of the cavity during mode-locked operation. Argon with a backing pressure of up to 10 bar can be injected into the cavity through a 50-µm opening diameter glass nozzle which is placed in the vicinity of the tight focus. A mass flow controller with a pressure sensor enables a precise delivery of the generation gas. A gas dump connected to the primary vacuum pump, placed on the opposite side of the tight focus than the nozzle, evacuates most of the gas, reducing

Optics EXPRESS

the gas load on the turbomolecular pumps [27]. The gas nozzle is mounted on a motorized xyz-stage for fine-adjustment of the XUV generation point. To extract the generated XUV light and to ensure p-polarized operation of the TDL, a 325-µm thick sapphire plate is placed under Brewster's angle for the fundamental laser wavelength at a distance of ~15 mm from the tight focus. Due to the simplicity of the aforementioned XUV out-coupling mechanism, the method has been routinely used in fsECs [28–30]. However, the maximum reflectivity of the sapphire plate is limited to 17% at a wavelength of 50 nm (25 eV) and decreases strongly for shorter and longer wavelengths (see, e.g., [31]). The generated XUV light is directed by an unprotected gold mirror towards a spectrometer (248/310 McPherson). The XUV flux is measured with an aluminum coated AXUV100Al photodiode. To suppress any residual infrared light from reaching the photodiode, an additional 200-nm thick aluminum filter is inserted in front.

Two turbomolecular pumps provide a vacuum level which prevents significant reabsorption of the generated XUV light within the distance of ~20 cm separating the detector from the generation point. The cavity components experiencing the highest intensities, the anti-reflection coated YAG plate and sapphire plate, are purged with oxygen from both sides to prevent contamination during laser operation. Optical coatings have been designed inhouse and grown in our ion-beam sputtering coating facility.

3. Experimental results

Without injection of gas into the tight focus, our laser runs with an intracavity average power of 640 W, an intracavity peak power of 520 MW, and an intracavity pulse energy of 55 µJ at a pump power of 285 W. This performance is reached after optimizing the distance between CM5 and CM6 with the piezo stage in mode-locked operation. Intensity autocorrelation trace, optical spectrum, and radiofrequency spectrum are shown in Figs. 3(a) to 3(c). The optical spectrum of the 99-fs soliton pulse is centered at 1027.8 nm with a full width at half maximum bandwidth (FWHM) of 14.0 nm. We confirmed single pulse operation by a 180-ps scan in the autocorrelator and by observing the pulse train with an 18.5-ps-rise-time photodetector on a 40-GHz sampling oscilloscope.

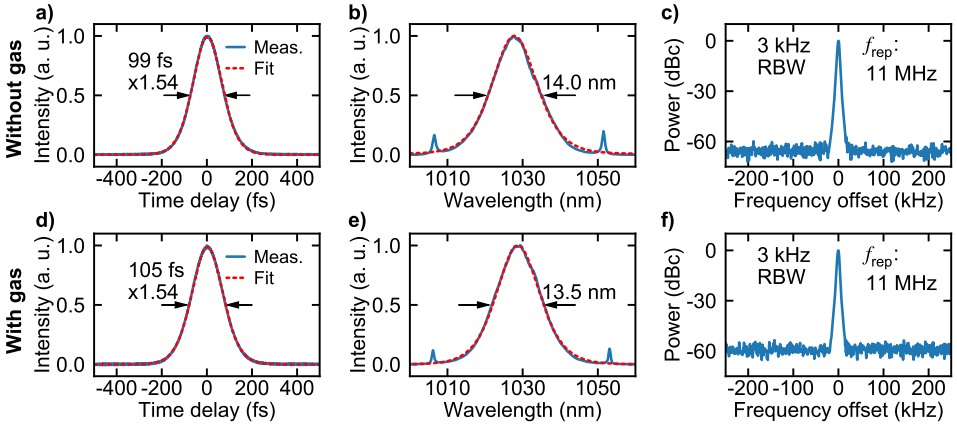

Fig. 3. Comparison of the thin-disk laser output parameters a) to c) without the injection of gas and d) to f) with injection of argon gas into the intracavity focus for HHG. a), d) Intensity autocorrelation traces with sech^2 fit. b), e) Optical spectra with spectral bandwidth and sech^2 fit. c), f) Radiofrequency spectra of the fundamental repetition rate (f_{rep}) with 3-kHz resolution bandwidth (RBW).

Optics EXPRESS

To initialize XUV generation, argon is injected into the tight focus of the laser cavity. In the current system, the gas plasma affects the laser: the position of CM5 has to be slightly shifted (< 500 µm) between operation with and without gas. We attribute this behavior to the lensing effect in the plasma since it can be compensated by this shift. With HHG, the laser operates with 105-fs pulse duration at an intracavity peak power of 365 MW and a pulse energy of 40 µJ. The intracavity average power is 470 W, which is obtained for a diode pump power of 180 W. Intensity autocorrelation trace, optical spectrum, and radiofrequency spectrum are shown in Figs. 3(d) to 3(f). Compared to operation without HHG, the optical spectrum shifts by 1 nm to a central wavelength of 1028.8 nm with a FWHM bandwidth of 13.5 nm.

The XUV optical spectrum attenuated by a 200-nm thick aluminum filter and generated in argon with a backing pressure of 3 bar is shown in Fig. 4. We generate up to H31 which corresponds to a wavelength of 33 nm and an energy of 37 eV. Utilizing the harmonic cut-off formula, the intracavity peak intensity in the tight focus is estimated to be $7{\cdot}10^{13}$ W/cm^2, corresponding to a focal radius of ~18 µm in mode-locked operation. A total generated XUV power of ~2 µW within the spectral range from H17 to H31 (20 - 37 eV) is conservatively estimated. We corrected by the tabulated values for the extraction efficiency of a sapphire plate (see, e.g. [31]), the reflectance of a gold mirror, and the transmission of a 200-nm thick aluminum filter. The absorption of XUV radiation in the gas background (oxygen: $\sim 9{\cdot}10^{-3}$ mbar; argon: $\sim 2.5{\cdot}10^{-3}$ mbar) to the detector is considerably small and therefore neglected. Assuming a flat spectral response of the XUV spectrometer, a generated average power of ~0.4 µW in H25 (30 eV) is estimated.

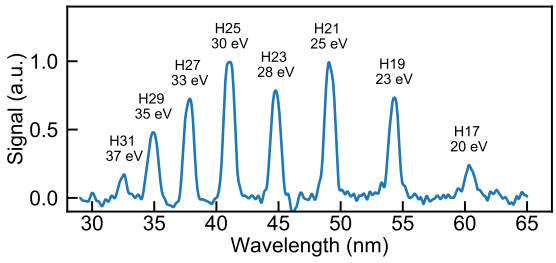

Fig. 4. Optical spectrum of XUV light generated in argon showing 17th to 31st harmonic. Peaks are labeled with harmonic order and corresponding photon energies. The XUV spectrum is attenuated by a 200-nm thick aluminum filter.

In the current study, thermal drift of uncooled cavity components limited operation to less than 15 minutes, which prevented a systematic optimization, especially with respect to the phase matching of the harmonics. Phase matching becomes increasingly difficult at repetition rates above ~10 MHz, due to a steady-state plasma accumulated in the generation volume [12]. Nevertheless, phase matching at even higher repetition rates has already been demonstrated, for instance, in single pass configuration at 10.7 MHz [8] and in a fsEC at 77 MHz [12]. After implementation of water-cooled mirror mounts in our cavity, which is currently in progress, we will investigate phase matching in detail. For this study, we plan to use an improved gas target similar to the system reported in [32].

4. Conclusion and outlook

We have demonstrated intra-oscillator HHG in a 105-fs KLM Yb:YAG TDL operating at 11-MHz repetition rate. In comparison to our previous result with XUV photon energies up to 20 eV (H17) and a total generated average power of ~0.55 nW in H11 (13 eV) in xenon [17], we now generate up to 37 eV (H31) with an average power of ~0.4 µW in H25 (30 eV) in argon, which

Optics EXPRESS

is an increase in XUV flux of three orders of magnitude. Combined with the decreased pulse duration of the TDL by a factor of more than two, our result presents a considerable advance in TDL based intra-oscillator XUV sources [17,19].

Following the intracavity peak power scaling concept for KLM TDLs introduced by Brons *et al.* [26] in combination with shorter pulse durations by operating the laser in the strongly SPM-broadened regime [33,34], we expect further advancement of our system towards sub-100-fs operation with gigawatt intracavity peak powers. Due to the strong dependency of the HHG efficiency on peak intensity and pulse duration, this should lead to a substantial improvement of the performance of the system [4,25]. Further advances are expected by more efficient XUV extraction. Instead of a sapphire plate under Brewster's angle for the fundamental wavelength, a grazing incidence plate or a pierced mirror can be employed. With a grazing incidence plate, an XUV reflectivity up to 70% can be reached at 80° angle of incidence and fused silica as top layer of the anti-reflection coating for the fundamental laser-wavelength [31]. The pierced mirror method is especially suited for the efficient extraction of highly energetic XUV light [11,15]. In addition to an improved XUV extraction efficiency, a further reduction of the pulse duration of the driving TDL, reducing the level of steady-state plasma adversely affecting the TDL and improving phase matching of the generated harmonics, is also desirable [8,15].

We believe that our approach of HHG inside a TDL oscillator will lead to a novel class of single-stage coherent XUV light sources operating at MHz repetition rate. As most of the volume in our vacuum chamber remains empty, we expect that the footprint of our system can be strongly reduced with sufficient engineering, leading to a more compact and transportable design. We expect that such systems will soon operate at a performance comparable to state-of-the-art megahertz repetition rate HHG systems.

Funding. H2020 European Research Council (279505); Schweizerischer Nationalfonds zur Förderung der Wissenschaftlichen Forschung (144970, 170772, 179146).

Acknowledgments. The authors acknowledge the support of the Ultrafast Laser Physics group of Ursula Keller (ETH Zürich) for lending the 248/310 McPherson spectrometer.

Disclosures. The authors declare that there are no conflicts of interest related to this article.

Data availability. Data underlying the results presented in this paper are available in Ref. [35].

References

1. C. M. Heyl, J. Güdde, A. L'Huillier, and U. Höfer, "High-order harmonic generation with μJ laser pulses at high repetition rates," J. Phys. B: At., Mol. Opt. Phys. **45**(7), 074020 (2012).
2. M. Keunecke, C. Möller, D. Schmitt, H. Nolte, G. S. M. Jansen, M. Reutzel, M. Gutberlet, G. Halasi, D. Steil, S. Steil, and S. Mathias, "Time-resolved momentum microscopy with a 1 MHz high-harmonic extreme ultraviolet beamline," Rev. Sci. Instrum. **91**(6), 063905 (2020).
3. S. Passlack, S. Mathias, O. Andreyev, D. Mittnacht, M. Aeschlimann, and M. Bauer, "Space charge effects in photoemission with a low repetition, high intensity femtosecond laser source," J. Appl. Phys. **100**(2), 024912 (2006).
4. C. M. Heyl, C. L. Arnold, A. Couairon, and A. L'Huillier, "Introduction to macroscopic power scaling principles for high-order harmonic generation," J. Phys. B: At., Mol. Opt. Phys. **50**(1), 013001 (2017).
5. A. K. Mills, T. J. Hammond, M. H. C. Lam, and D. J. Jones, "XUV frequency combs via femtosecond enhancement cavities," J. Phys. B: At., Mol. Opt. Phys. **45**(14), 142001 (2012).
6. C. Gohle, T. Udem, M. Herrmann, J. Rauschenberger, R. Holzwarth, H. A. Schuessler, F. Krausz, and T. W. Hänsch, "A frequency comb in the extreme ultraviolet," Nature **436**(7048), 234–237 (2005).
7. J. Boullet, Y. Zaouter, J. Limpert, S. Petit, Y. Mairesse, B. Fabre, J. Higuet, E. Mével, E. Constant, and E. Cormier, "High-order harmonic generation at a megahertz-level repetition rate directly driven by an ytterbium-doped-fiber chirped-pulse amplification system," Opt. Lett. **34**(9), 1489–1491 (2009).
8. S. Hädrich, M. Krebs, A. Hoffmann, A. Klenke, J. Rothhardt, J. Limpert, and A. Tünnermann, "Exploring new avenues in high repetition rate table-top coherent extreme ultraviolet sources," Light: Sci. Appl. **4**(8), e320 (2015).
9. S. Hädrich, A. Klenke, J. Rothhardt, M. Krebs, A. Hoffmann, O. Pronin, V. Pervak, J. Limpert, and A. Tünnermann, "High photon flux table-top coherent extreme-ultraviolet source," Nat. Photonics **8**(10), 779–783 (2014).
10. R. J. Jones, K. D. Moll, M. J. Thorpe, and J. Ye, "Phase-Coherent Frequency Combs in the Vacuum Ultraviolet via High-Harmonic Generation inside a Femtosecond Enhancement Cavity," Phys. Rev. Lett. **94**(19), 193201 (2005).

Optics EXPRESS

11. H. Carstens, M. Högner, T. Saule, S. Holzberger, N. Lilienfein, A. Guggenmos, C. Jocher, T. Eidam, D. Esser, V. Tosa, V. Pervak, J. Limpert, A. Tünnermann, U. Kleineberg, F. Krausz, and I. Pupeza, "High-harmonic generation at 250 MHz with photon energies exceeding 100 eV," Optica **3**(4), 366–369 (2016).
12. G. Porat, C. M. Heyl, S. B. Schoun, C. Benko, N. Dörre, K. L. Corwin, and J. Ye, "Phase-matched extreme-ultraviolet frequency-comb generation," Nat. Photonics **12**(7), 387–391 (2018).
13. J. Brons, V. Pervak, D. Bauer, D. Sutter, O. Pronin, and F. Krausz, "Powerful 100-fs-scale Kerr-lens mode-locked thin-disk oscillator," Opt. Lett. **41**(15), 3567–3570 (2016).
14. N. Modsching, J. Drs, J. Fischer, C. Paradis, F. Labaye, M. Gaponenko, C. Kränkel, V. J. Wittwer, and T. Südmeyer, "Sub-100-fs Kerr lens mode-locked Yb:Lu2O3 thin-disk laser oscillator operating at 21 W average power," Opt. Express **27**(11), 16111–16120 (2019).
15. I. Pupeza, S. Holzberger, T. Eidam, H. Carstens, D. Esser, J. Weitenberg, P. Rußbüldt, J. Rauschenberger, J. Limpert, T. Udem, A. Tünnermann, T. W. Hänsch, A. Apolonski, F. Krausz, and E. Fill, "Compact high-repetition-rate source of coherent 100 eV radiation," Nat. Photonics **7**(8), 608–612 (2013).
16. K. D. Moll, R. J. Jones, and J. Ye, "Output coupling methods for cavity-based high-harmonic generation," Opt. Express **14**(18), 8189–8197 (2006).
17. F. Labaye, M. Gaponenko, V. J. Wittwer, A. Diebold, C. Paradis, N. Modsching, L. Merceron, F. Emaury, I. J. Graumann, C. R. Phillips, C. J. Saraceno, C. Kränkel, U. Keller, and T. Südmeyer, "Extreme ultraviolet light source at a megahertz repetition rate based on high-harmonic generation inside a mode-locked thin-disk laser oscillator," Opt. Lett. **42**(24), 5170–5173 (2017).
18. N. Kanda, T. Imahoko, K. Yoshida, A. A. Eilanlou, Y. Nabekawa, T. Sumiyoshi, M. Kuwata-Gonokami, K. Midorikawa, K. Midorikawa, K. Midorikawa, and K. Midorikawa, "Multi-port Intra-Cavity High Harmonic Generation in a Yb:YAG Thin Disk Mode-Locked Oscillator with MHz Repetition Rate," in Frontiers in Optics 2017, OSA Technical Digest (Online) (Optical Society of America, 2017), paper LW5F.4.
19. N. Kanda, T. Imahoko, K. Yoshida, A. Tanabashi, A. Amani Eilanlou, Y. Nabekawa, T. Sumiyoshi, M. Kuwata-Gonokami, and K. Midorikawa, "Opening a new route to multiport coherent XUV sources via intracavity high-order harmonic generation," Light: Sci. Appl. **9**(1), 168 (2020).
20. F. Labaye, M. Gaponenko, N. Modsching, P. Brochard, C. Paradis, S. Schilt, V. J. Wittwer, and T. Sudmeyer, "XUV Sources Based on Intra-Oscillator High Harmonic Generation With Thin-Disk Lasers: Current Status and Prospects," IEEE J. Sel. Top. Quantum Electron. **25**(4), 1–19 (2019).
21. F. Saltarelli, I. J. Graumann, L. Lang, D. Bauer, C. R. Phillips, and U. Keller, "Power scaling of ultrafast oscillators: 350-W average-power sub-picosecond thin-disk laser," Opt. Express **27**(22), 31465–31474 (2019).
22. F. Saltarelli, A. Diebold, I. J. Graumann, C. R. Phillips, and U. Keller, "Modelocking of a thin-disk laser with the frequency-doubling nonlinear-mirror technique," Opt. Express **25**(19), 23254–23265 (2017).
23. I. J. Graumann, F. Saltarelli, L. Lang, V. J. Wittwer, T. Südmeyer, C. R. Phillips, and U. Keller, "Power-scaling of nonlinear-mirror modelocked thin-disk lasers," Opt. Express **27**(26), 37349–37363 (2019).
24. J. Fischer, J. Drs, F. Labaye, N. Modsching, C. Kränkel, V. J. Wittwer, and T. Südmeyer, "Intra-Oscillator High Harmonic Generation in a ~100-fs Kerr-Lens Mode-Locked Thin-Disk Laser," in *Conference on Lasers and Electro-Optics, OSA Technical Digest* (Optical Society of America, 2020), paper SF3H.3.
25. S. Hädrich, J. Rothhardt, M. Krebs, S. Demmler, A. Klenke, A. Tünnermann, and J. Limpert, "Single-pass high harmonic generation at high repetition rate and photon flux," J. Phys. B: At., Mol. Opt. Phys. **49**(17), 172002 (2016).
26. J. Brons, V. Pervak, E. Fedulova, D. Bauer, D. Sutter, V. Kalashnikov, A. Apolonskiy, O. Pronin, and F. Krausz, "Energy scaling of Kerr-lens mode-locked thin-disk oscillators," Opt. Lett. **39**(22), 6442–6445 (2014).
27. D. C. Yost, "Development of an Extreme Ultraviolet Frequency Comb for Precision Spectroscopy," PhD Thesis, University of Colorado (2011).
28. C. Benko, T. K. Allison, A. Cingöz, L. Hua, F. Labaye, D. C. Yost, and J. Ye, "Extreme ultraviolet radiation with coherence time greater than 1 s," Nat. Photonics **8**(7), 530–536 (2014).
29. C. Benko, L. Hua, T. K. Allison, F. Labaye, and J. Ye, "Cavity-Enhanced Field-Free Molecular Alignment at a High Repetition Rate," Phys. Rev. Lett. **114**(15), 153001 (2015).
30. A. Ozawa, Z. Zhao, M. Kuwata-Gonokami, and Y. Kobayashi, "High average power coherent vuv generation at 10 MHz repetition frequency by intracavity high harmonic generation," Opt. Express **23**(12), 15107–15118 (2015).
31. O. Pronin, V. Pervak, E. Fill, J. Rauschenberger, F. Krausz, and A. Apolonski, "Ultrabroadband efficient intracavity XUV output coupler," Opt. Express **19**(11), 10232–10240 (2011).
32. C. M. Heyl, S. B. Schoun, G. Porat, H. Green, and J. Ye, "A nozzle for high-density supersonic gas jets at elevated temperatures," Rev. Sci. Instrum. **89**(11), 113114 (2018).
33. J. Zhang, J. Brons, M. Seidel, V. Pervak, V. Kalashnikov, Z. Wei, A. Apolonski, F. Krausz, and O. Pronin, "49-fs Yb:YAG thin-disk oscillator with distributed Kerr-lens mode-locking," in *2015 European Conference on Lasers and Electro-Optics - European Quantum Electronics Conference* (Optical Society of America, 2015), paper PD_A_1.
34. C. Paradis, N. Modsching, V. J. Wittwer, B. Deppe, C. Kränkel, and T. Südmeyer, "Generation of 35-fs pulses from a Kerr lens mode-locked Yb:Lu2O3 thin-disk laser," Opt. Express **25**(13), 14918–14925 (2017).
35. J. Fischer, J. Drs, F. Labaye, N. Modsching, V. J. Wittwer, and T. Südmeyer, Data presented in this work are available on http://doi.org/10.23728/b2share.2c19736994b8437995c99aa48eb15da4 (2021).

Research Article | Vol. 30, No. 17 / 15 Aug 2022 / Optics Express 30969

Optics EXPRESS

Efficient XUV-light out-coupling of intra-cavity high harmonics by a coated grazing-incidence plate

JULIAN FISCHER,* JAKUB DRS, FRANÇOIS LABAYE, NORBERT MODSCHING, MICHAEL MÜLLER, VALENTIN J. WITTWER, AND THOMAS SÜDMEYER

Laboratoire Temps-Fréquence (LTF), Institut de Physique, Université de Neuchâtel, Avenue de Bellevaux 51, 2000 Neuchâtel, Switzerland
julian.fischer@unine.ch

Abstract: We experimentally demonstrate an efficient and broadband extreme-ultraviolet light (XUV) out-coupling mechanism of intra-cavity generated high harmonics. The mechanism is based on a coated grazing-incidence plate (GIP), which utilizes the enhanced reflectivity of s-polarized light in comparison to p-polarized light for large angles of incidence (AoI). We design and produce a 60°-AoI coated GIP, tailored specifically for the high demands inside a sub-50-fs Kerr-lens mode-locked Yb:YAG thin-disk laser oscillator in which high harmonic generation (HHG) is driven at ~450 MW peak power and 17 MHz repetition rate. The coated GIP features an XUV out-coupling efficiency of >25% for photon energies ranging from 10 eV to 60 eV while being anti-reflective for the driving laser field. The XUV spectra reach up to 52 eV in argon and 30 eV in xenon. In a single harmonic, we out-couple 1.3 µW of XUV average power at 37 eV in argon and 5.4 µW at 25 eV in xenon. The combination of an improved HHG driving laser performance and the out-coupling via the coated GIP enabled us to increase the out-coupled XUV average power in a single harmonic by a factor of 20 compared to previous HHG inside ultrafast laser oscillators. Our source approaches the state-of-the-art out-coupled XUV power levels per harmonic of femtosecond enhancement cavities operating at comparable photon energies.

© 2022 Optica Publishing Group under the terms of the Optica Open Access Publishing Agreement

1. Introduction

Ultrafast lasers driving high harmonic generation (HHG) in a noble gas target have brought coherent extreme-ultraviolet light (XUV) into laboratories. In recent years, there has been a strong progress in the transition of HHG sources operating from kilohertz to megahertz repetition rates (MHz-HHG). Higher repetition rates enable shorter measurement times in space-charge-limited photoelectron spectroscopy experiments [1,2] and allow for frequency- comb applications in the XUV spectral range [3,4]. To increase the repetition rate, the driving laser system must deliver ever higher average power to maintain the pulse energy required for HHG. Nowadays, laser systems based on Yb-doped gain materials are most suitable at the required average power and several concepts capable of driving MHz-HHG have been developed.

The highest XUV average power per harmonic at MHz repetition rate is currently delivered by a high-power fiber chirped-pulse amplifier (FCPA) system driving HHG in single-pass configuration after frequency-doubling and temporal post-compressing the laser output [5].

Utilizing the field enhancement inside passive femtosecond enhancement cavities (fsEC) or inside mode-locked high-power laser oscillators is another approach suitable for reaching the required high average and peak powers for MHz-HHG at even higher repetition rates. In passive fsECs, a high repetition rate laser is coupled into an actively stabilized high finesse cavity that contains the HHG generation target [3,4]. In contrast, gain inside the cavity allows for the formation of a powerful soliton directly inside the cavity of a mode-locked thin-disk laser (TDL)

#458946 https://doi.org/10.1364/OE.458946
Journal © 2022 Received 24 Mar 2022; revised 27 May 2022; accepted 7 Jun 2022; published 10 Aug 2022

Optics EXPRESS

oscillator. This intra-oscillator HHG approach circumvents the need for coherent coupling, enabling a single-stage XUV source [6,7].

However, in most cavity-enhanced HHG systems, higher harmonics are generated collinearly with the driving laser and need to be out-coupled. Efficient out-coupling of the XUV light without losing the intra-cavity enhancement is a major challenge and out-coupling efficiencies are often restricted to a few percent. Figure 1 shows the most-commonly used XUV out-coupling methods inside fsECs and mode-locked oscillators which will be briefly introduced in the following.

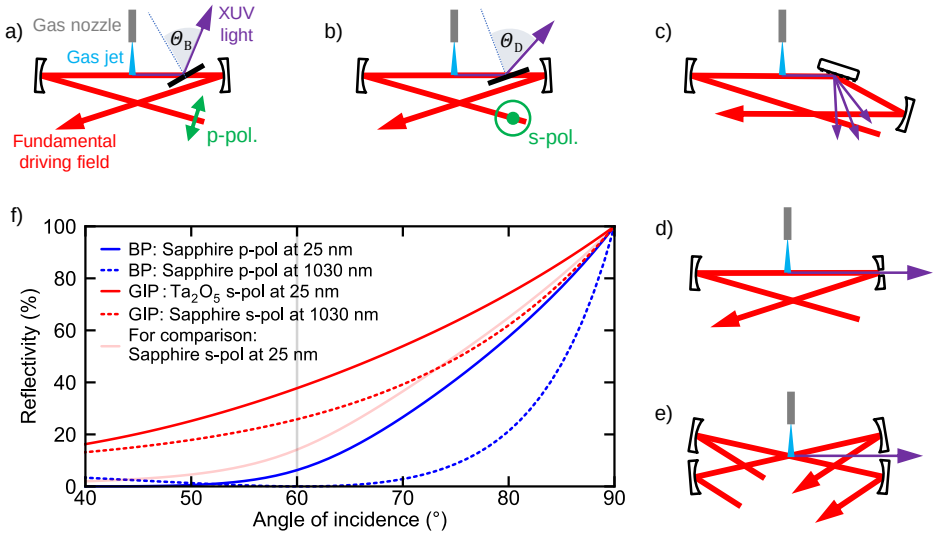

Fig. 1. Operation principle of common intra-cavity XUV out-coupling mechanisms. (a) Brewster's plate method with the fundamental driving field in p-polarization. Θ_B: Brewster's angle. (b) Coated-GIP method presented in this work with the fundamental driving field in s-polarization. Θ_D: angle of incidence on the GIP. (c) XUV diffraction grating method spatially disperses the generated harmonics. (d) Pierced-mirror method lets less diverging XUV light pass through a hole in the mirror. (e) Non-collinear crossed-beam XUV out-coupling mechanism. (f) Illustration of the enhanced XUV reflectivity of s-polarized in comparison to p-polarized light for coated GIP XUV out-coupling in comparison to the Brewster's plate (BP) method, respectively. Angle-dependent reflectivity of s-polarized light with 25 nm wavelength (our XUV cut-off) from Ta_2O_5, the top layer of our coated GIP, in comparison to the 25 nm p-polarized one from sapphire, as in the Brewster's plate method. The p-polarized reflectivity of 1030-nm light from sapphire vanishes at Brewster's angle. The high reflectivity losses for the s-polarized 1030 nm light from the sapphire substrate of the GIP are reduced by anti-reflection coatings applied to both sides of the GIP (further details are described in Section 3). Depending on the desired XUV photon energies, different materials can be chosen as the top layer of the coated GIP. The s-polarized XUV reflectivity at 25 nm of sapphire, shown for comparison, is inferior to the one of Ta_2O_5 at an AoI of 60°.

The simplest XUV out-coupling method is based on placing a thin dielectric plate, typically sapphire, under Brewster's angle for the p-polarized fundamental driving field into the cavity [Fig. 1(a)]. The difference in the refractive index of the plate for the XUV and the fundamental light leads to a partial reflection of the XUV light. However, the reflectivity of the sapphire plate is relatively narrowband and limited to a maximum of 17% at 25 eV [8]. From ~600 µW of generated XUV average power in a single harmonic at 15 eV and 50 MHz, only 77 µW were out-coupled (12% XUV out-coupling efficiency) from the fsEC in [9]. Thanks to its technical simplicity, until now, all intra-oscillator HHG TDL systems utilized the sapphire Brewster's plate

Optics EXPRESS

XUV out-coupling method [6,7,10]. Recently, 0.4 μW of XUV average power at 30 eV and 11 MHz were generated inside a ~100-fs Kerr-lens mode-locked (KLM) Yb:YAG TDL oscillator [10], but only 0.06 μW were out-coupled (14% XUV out-coupling efficiency).

XUV out-coupling via an XUV diffraction grating etched into the top layer of one of the highly reflective cavity mirrors is a method successfully implemented in fsECs [Fig. 1(c)] [11]. While this method features the advantage of no material propagation inside the cavity, the out-coupled XUV light is spatially dispersed and the XUV extraction efficiency typically reaches only around 10% [8,11]. Using this method, the up to now highest generated XUV average power inside a fsEC, amounting to 2 mW at 13 eV and 77 MHz, was demonstrated [12]. Nevertheless, just 130 μW were out-coupled, resulting in a 7% XUV out-coupling efficiency.

Another XUV out-coupling method successfully implemented in fsECs is the pierced mirror [Fig. 1(d)]. The concept is based on the smaller divergence of the short-wavelength XUV light in comparison to fundamental driving field. The less-divergent XUV light can escape the cavity through a small on-axis hole, typically in the ~100-μm diameter range [13], drilled into one of the cavity mirrors. The out-coupling efficiency increases strongly towards higher photon energies and is spectrally not limited. In the 18-MHz fsEC in [14] for example, only 14 μW of XUV average power were out-coupled with 5% efficiency at 37 eV while towards higher photon energies, the XUV out-coupling efficiency increased to 45% at 60 eV.

Recently, a new XUV out-coupling mechanism based on a non-collinear crossed-beam geometry was experimentally demonstrated inside a fsEC [Fig. 1(e)]. The mechanism was proposed before [15] and utilizes a cavity that is twice as long as the driving laser cavity, enabling two pulses to circulate inside the cavity which meet simultaneously in the gas target. The generated harmonics and the fundamental driving field propagated in different directions and can thus be easily separated, e.g., by a gap in between two mirrors. A record high power level of 600 μW at 13 eV and 154 MHz was out-coupled with >60% efficiency using this method [16].

XUV out-coupling of intra-cavity high harmonics by a coated grazing-incidence plate (GIP) was proposed by [8]. The mechanism is based on the higher reflectivity of s-polarized light in comparison to p-polarized light for large angles of incidence (AoI) [Figs. 1(b),(f)]. For the s-polarized near-infrared (NIR) driving laser field, a low-loss transmission is enabled by NIR-anti-reflection (AR) coatings on both sides of the GIP. Despite the common use of GIPs to separate XUV and NIR light in single-pass HHG systems [17,18], XUV out-coupling of intra-cavity high harmonics by a coated GIP has not been experimentally demonstrated until now. Even the by [8] produced coated GIP was characterized extra-cavity only. Potential reasons preventing so far an intra-cavity application might have been the introduced losses of the coated GIP for the fundamental light, thermal lensing, nonlinear effects, or the damage threshold of the coated GIP due to the high intra-cavity average and peak powers [8].

In this work, we demonstrate for the first time out-coupling of intra-cavity high harmonics by a coated GIP [Fig. 1(b)]. We designed and produced a 60°-AoI coated GIP in our ion-beam-sputtering (IBS) coating facility and placed it inside the cavity of a high-power ultrafast TDL oscillator. We present the coating structure and design parameters of our GIP and discuss the trade-off between XUV reflectivity and bandwidth of the AR coatings for the NIR fundamental driving field. As shown by Fig. 2, our intra-oscillator HHG source based on GIP XUV out-coupling approaches the state-of-the-art out-coupled XUV power levels per harmonic of fsEC sources at comparable photon energies.

Optics EXPRESS

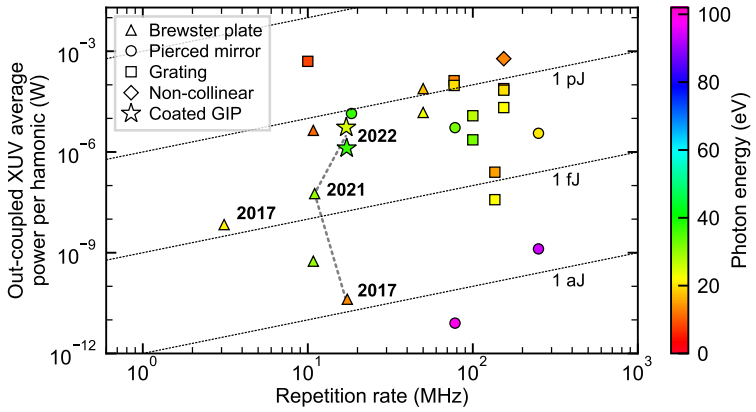

Fig. 2. Overview of intra-cavity XUV sources based on fsEC and intra-oscillator HHG. The plot shows the out-coupled XUV average power per harmonic and the color code represents the photon energy of the out-coupled harmonic. The applied XUV out-coupling mechanism is distinguished by the marker symbol. Intra-oscillator sources are labeled by year of publication. The dashed line indicates the progress of our intra-oscillator HHG system and the stars at "2022" show the results we achieved in argon and xenon using the here presented coated GIP for XUV out-coupling. References: [3,6,7,9–14,16,19–23].

2. Experimental setup

The scheme of our KLM TDL oscillator is shown in Fig. 3. The oscillator is housed in a vacuum chamber with a footprint of 0.8 m × 1.6 m and operates at $<1{\cdot}10^{-2}$ mbar pressure, limiting reabsorption of the generated XUV light. Most characteristics of the TDL setup are described in our recent publication [24]. Compared to the publication, we mode-lock the laser using a 2-mm-thick Kerr medium to decrease the intra-cavity power of the TDL due to a power limitation we observe when using the coated GIP (more details in Section 4). Furthermore, the laser operates in s-polarization which is required for efficient XUV out-coupling through the coated GIP.

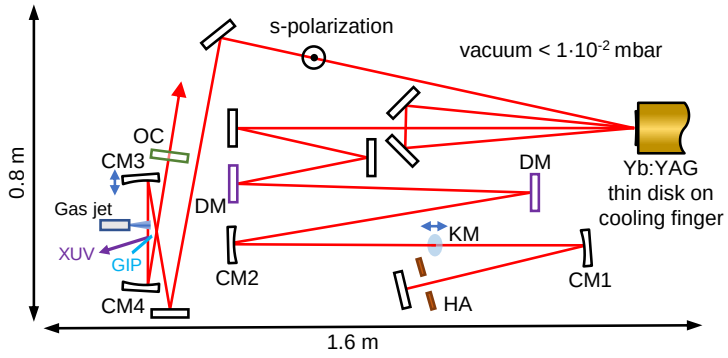

Fig. 3. Schematic of the KLM Yb:YAG TDL oscillator with double pass over the disk. High harmonics are generated in the tight focus between two concave mirrors, CM3 and CM4. A coated GIP placed after the tight focus is used to couple the generated XUV light out of the oscillator. As indicated by the double arrow, CM3 is mounted on a translation stage used for fine-tuning of the laser cavity during mode-locked operation. HA: hard aperture; CM1/2: concave mirror; KM: Kerr medium; DM: dispersive mirror; OC: output coupler.

Optics EXPRESS

The output-coupling arm of the oscillator contains a tight focus extension for HHG, which consists of two concave mirrors (CM3 and CM4). Due to the different peak intensity requirements for driving HHG in argon and xenon, we employed CM3 with a radius of curvature (RoC) of 100 mm and 150 mm, respectively, while CM4 always had a RoC of 250 mm. The noble gas is injected into the focus with a tapered glass gas nozzle with a ~100-µm opening diameter. The gas nozzle is placed on a motorized xyz-stage to fine-adjust the XUV generation point. The coated GIP is placed after the focus between CM3 and CM4 to out-couple the XUV light out of the oscillator. The XUV light is directed by an unprotected gold mirror in the case of xenon or another extra-cavity coated GIP in the case of argon towards a 248/310 McPherson spectrometer and a photodiode. The overall XUV flux is measured with an aluminum coated AXUV100Al photodiode, while an additional 200-nm-thick aluminum filter is inserted to block the residual NIR. We use tabulated values for the transmission of the aluminum filter, for the reflectivity of the gold mirror, and for the reflectivity of the Ta_2O_5 top layer of the GIP to determine the generated and out-coupled XUV flux. For the determination of the flux in a single harmonic order, we assume a flat spectral response of the XUV spectrometer [10]. CM3 is placed on a motorized linear stage, allowing to compensate the lens effect of the plasma in the generation gas on the oscillator.

The optical coatings of the dispersive mirrors as well as of the coated GIP were designed inhouse and grown in our IBS coating facility. The Kerr medium and the coated GIP are purged with oxygen from both sides to prevent contamination during laser operation [10].

3. Design of the coated grazing-incidence plate

The coated GIP out-coupling method utilizes the increasing Fresnel reflection at the vacuum-top layer interface with increasing AoI in s-polarization for the XUV light [8]. In comparison to [8], we chose Ta_2O_5 as top layer instead of SiO_2 due to its higher XUV reflectivity, especially for a moderate AoI of 60°. Since the XUV light is typically absorbed in the first tens of nanometers in the top layer, interference with all underlying layers can be neglected. This allows to freely minimize the reflectance of the NIR light for s-polarization at the same AoI by using the interference of the material interfaces in the layer stack. The chosen materials are transparent in the NIR. Especially for the coated GIP that is placed inside a cavity, it is important that the NIR pulse with its full spectral bandwidth experiences low losses and therefore the AR-coating properties in the NIR needs to cover this bandwidth. Low losses at the GIP for the NIR pulse are achieved by applying the same coating on both sides of the GIP. Benefitting from gain in the cavity, we can tolerate higher losses compared to fsECs. Recently, we showed operation of our TDL oscillator with an intra-cavity peak power of more than 1 GW at an output coupling rate of 8.5% [24]. In the following, we assume that 0.5% per coating, resulting in 2% losses per cavity round-trip, can be easily tolerated.

The design of a coated GIP and the choice of the AoI is based on a trade-off between a desired high XUV reflectivity and low reflection losses over the spectral bandwidth of the driving NIR pulse. While a larger AoI favors a higher XUV reflectivity, low reflection losses for the fundamental NIR pulse become increasingly more difficult as the supported spectral bandwidth decreases. To visualize this trade-off, we designed several GIP coatings, each optimized for a different AoI and maximal NIR bandwidth (reflectivity <0.5% per coating), yet not exceeding a total coating thickness of 3.5 µm, allowing reliable production [Fig. 4]. A larger NIR bandwidth at high AoI could be potentially realized by designing thicker AR coatings, but this is outside of the scope of this investigation since it comes with other challenges related to the manufacturing of such coatings [8]. The design study in Fig. 4(a) shows the wavelength and AoI-dependent XUV reflectivity of the Ta_2O_5 top layer whereas Fig. 4(b) visualizes the AoI-dependent supported spectral bandwidth of the AR coatings for the NIR pulse.

Optics EXPRESS

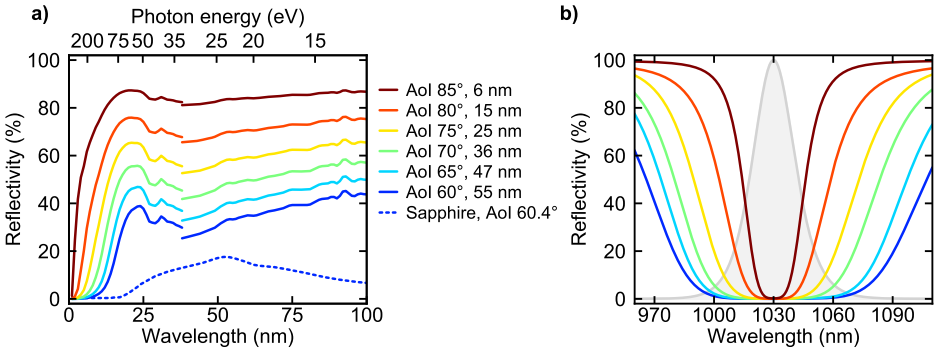

Fig. 4. Coated GIP design study and trade-off parameters for AoI ranging from 60° to 85°. (a) Wavelength-dependent reflectivity of s-polarized XUV light from the Ta_2O_5 top layer of the GIP. The steps in the reflectivity curves are due to the use of two different reference data sets – high energy side is from [25] and low energy side from [26]. The p-polarized XUV reflectivity from a sapphire plate placed under Brewster's angle (60.4°) is shown for comparison (blue dashed line). (b) Wavelength dependent reflectivity of the fundamental driving field. The maximum bandwidth (reflectivity <0.5%) for the respective AoI of the GIP is shown in the legend of (a). A transform limited soliton spectrum of a 45-fs pulse is shown for comparison (shaded gray area).

Due to our broadband pulses (~45 fs), we choose a 60°-AoI design of the coated GIP. Furthermore, the choice of an AoI of 60° simplifies the comparison to the sapphire Brewster's plate method (Brewster's angle of 60.4°), which is commonly used for intra-cavity applications, in this first proof-of-principle experiment. Another reason is that for the intra-cavity use of a coated GIP, in comparison to its single-pass application, it is crucial to minimize any influence on the NIR beam propagation, which becomes more challenging for larger AoIs. Due to slight production deviations, the produced coated GIPs turned out to be centered at an AoI of 62° for the laser wavelength. Figure 5(a) shows the wavelength dependent reflectivity of the s-polarized fundamental wavelength at 1030 nm of the coated GIP device with the same coating applied on both sides. The measured reflectivity of a single AR coating is below 1% in the 1000 nm to 1060 nm wavelength range. In comparison, the reflectivity of the p-polarized fundamental light of the applied AR coating is >6%. The high difference in reflectivity for s- and p-polarized radiation should thus enable an automatic selection of an s-polarized laser operation without the need of an additional polarization selecting intra-cavity element. The design of the AR coating and the s-polarized electric-field distribution of the fundamental light is shown in Fig. 5(b). The coating has a total thickness of 3.35 µm and consists of alternating layers of SiO_2 and Ta_2O_5. To further enhance the XUV reflectivity, the 263-nm-thick top layer is made from Ta_2O_5, a high refractive index material in the XUV range. Our coated GIP with 60° AoI features a broadband XUV reflectivity >25% for photon energies between 10 and 60 eV. For higher AoIs, the reflectivity could be increased to >50% while simultaneously extending the high photon energy cut-off. In comparison, a sapphire plate placed under Brewster's angle for the p-polarized fundamental light would feature a narrower reflectivity band with a maximum of 17% at 25 eV [Fig. 4(a)].

Optics EXPRESS

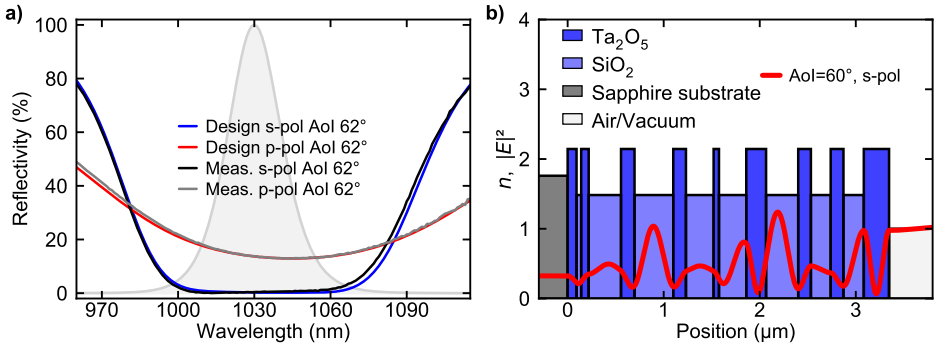

Fig. 5. Characterization and design properties of the fabricated coated GIP. (a) Reflectivity of the s- and p-polarized fundamental light from the both-side AR-coated GIP at an AoI of 62°. The curves according to the design and the measured data are shown. A transform-limited soliton spectrum of a 45-fs pulse is shown for comparison (gray shaded area). (b) Coating design of the GIP for an AoI of 60°. The red line shows the light intensity distribution of the fundamental laser light within the dielectric coating.

4. Experimental results

Table 1 summarizes the laser parameters and XUV performance of our TDL oscillator. In the here presented experiment, we operated our TDL oscillator based on Yb:YAG as gain material with sub-50-fs pulse duration at ~17 MHz repetition rate. The optical bandwidth of the sub-50-fs pulses exceed the gain bandwidth of Yb:YAG by a factor of more than two. Such short pulses from Yb:YAG are enabled by operating the oscillator in a regime of strong self-phase-modulation inside the laser cavity [27]. Without the coated GIP introduced into the oscillator, our TDL oscillator delivers 43-fs pulses at 220 W of pump power. Intra-cavity, we achieve a peak and average power of 950 MW and 800 W, respectively. When the coated GIP is introduced into the oscillator, the performance was limited to less than 500 MW of intra-cavity peak power. We assume that this limitation comes from a thermal lens originating from the coatings of the GIP, which is for the argon experiment at an incident average intensity on the GIP of ~10 kW/cm^2 and for xenon at ~40 kW/cm^2. The respective incident peak intensities and peak fluences on the GIP are ~20 GW/cm^2 and ~1 J/cm^2 for argon and ~80 GW/cm^2 and ~5 J/cm^2 for xenon. Please note that the stated intensities and fluences are error-prone due to their high sensitivity to the respective length measurements of the HHG focus to the GIP. During the experiment we did not observe damage of the coated GIP.

We inject argon with a backing pressure of 5 bar and use a CM3 with 100-mm RoC. At a pump power of ~200 W, the laser operates with 46 fs pulse duration at an intra-cavity peak and average power of 480 MW and 430 W, respectively. The optical spectrum [Fig. 6(b)] is centered at 1024.9 nm with a FWHM bandwidth of 24.5 nm. The ~5-nm blueshift of the optical spectrum away from the gain peak of Yb:YAG at 1030 nm is explained by the ionization blue-shift in the plasma. The harmonic spectrum is shown in Fig. 7 and extents up to the 43rd harmonic (52 eV). We out-couple an XUV average power of 1.3 μW in the 31st harmonic (37 eV). With an XUV out-coupling efficiency of ~30%, 1.3 μW of out-coupled correspond to 4.3 μW of generated XUV average power.

Due to the lower ionization potential of xenon, we use a slightly larger focus with a 150-mm RoC for CM3. At a pump power of ~200 W, the laser operates with 45 fs pulse duration at an intra-cavity peak and average power of 410 MW and 360 W, respectively. The optical spectrum is centered at 1031.1 nm with a FWHM bandwidth of 26.9 nm [Fig. 6(e)]. The harmonic spectrum in xenon with a backing pressure of 3 bar extents up to the 25th harmonic (30 eV) and we

Optics EXPRESS

Table 1. Summary of the laser parameters and XUV performance of our TDL oscillator with HHG in argon and xenon.

Generation gas	Argon	Xenon
Gas backing pressure (bar)	5	3
Harmonic cut-off (# | eV)	43 | 52	25 | 30
Out-coupled overall XUV flux (μW)	9.0	11.0
Out-coupled XUV flux in harmonic (μW | eV)	1.3 | 37	5.4 | 25
Generated XUV flux in harmonic (μW | eV)	4.3 | 37	18.0 | 25
Pump power (W)	200	200
Concave RoC of CM3 (mm)	100	150
NIR beam radius incident on GIP (μm × μm)	950 × 1900	400 × 800
Intra-cavity peak power (MW)	480	410
Intra-cavity average power (W)	430	360
Intra-cavity pulse energy (μJ)	23	19
Pulse duration (fs)	46	45
Central wavelength (nm)	1024.9	1031.1
FWHM spectral bandwidth (nm)	24.5	26.9
Repetition rate (MHz)	17.2	17.1

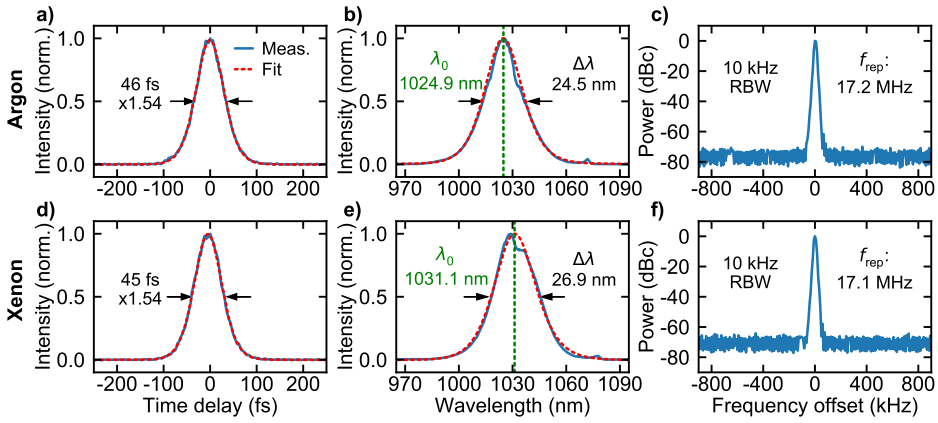

Fig. 6. Characterization of the KLM Yb:YAG TDL oscillator with HHG in argon (a) to (c) and xenon (d) to (f). (a), (d) Intensity autocorrelation with fit for sech^2-soliton pulses. (b), (e) Optical spectrum with central wavelength (λ_0), spectral FWHM bandwidth ($\Delta\lambda$), and sech^2 fit. (c), (f) Radio-frequency (RF) spectrum of the fundamental repetition rate (f_{rep}) measured with 10-kHz resolution bandwidth (RBW).

Optics EXPRESS

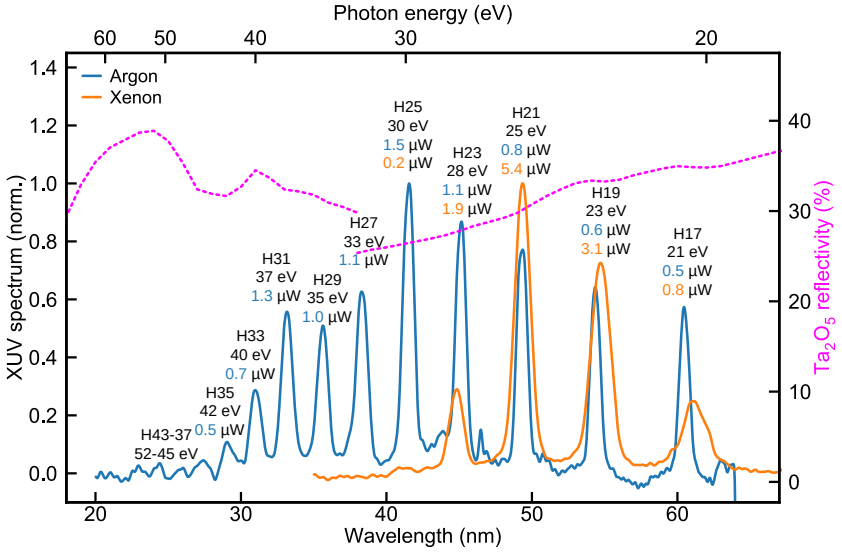

Fig. 7. Detected XUV spectra in argon and xenon filtered by a 200-nm-thick aluminum filter. Harmonics are labelled with harmonic order, energy, and out-coupled XUV average power per harmonic. The s-polarized XUV reflectivity of the Ta_2O_5 top layer of the 60°-AoI GIP is shown for comparison. The step in the reflectivity curve is due to the use of two different reference data sets – high energy side is taken from [25] and low energy side from [26].

out-couple an XUV average power of 5.4 µW in the 21st harmonic (25 eV) [Fig. 7]. With an XUV out-coupling efficiency of ~30%, 5.4 µW of out-coupled correspond to 18.0 µW of generated XUV average power.

While driving HHG in both gases, the intensity autocorrelation traces [Figs. 6(a),(d)] and the optical spectra [Figs. 6(b),(e)] agree well with the fit for sech^2-soliton pulses. The radio-frequency spectra measured at the fundamental repetition frequency of ~17 MHz show no side peaks [Figs. 6(c),(f)], indicating clean soliton mode-locking. Within a few hours of XUV experiments, we did not observe degradation of the coated GIP.

5. Conclusion and outlook

We have, for the first time, experimentally implemented a coated GIP for efficient and broadband XUV out-coupling of intra-cavity generated high harmonics. We have designed and produced a 60°-AoI GIP, tailored specifically for the high demands of intra-cavity HHG. We have shown that XUV sources based on intra-oscillator HHG can deliver µW power levels, approaching the state-of-the-art of out-coupled XUV power levels delivered by fsECs at comparable photon energies [Fig. 2].

In comparison to previous intra-oscillator HHG in argon inside a ~100-fs KLM Yb:YAG TDL oscillator where ~0.06 µW of XUV were out-coupled in the 25th harmonic (30 eV) by a sapphire Brewster's plate [10], the combination of increased driving laser performance with more efficient XUV out-coupling by the coated GIP allowed us to out-couple 1.3 µW in the 31st harmonic (37 eV). Hence, we have increased the out-coupled XUV average power by a factor of 20 while simultaneously increasing the photon energy. With xenon as generation gas, our out-coupled

Optics EXPRESS

XUV average power has increased even further and has reached 5.4 µW in the 21st harmonic (25 eV).

Currently, the intra-cavity HHG laser performance of our TDL oscillator is limited, which presumably originates from a thermal effect in the AR coatings of the GIP. By investigating and optimizing the residual absorption of the employed AR coatings, we expect to be able to increase our laser performance and the XUV output. Further possibilities to increase the XUV output of the system, including, e.g., the implementation of a high-pressure gas target, have been discussed in our previous publication [10].

In a future study, we plan to optimize the structure of our coated GIP. A first parameter is the design angle of the coated GIP, which can be used to further optimize the discussed trade-off between XUV reflectivity and supported driving laser pulse duration. Also, the top-layer material can be changed. Instead of Ta_2O_5, also the low index material SiO_2 can be used [8]. This brings the advantage of having the low index material at the interface to vacuum, simplifying the AR coating. Alternatively, also the high index material Ta_2O_5 can be exchanged by another one such as Nb_2O_5, Al_2O_3, or HfO_2. A change of the substrate material from sapphire to fused silica (lower refractive index in the NIR) reduces the complexity of the NIR AR coatings, leading potentially to lower NIR losses. This would be beneficial for the use of a coated GIP in a fsEC, which is more sensitive to losses than a TDL oscillator.

We have shown that efficient and broadband intra-cavity XUV out-coupling by a coated GIP is a well-suited approach to improve the performance of intra-cavity XUV sources based on fsECs or TDL oscillators.

Funding. Schweizerischer Nationalfonds zur Förderung der Wissenschaftlichen Forschung (200020_179146, 200020_200774, 206021_144970, 206021_170772, 206021_198176).

Acknowledgments. The authors acknowledge the support of the Ultrafast Laser Physics group of Ursula Keller (ETH Zürich) for lending the 248/310 McPherson spectrometer.

Disclosures. The authors declare no conflicts of interest.

Data availability. Data underlying the results presented in this paper are available in Ref. [28].

References

1. S. Passlack, S. Mathias, O. Andreyev, D. Mittnacht, M. Aeschlimann, and M. Bauer, "Space charge effects in photoemission with a low repetition, high intensity femtosecond laser source," J. Appl. Phys. **100**(2), 024912 (2006).
2. T. Südmeyer, S. V. Marchese, S. Hashimoto, C. R. E. Baer, G. Gingras, B. Witzel, and U. Keller, "Femtosecond laser oscillators for high-field science," Nat. Photonics **2**(10), 599–604 (2008).
3. C. Gohle, T. Udem, M. Herrmann, J. Rauschenberger, R. Holzwarth, H. A. Schuessler, F. Krausz, and T. W. Hänsch, "A frequency comb in the extreme ultraviolet," Nature **436**(7048), 234–237 (2005).
4. R. J. Jones, K. D. Moll, M. J. Thorpe, and J. Ye, "Phase-Coherent Frequency Combs in the Vacuum Ultraviolet via High-Harmonic Generation inside a Femtosecond Enhancement Cavity," Phys. Rev. Lett. **94**(19), 193201 (2005).
5. R. Klas, A. Kirsche, M. Gebhardt, J. Buldt, H. Stark, S. Hädrich, J. Rothhardt, and J. Limpert, "Ultra-short-pulse high-average-power megahertz-repetition-rate coherent extreme-ultraviolet light source," PhotoniX **2**(1), 4–8 (2021).
6. F. Labaye, M. Gaponenko, V. J. Wittwer, A. Diebold, C. Paradis, N. Modsching, L. Merceron, F. Emaury, I. J. Graumann, C. R. Phillips, C. J. Saraceno, C. Kränkel, U. Keller, and T. Südmeyer, "Extreme ultraviolet light source at a megahertz repetition rate based on high-harmonic generation inside a mode-locked thin-disk laser oscillator," Opt. Lett. **42**(24), 5170–5173 (2017).
7. N. Kanda, T. Imahoko, K. Yoshida, A. Tanabashi, A. Amani Eilanlou, Y. Nabekawa, T. Sumiyoshi, M. Kuwata-Gonokami, and K. Midorikawa, "Opening a new route to multiport coherent XUV sources via intracavity high-order harmonic generation," Light: Sci. Appl. **9**(1), 168 (2020).
8. O. Pronin, V. Pervak, E. Fill, J. Rauschenberger, F. Krausz, and A. Apolonski, "Ultrabroadband efficient intracavity XUV output coupler," Opt. Express **19**(11), 10232–10240 (2011).
9. J. Lee, D. R. Carlson, and R. J. Jones, "Optimizing intracavity high harmonic generation for XUV fs frequency combs," Opt. Express **19**(23), 23315–23326 (2011).
10. J. Fischer, J. Drs, F. Labaye, N. Modsching, V. Wittwer, and T. Südmeyer, "Intra-oscillator high harmonic generation in a thin-disk laser operating in the 100-fs regime," Opt. Express **29**(4), 5833–5839 (2021).
11. D. C. Yost, T. R. Schibli, and J. Ye, "Efficient output coupling of intracavity high-harmonic generation," Opt. Lett. **33**(10), 1099–1101 (2008).
12. G. Porat, C. M. Heyl, S. B. Schoun, C. Benko, N. Dörre, K. L. Corwin, and J. Ye, "Phase-matched extreme-ultraviolet frequency-comb generation," Nat. Photonics **12**(7), 387–391 (2018).

Optics EXPRESS

13. I. Pupeza, S. Holzberger, T. Eidam, H. Carstens, D. Esser, J. Weitenberg, P. Rußbüldt, J. Rauschenberger, J. Limpert, T. Udem, A. Tünnermann, T. W. Hänsch, A. Apolonski, F. Krausz, and E. Fill, "Compact high-repetition-rate source of coherent 100 eV radiation," Nat. Photonics **7**(8), 608–612 (2013).
14. T. Saule, S. Heinrich, J. Schötz, N. Lilienfein, M. Högner, O. deVries, M. Plötner, J. Weitenberg, D. Esser, J. Schulte, P. Russbueldt, J. Limpert, M. F. Kling, U. Kleineberg, and I. Pupeza, "High-flux ultrafast extreme-ultraviolet photoemission spectroscopy at 18.4 MHz pulse repetition rate," Nat. Commun. **10**(1), 458 (2019).
15. K. D. Moll, R. J. Jones, and J. Ye, "Output coupling methods for cavity-based high-harmonic generation," Opt. Express **14**(18), 8189–8197 (2006).
16. C. Zhang, S. B. Schoun, C. M. Heyl, G. Porat, M. B. Gaarde, and J. Ye, "Noncollinear Enhancement Cavity for Record-High Out-coupling Efficiency of an Extreme-UV Frequency Comb," Phys. Rev. Lett. **125**(9), 093902 (2020).
17. R. Klas, A. Kirsche, M. Tschernajew, J. Rothhardt, and J. Limpert, "Annular beam driven high harmonic generation for high flux coherent XUV and soft X-ray radiation," Opt. Express **26**(15), 19318–19327 (2018).
18. A. Comby, D. Descamps, S. Beauvarlet, A. Gonzalez, F. Guichard, S. Petit, Y. Zaouter, and Y. Mairesse, "Cascaded harmonic generation from a fiber laser: a milliwatt XUV source," Opt. Express **27**(15), 20383–20396 (2019).
19. H. Carstens, M. Högner, T. Saule, S. Holzberger, N. Lilienfein, A. Guggenmos, C. Jocher, T. Eidam, D. Esser, V. Tosa, V. Pervak, J. Limpert, A. Tünnermann, U. Kleineberg, F. Krausz, and I. Pupeza, "High-harmonic generation at 250 MHz with photon energies exceeding 100 eV," Optica **3**(4), 366–369 (2016).
20. J. Nauta, J.-H. Oelmann, A. Borodin, A. Ackermann, P. Knauer, I. S. Muhammad, R. Pappenberger, T. Pfeifer, and J. R. Crespo López-Urrutia, "XUV frequency comb production with an astigmatism-compensated enhancement cavity," Opt. Express **29**(2), 2624–2636 (2021).
21. A. Ozawa, J. Rauschenberger, C. Gohle, M. Herrmann, D. R. Walker, V. Pervak, A. Fernandez, R. Graf, A. Apolonski, R. Holzwarth, F. Krausz, T. W. Hänsch, and T. Udem, "High Harmonic Frequency Combs for High Resolution Spectroscopy," Phys. Rev. Lett. **100**(25), 253901 (2008).
22. A. Cingöz, D. C. Yost, T. K. Allison, A. Ruehl, M. E. Fermann, I. Hartl, and J. Ye, "Direct frequency comb spectroscopy in the extreme ultraviolet," Nature **482**(7383), 68–71 (2012).
23. A. Ozawa, Z. Zhao, M. Kuwata-Gonokami, and Y. Kobayashi, "High average power coherent vuv generation at 10 MHz repetition frequency by intracavity high harmonic generation," Opt. Express **23**(12), 15107–15118 (2015).
24. J. Fischer, J. Drs, N. Modsching, F. Labaye, V. J. Wittwer, and T. Südmeyer, "Efficient 100-MW, 100-W, 50-fs-class Yb:YAG thin-disk laser oscillator," Opt. Express **29**(25), 42075–42081 (2021).
25. B. L. Henke, E. M. Gullikson, and J. C. Davis, "X-Ray Interactions: Photoabsorption, Scattering, Transmission, and Reflection at E = 50-30,000 eV, Z = 1-92," At. Data Nucl. Data Tables **54**(2), 181–342 (1993).
26. L. V. Rodríguez-de Marcos, J. I. Larruquert, J. A. Méndez, and J. A. Aznárez, "Self-consistent optical constants of SiO_2 and Ta_2O_5 films," Opt. Mater. Express **6**(11), 3622–3637 (2016).
27. J. Drs, J. Fischer, N. Modsching, F. Labaye, V. J. Wittwer, and T. Südmeyer, "Sub-30-fs Yb:YAG thin-disk laser oscillator operating in the strongly self-phase modulation broadened regime," Opt. Express **29**(22), 35929–35937 (2021).
28. J. Fischer, Data for "Efficient XUV-light out-coupling of intra-cavity high harmonics by a coated grazing-incidence plate," B2Share (2022), http://doi.org/10.23728/b2share.180c5e438a7240eebf3da181112054b2.

3.3 Pierced mirror out-coupling of intra-oscillator generated high harmonic XUV light

Introduction

A pierced mirror was investigated during this thesis as another intra-cavity XUV out-coupling mechanism. This approach is commonly used in femtosecond enhancement cavities (fsEC) [1–3]. It has however not yet been demonstrated inside an ultrafast laser oscillator. In the context of intra-oscillator HHG, the pierced mirror is placed inside the laser cavity after the HHG focus. The small on-axis hole with a diameter in the 100-µm range enables out-coupling of the XUV light which is much less divergent in comparison to the driving infrared laser. The advantage of this approach is that the XUV out-coupling efficiency increases towards higher XUV photon energies and is spectrally not limited. Compared to the Brewster plate and the coated GIP out-coupling, the pierced mirror circumvents unwanted material transmission for the infrared driving field inside the cavity. Material transmission can lead to thermal effects, which detrimentally affect laser performance at high laser powers [section 3.2]. Further details including a comparison to other commonly applied intra-cavity XUV out-coupling methods is provided by section 3.2.

The following preliminary and not yet published experimental study demonstrates the suitability of a pierced mirror for out-coupling of XUV light generated in neon and argon inside an ultrafast TDL oscillator.

Experimental setup

An experimental schematic of HHG inside a KLM Yb:YAG TDL oscillator with a pierced mirror (PM) as XUV out-coupler is shown in Fig. 3.3. The setup includes three sections, which are Chamber 1, Chamber 2, and an XUV spectrometer.

The TDL oscillator, which main characteristics are described in section 2.4, is placed in Chamber 1. In the current configuration, the laser operates in p-polarization and is characterized via the output-coupler leakage for the infrared beam with a transmission of 0.77%. A high peak-power configuration based on an 1-mm-thick sapphire plate as Kerr medium is selected for driving HHG in neon. For HHG in argon, a reduced peak-power configuration based on a 2-mm-thick sapphire plate is chosen. The noble gas is injected by a ∼100-µm-opening-diameter tapered glass nozzle into a tight intra-cavity focus between the concave mirrors PM and CM3. The CM3 has a radius of curvature (ROC) of 100 mm while the PM has a ROC of 250 mm. The resulting beam expansion

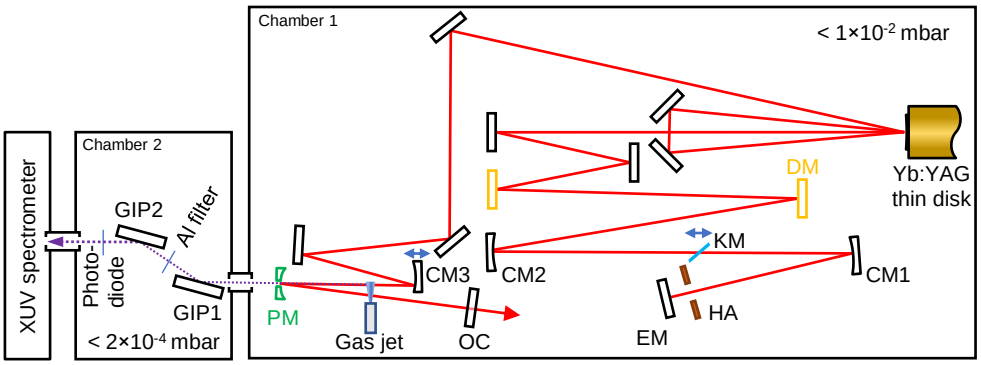

Figure 3.3: Schematic of the KLM Yb:YAG TDL oscillator with pierced mirror (PM) XUV light out-coupling. The setup includes three sections (Chamber 1, Chamber 2, and XUV spectrometer). Intra-oscillator HHG is driven in the tight focus between two concave mirrors (CM3 and PM), which are placed in Chamber 1. CM3 and PM have a ROC of 100 mm and 250 mm, respectively. The out-coupled XUV light is stripped of the residual infrared light using two 75° angle of incidence grazing-incidence plates (GIP1 and GIP2), which are placed in Chamber 2. EM: end mirror; HA: hard aperture; CM: concave mirror; DM: dispersive mirror; KM: Kerr medium; OC: output coupler; GIP: grazing-incidence plate. Further details of the TDL setup are given in section 2.4.

on the PM by a factor of 1.67 leads to reduced losses of the driving laser, but also limits the out-coupling efficiency of lower-energetic stronger-diverging harmonics. CM3 is placed on a linear translation stage. Shifting the position of CM3 is used to compensate the plasma lens in the generation gas and to optimize the oscillator performance in mode-locked operation.

The out-coupled XUV light is stripped of the residual infrared light using two 75° angle of incidence grazing-incidence plates (GIP), which are placed in Chamber 2. The high-refractive-index Ta_2O_5 top-layer of the GIPs is suitable for a broadband p-polarized XUV reflectivity up to ∼100 eV. XUV light is subsequently characterized by an aluminum coated photodiode (AXUV100Al, OPTO DIODE) and an in-house built XUV spectrometer. A 200-nm-thick aluminum filter can be used to suppress residual infrared light from reaching the photodiode or spectrometer. Tabulated values for the reflectivity of the Ta_2O_5 top layer of the GIP, the transmission of the aluminum filter, and simulated values for the grating efficiency are used to determine the XUV flux.

Experimental results

Figure 3.4 shows details of the pierced mirror implemented inside the TDL cavity. A picture of the pierced mirror is shown in Fig. 3.4 a). The XUV extraction hole has the shape of a cone with the tip facing to the front side of the mirror. Fig. 3.4 b) shows a microscope image of the frontside of the respective hole where the XUV light can exit the cavity through a ∼120-µm diameter opening. Without hard aperture for KLM inside the cavity, the induced losses favor a laser operation in the TEM_{10}, TEM_{01}, or TEM_{11} transverse-electromagnetic mode when aligned in continuous-wave operation to the center of the hole. The presence of the hard aperture in the cavity forces the favored TEM_{00} operation. Depending on the employed Kerr medium thickness, different mode-locking procedures are followed. Using the 2-mm-thick Kerr medium, the driving laser can be directly mode-locked when aligned on the XUV extraction hole. In the 1-mm-thick Kerr medium configuration, initiating mode-locking with the driving

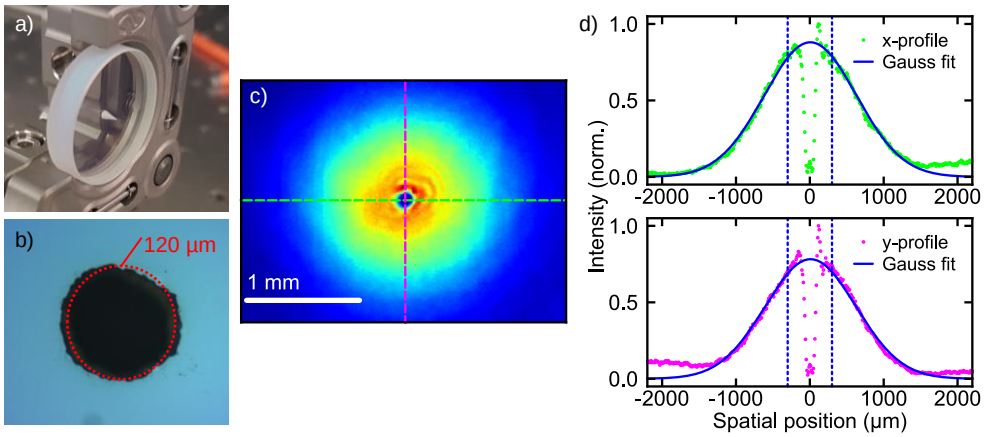

Figure 3.4: Experimental details of pierced mirror XUV out-coupling from a KLM Yb:YAG TDL oscillator. a) Picture of the pierced mirror with 6 mm thickness and 25 mm diameter. The XUV extraction hole is drilled in the form of a cone with the cone tip facing to the front side of the mirror. b) Microscope image of the front side of the XUV extraction hole. XUV can exit through a ∼120-µm diameter opening. c) Image of the infrared beam on the pierced mirror in mode-locked operation while driving HHG in neon. The beam is centered on the XUV extraction hole. The magenta- and lime-colored dashed lines mark the x- and y-positions of the hole and d) shows the intensity profiles of the beam along these two lines. A Gaussian is fitted to the intensity profile where the region between the two blue vertical dashed lines is excluded from the fit.

laser field aligned on the hole was not possible. Instead, the losses induced by the pierced mirror hole are reduced by "misaligning" the laser beam without hard aperture away from the hole until the laser operates again in a TEM_{00} mode. In this state, the hard aperture is moved in the cavity and mode-locking is initialized by shaking one of the cavity mirrors by a piezo actuator. Afterwards, the beam is realigned on the hole by steering the beam with the cavity end mirror [EM in Fig. 3.3] in mode-locked operation. Fig. 3.4 c) shows an image of the infrared laser beam centered on the pierced mirror hole in mode-locked operation while driving HHG in neon. Fig. 3.4 d) depicts the corresponding intensity profiles along the dashed line cuts shown in Fig. 3.4 c). A Gaussian is fitted to the intensity profiles while the position of the hole is excluded from the fit. According to the fit, the beam radius ($1/e^2$) in x- and y-direction is 1250 µm and 1230 µm, respectively.

Comparing the average beam radius of 1240 µm to the XUV extraction hole radius of 60 µm, yields a radius overlap of ∼5%, which results in a calculated intensity loss of ∼0.5% per pass or ∼1% per cavity round-trip of the infrared beam. The achieved overlap is comparable to or higher than the one achieved in fsECs, where, e.g., overlaps of ∼3% (80-µm hole radius and 2700-µm infrared beam radius) [1] or ∼5% (170-µm hole radius and 3650-µm infrared beam radius) [2] are reached. It is important to note that fsECs are typically build in the form of a ring cavity [1–5], whereas the here presented oscillator is a

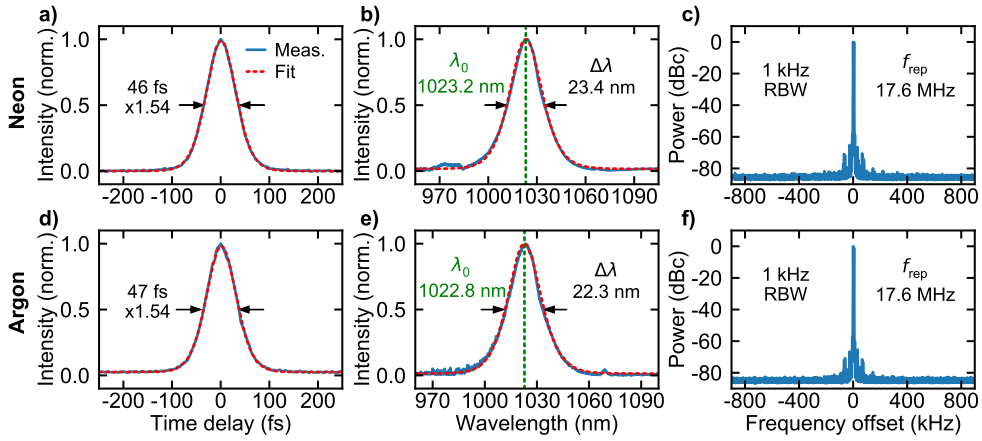

Figure 3.5: Characterization of the KLM Yb:YAG TDL oscillator driving HHG in neon a) to c) and argon d) to f) and XUV out-coupling by a pierced mirror. a), d) Intensity autocorrelation with a fit for sech²-soliton pulses. b), e) Optical spectrum centered at λ_0, spectral FWHM bandwidth $\Delta\lambda$, and sech² fit. c), f) Radio-frequency spectrum of the fundamental repetition rate (f_{rep}) measured with 1-kHz resolution bandwidth (RBW).

Table 3.1: Laser parameters and XUV performance of the KLM Yb:YAG TDL oscillator driving HHG in neon and argon. XUV light generated inside the oscillator is out-coupled by a pierced mirror.

Generation gas	**Neon**	**Argon**
Gas backing pressure (bar)	10	5
Harmonic cut-off (# | eV)	59 | 71	49 | 59
Out-coupled overall XUV flux (µW)	-	∼6
Out-coupled XUV flux in harmonic (µW | eV)	∼0.001 | 61	∼1 | 40
Intra-cavity average power (W)	1130	440
Intra-cavity peak power (MW)	1230	470
Pulse duration (fs)	46	47
Central wavelength (nm)	1023.2	1022.8
FWHM optical bandwidth (nm)	23.4	22.3
Repetition rate (MHz)	17.6	17.6
Pump power (W)	470	320
Introduced roundtrip GDD (fs^2)	-2000	-2000
Kerr medium thickness (mm)	1	2
Hard aperture diameter (mm)	4.0	4.0

standing-wave cavity-type with the pierced mirror in folding configuration. In the standing-wave configuration, the pierced mirror features twice the round-trip losses compared to the ring configuration. Whereas the achievable enhancement inside a fsEC strongly decreases with increasing losses of the driving laser on the pierced mirror, gain inside a TDL oscillator in every cavity round-trip can compensate the losses. TDL oscillators can thus be expected to tolerate comparably higher round-trip losses, meaning relatively larger hole sizes.

Table 3.1 shows the mode-locked laser and XUV performance while driving HHG in neon and argon. In the high-peak-power configuration with 10 bar backing pressure[2] of neon, the TDL operates with 46 fs pulse duration at an intra-cavity average and peak power of 1130 W and 1230 MW, respectively. The 23.4-nm FWHM optical spectrum is centered at 1023.2 nm [Fig. 3.5 b)]. The laser operation at a central wavelength away from the Yb:YAG gain maximum at 1030 nm is explained by a plasma-induced blue shift. The achieved intra-cavity peak power of 1.2 GW significantly exceeds previous TDLs operating with XUV out-couplers based on infrared-transmissive elements [section 3.1, section 3.2, and [6]]. The XUV spectrum in neon extends up to 71 eV (59^{th}

[2] 10 bar backing pressure represents the maximum gas pressure of the employed gas delivery system, which means that higher pressures could potentially further increase the XUV flux.

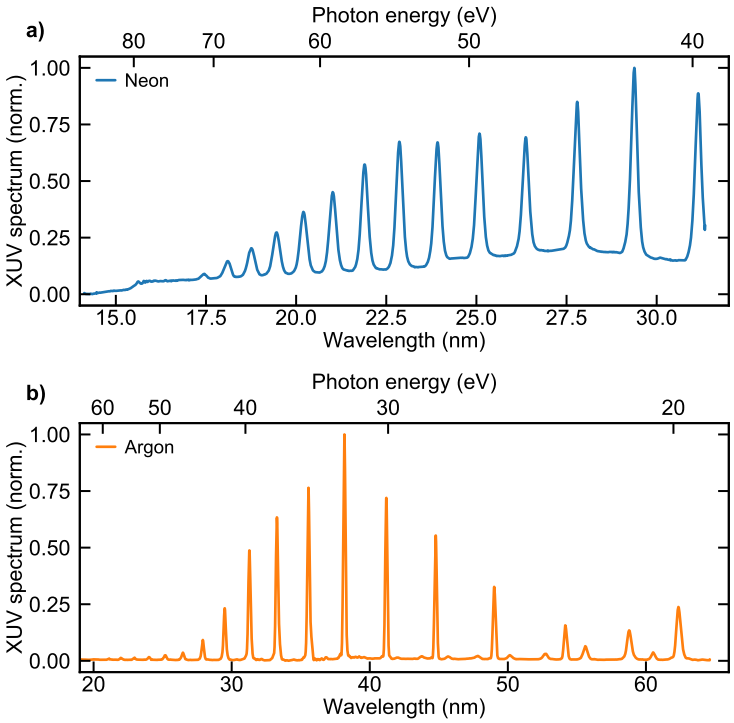

Figure 3.6: Detected XUV spectra in neon a) and argon b). XUV light is generated inside the tight focus of a KLM Yb:YAG TDL oscillator, out-coupled by a pierced mirror, and guided by two grazing incidence plates towards the XUV spectrometer. The argon spectrum is filtered by a 200-nm-thick aluminum filter, which is inserted in the space between the two grazing incidence plates.

harmonic) [Fig. 3.6 a)] and the out-coupled XUV flux within a single harmonic order at 61 eV (51$^{\text{st}}$ harmonic) is determined to be ∼1 nW.[3] In the reduced peak-power configuration with 5 bar backing pressure of argon, the TDL operates with 47 fs pulse duration at an intra-cavity average and peak power of 440 W and 470 MW, respectively. The 22.3-nm FWHM optical spectrum is centered at 1022.8 nm [Fig. 3.5 e)]. The XUV spectrum extends up to 59 eV (49$^{\text{th}}$ harmonic) [Fig. 3.6 b)] and the out-coupled XUV flux within a single harmonic order at 40 eV (33$^{\text{rd}}$ harmonic) is determined to be ∼1 µW.[4] In both

[3]The out-coupled flux within the 51$^{\text{st}}$ harmonic is calculated from the detected flux on the camera of the XUV spectrometer.

[4]The overall out-coupled XUV flux in argon is determined with the photodiode. The flux within the 33$^{\text{rd}}$ harmonic is determined with two different methods: 1. Determining the overall flux with the photodiode and then calculating the flux in the 33$^{\text{rd}}$ harmonic using the detected XUV spectrum. 2. Directly from the detected flux on the camera of the XUV spectrometer. The results of method 1 and 2 agree well within error margins.

gases, neon and argon, the intensity autocorrelation [Fig. 3.5 a), d)] and optical spectrum [Fig. 3.5 b), e)] agree well with the fit for sech^2-soliton pulses. The radio-frequency spectra measured at the fundamental repetition frequency of 17.6 MHz show a suppression of side peaks below -65 dBc. This indicates stable mode-locking, but also high mechanical noise present in the system. The noise is attributed to the operating turbo pumps mounted on top of the vacuum chamber and water-cooling induced vibrations. During several hours of XUV generation, no damage of the pierced mirror was observed.

Conclusion and outlook

XUV out-coupling of intra-oscillator generated high harmonic XUV light by a pierced mirror has been demonstrated for the first time. This approach enables spectrally unlimited XUV out-coupling towards higher photon energies and presents a crucial component towards a 100-eV intra-oscillator HHG source. For photon energies exceeding 50 eV, the pierced mirror complements the coated GIP as XUV out-coupler, which features efficient out-coupling in the 10 to 60 eV photon energy range [section 3.2]. The with pierced mirror achieved intra-cavity peak power of 1.2 GW significantly exceeds the peak power of previous TDLs operating with XUV out-couplers based on infrared-transmissive elements [section 3.1, section 3.2, and [6]]. The improved driving laser performance has enabled HHG in neon with photon energies up to 71 eV (59$^{\text{th}}$ harmonic).

To reach 100-eV photon energies with the developed intra-oscillator XUV source, the peak intensity inside the HHG focus must be further increased. A first option is using an even tighter focus by adapting the cavity design. A second option is to increase the intra-cavity peak power of the TDL system. For this, the currently employed 1-mm-thick sapphire Kerr medium can be replaced by an 0.5-mm-thick one, which should enable up to 2 GW of intra-cavity peak power [7].

References

1. Pupeza, I., Holzberger, S., Eidam, T., Carstens, H., Esser, D., Weitenberg, J., Rußbüldt, P., Rauschenberger, J., Limpert, J., Udem, T., Tünnermann, A., Hänsch, T. W., Apolonski, A., Krausz, F. & Fill, E. Compact high-repetition-rate source of coherent 100 eV radiation. *Nature Photonics* **7**, 608 (2013).

2. Saule, T., Heinrich, S., Schötz, J., Lilienfein, N., Högner, M., deVries, O., Plötner, M., Weitenberg, J., Esser, D., Schulte, J., Russbueldt, P., Limpert, J., Kling, M. F., Kleineberg, U. & Pupeza, I. High-flux ultrafast extreme-ultraviolet photoemission spectroscopy at 18.4 MHz pulse repetition rate. *Nature Communications* **10**, 1 (2019).

3. Carstens, H., Högner, M., Saule, T., Holzberger, S., Lilienfein, N., Guggenmos, A., Jocher, C., Eidam, T., Esser, D., Tosa, V., Pervak, V., Limpert, J., Tünnermann, A., Kleineberg, U., Krausz, F. & Pupeza, I. High-harmonic generation at 250 MHz with photon energies exceeding 100 eV. *Optica* **3**, 366 (2016).

4. Gohle, C., Udem, T., Herrmann, M., Rauschenberger, J., Holzwarth, R., Schuessler, H. A., Krausz, F. & Hänsch, T. W. A frequency comb in the extreme ultraviolet. *Nature* **436**, 234 (2005).

5. Jones, R. J., Moll, K. D., Thorpe, M. J. & Ye, J. Phase-Coherent Frequency Combs in the Vacuum Ultraviolet via High-Harmonic Generation inside a Femtosecond Enhancement Cavity. *Physical Review Letters* **94**, 193201 (2005).

6. Kanda, N., Imahoko, T., Yoshida, K., Tanabashi, A., Amani Eilanlou, A., Nabekawa, Y., Sumiyoshi, T., Kuwata-Gonokami, M. & Midorikawa, K. Opening a new route to multiport coherent XUV sources via intracavity high-order harmonic generation. *Light: Science & Applications* **9**, 168 (2020).

7. Fischer, J., Drs, J., Labaye, F., Modsching, N., Müller, M., Wittwer, V. J. & Südmeyer, T. *High Harmonic Generation Inside Thin-Disk Laser Oscillators – An Efficient and Single-Stage XUV Source* in *Optica High-brightness Sources and Light-driven Interactions Congress 2022* (Optica Publishing Group, 2022), paper HW2B.3.

4 Conclusion and outlook

This PhD thesis focused on (i) pushing the output performance of high-peak-power sub-100-fs thin-disk laser (TDL) oscillators and on (ii) driving the extreme nonlinear process of high harmonic generation (HHG) directly inside the cavity of ultrafast TDL oscillators. The high-power development has resulted in reaching the shortest pulse duration as well as the first more than 100 MW peak-power TDL oscillator. While being implemented for the first time five years ago in 2017, this thesis has demonstrated that intra-oscillator HHG is a viable approach capable of reaching a state-of-the-art XUV flux comparable to other table-top megahertz repetition rate XUV sources.

In detail: The during this thesis developed Kerr lens mode-locked (KLM) Yb:YAG TDL presents not only with 27 fs the shortest pulse-duration TDL oscillator, but also with 102 MW peak power in 52-fs pulses the first >100 MW peak-power oscillator. The results demonstrate that KLM TDL oscillators which operate in the regime of strong intra-cavity self-phase modulation can deliver highest performance even far beyond the supported spectral bandwidth of the used gain material. The results furthermore show that Yb:YAG is currently still the best choice for the TDL oscillator technology to reach shortest pulses and highest peak powers. This statement also holds compared to TDL oscillators based on more broadband gain materials. The 102-MW peak power and ideally soliton-shaped 52-fs output pulses can directly be used for driving nonlinear interactions such as optical rectification for broadband terahertz (THz) generation [1–3] and are as well very promising to reach the few-cycle regime within a single temporal pulse compression stage [4–6]. According to simulations, it is expected that these pulses can be compressed within a single argon-filled multi-pass gas cell to ∼7 fs and ∼500 MW peak power. Compared to previous compression experiments of megahertz pulse trains, this source should reach such pulse durations with a superior pulse contrast, making the source attractive for megahertz repetition rate pump-probe experiments requiring a high temporal pulse contrast.

No fundamental limitation preventing further power-scaling was identified during this thesis. An output peak-power scaling by a factor well above two of the KLM Yb:YAG TDL oscillator should be possible by increasing the pump-spot diameter on the disk combined with an appropriate adaptation of the cavity

design and KLM mechanism [7, 8]. To prevent any damage of the disk, the current system was limited to a pump intensity of ∼6 kW/cm². However, pump intensities of up to 10 kW/cm² have already been reported in the literature [7]. Thus, pumping the current system with 10 kW/cm² should allow theoretically for a 60% increase in output peak power considering that the here demonstrated optical-to-optical efficiency can be maintained and no limiting thermal effects appear. Additionally, the industrial dielectric coatings of the disk have not yet been optimized for the spectral bandwidth achieved in the shortest pulse configuration here presented. This might currently represent a limit for the efficient generation of even shorter pulse durations in the order of 30 fs. Altogether, it can be expected that ultrafast thin-disk laser oscillators operating with several 100 MW peak power at tens of megahertz repetition rate will become soon available.

In order to reach a state-of-the-art XUV output flux, the efforts were focused on increasing the intra-cavity peak power and on improving the XUV out-coupling efficiency of the intra-oscillator generated harmonics. Scaling of the intra-cavity peak power was mainly enabled by changing the employed mode-locking mechanism from semiconductor saturable absorber mirror (SESAM) to KLM, selecting Yb:YAG as gain material, and broadband dispersion engineering using in-house developed dispersive mirrors. This resulted with an intra-cavity peak power of 2 GW at 51 fs pulse duration in the highest intra-cavity peak power so far demonstrated by any ultrafast laser oscillator. Two broadband and efficient intra-cavity XUV out-coupler, i.e., a coated grazing-incidence plate (GIP) and a pierced mirror were investigated. A coated GIP with a broadband XUV reflectivity of >25% between 10 and 60 eV was developed and for the first time implemented for out-coupling of intra-cavity generated high harmonics. The presented intra-oscillator HHG system with a coated GIP enabled out-coupling of 1.3 µW XUV average power in a single harmonic at 37 eV in argon and 5.4 µW at 25 eV in xenon. Compared to the initial result from 2017, the out-coupled average XUV power has been increased by more than four orders of magnitude. Furthermore, these XUV power levels approach the state-of-the-art out-coupled XUV average power levels of femtosecond enhancement cavities (fsEC) operating at comparable photon energies. Besides a coated GIP, preliminary results for the first out-coupling of intra-oscillator generated high harmonics from a KLM TDL by a pierced mirror were presented. A pierced mirror enables efficient and spectrally not-limited XUV out-coupling towards high photon energies. The 1.2 GW peak-power TDL oscillator operating with pierced mirror has enabled HHG in neon with photon energies up to 71 eV.

While the XUV power levels and energies of the current intra-oscillator HHG system should already enable first applications, further scaling towards higher

XUV flux and higher photon energy in the direction of 100 eV is of high interest. One promising step towards a higher XUV flux is the implementation of a high-pressure gas nozzle allowing a better suppression of detrimental plasma effects [9]. All prerequisites for a 100-eV intra-oscillator HHG source are fulfilled by demonstrating HHG in neon combined with the pierced mirror XUV out-coupling. Increasing the intra-cavity peak power from currently 1.2 GW to 2 GW, demonstrated during this thesis, should enable reaching the desired 100 eV photon energies. A single-stage 100-eV coherent-XUV source is highly attractive for coherent diffraction imaging and finds broad application especially in the semiconductor industry for optical inspection.

References

1. Paradis, C., Drs, J., Modsching, N., Razskazovskaya, O., Meyer, F., Kränkel, C., Saraceno, C. J., Wittwer, V. J. & Südmeyer, T. Broadband terahertz pulse generation driven by an ultrafast thin-disk laser oscillator. *Optics Express* **26**, 26377 (2018).
2. Drs, J., Modsching, N., Paradis, C., Kränkel, C., Wittwer, V. J., Razskazovskaya, O. & Südmeyer, T. Optical rectification of ultrafast Yb lasers: pushing power and bandwidth of terahertz generation in GaP. *JOSA B* **36**, 3039 (2019).
3. Saraceno, C. J. Mode-locked thin-disk lasers and their potential application for high-power terahertz generation. *Journal of Optics* **20**, 044010 (2018).
4. Pronin, O., Seidel, M., Lücking, F., Brons, J., Fedulova, E., Trubetskov, M., Pervak, V., Apolonski, A., Udem, T. & Krausz, F. High-power multi-megahertz source of waveform-stabilized few-cycle light. *Nature Communications* **6**, 6988 (2015).
5. Tsai, C.-L., Meyer, F., Omar, A., Wang, Y., Liang, A.-Y., Lu, C.-H., Hoffmann, M., Yang, S.-D. & Saraceno, C. J. Efficient nonlinear compression of a mode-locked thin-disk oscillator to 27 fs at 98 W average power. *Optics Letters* **44**, 4115 (2019).
6. Barbiero, G., Wang, H., Graßl, M., Gröbmeyer, S., Kimbaras, D., Neuhaus, M., Pervak, V., Nubbemeyer, T., Fattahi, H. & Kling, M. F. Efficient nonlinear compression of a thin-disk oscillator to 8.5 fs at 55 W average power. *Optics Letters* **46**, 5304 (2021).
7. Brons, J., Pervak, V., Fedulova, E., Bauer, D., Sutter, D., Kalashnikov, V., Apolonskiy, A., Pronin, O. & Krausz, F. Energy scaling of Kerr-lens mode-locked thin-disk oscillators. *Optics Letters* **39**, 6442 (2014).

8. Poetzlberger, M., Zhang, J., Gröbmeyer, S., Bauer, D., Sutter, D., Brons, J. & Pronin, O. Kerr-lens mode-locked thin-disk oscillator with 50% output coupling rate. *Optics Letters* **44**, 4227 (2019).

9. Heyl, C. M., Schoun, S. B., Porat, G., Green, H. & Ye, J. A nozzle for high-density supersonic gas jets at elevated temperatures. *Review of Scientific Instruments* **89**, 113114 (2018).

Curriculum vitae

Name	Julian Benedikt Fischer
Date of birth	5 April 1994
Citizenship	German

Education

2018 - 2022	Doctoral studies, University of Neuchâtel, Switzerland.
2018 - 2021	Master of Science in Management, Technical University of Munich, Germany.
2015 - 2018	Master of Science in Physics, Technical University of Munich, Germany.
2012 - 2015	Bachelor of Science in Physics, Technical University of Munich, Germany.

Research experience

2018 - 2022	Doctoral studies at Laboratoire Temps-Fréquence under supervision of Prof. Thomas Südmeyer, University of Neuchâtel. *Power-scaling of ultrafast thin-disk laser oscillators for intra-oscillator high harmonic generation.*
2021	Master's thesis under supervision of Prof. Christoph Kaserer and Prof. Tim Kroencke, Technical University of Munich and University of Neuchâtel. *Analysis of the United States Equity Portfolio of the Swiss National Bank*.
2017 - 2018	Master's thesis under supervision of Prof. Reinhard Kienberger, Technical University of Munich. *Ultrafast Electron Transfer in Light-to-Chemical Energy Conversion.*
2015	Bachelor's thesis under supervision of Prof. Peter Müller-Buschbaum, Technical University of Munich. *In-situ degradation of thin films for organic photovoltaics*.

Acknowledgments

First, I would like to thank all my colleagues at the Laboratoire Temps-Fréquence for creating such an excellent environment – professionally as well as personally. I really enjoyed the last four years with you!

In detail: I would like to thank Thomas for giving me the opportunity to work in his research group. Thank you for putting so much trust in your PhD students, giving us so much freedom. It was a pleasure to work under your supervision. Many thanks also to Valentin. You were always reachable and your deep technical knowledge of almost any technical device were extremely helpful. Most of our result were not possible without your customized coatings. I would like to thank Jakub for your great collaboration on the HHG project. Our individual tasks complemented each other very well and without your work, we would definitely not be where we are today. Thank you to Norbert for the hands-on introduction to the TDL technology and the great support for the paper writing. Thank you to François for introducing me to the HHG project in the beginning of my PhD and for all your knowledge support thereafter. Thank you to Michael and Marin for your support in the lab. Finally, Kenichi, while we did not work together on the same projects, I really enjoyed visiting conferences with you.

Outside of the Laboratoire Temps-Fréquence, I would like to thank my friends and family.